การเตรียมและการศึกษาลักษณะสมบัติของไฮโดรเจลเจลาติน/พีวีเอ ที่มีอนุภาคนาโนของเงินที่ได้จากการฉายรังสีแกมมา

นางสาวนุชนันท์ เลียวหิรัญ

วิทยานิพนธ์นี้เป็นส่วนหนึ่งของการศึกษาตามหลักสูตรปริญญาวิทยาศาสตรดุษฎีบัณฑิต
สาขาวิชาวิศวกรรมชีวเวช
คณะวิศวกรรมศาสตร์ จุฬาลงกรณ์มหาวิทยาลัย
ปีการศึกษา 2557

PREPARATION AND CHARACTERIZATION OF GAMMA-RAY IRRADIATED GELATIN/PVA HYDROGEL CONTAINING SILVER NANOPARTICLES

Miss Nuchanan Leawhiran

A Dissertation Submitted in Partial Fulfillment of the Requirements

for the Degree of Doctor of Philosophy Program in Biomedical Engineering

Faculty of Engineering

Chulalongkorn University

Academic Year 2014

Thesis Title	PREPARATION AND CHARACTERIZATION OF GAMMA-RAY IRRADIATED GELATIN/PVA HYDROGEL CONTAINING SILVER NANOPARTICLES
By	Miss Nuchanan Leawhiran
Field of Study	Biomedical Engineering
Thesis Advisor	Professor Pitt Supaphol, Ph.D.
Thesis Co-Advisor	Assistant Professor Kumpanart Soontornvipart, DVM, Ph.D.

Accepted by the Faculty of Engineering, Chulalongkorn University in Partial Fulfillment of the Requirements for the Doctoral Degree

.....Dean of the Faculty of Engineering

(Professor Bundhit Eua-arporn, Ph.D.)

THESIS COMMITTEE

.....Chairman

(Professor Prasit Pavasant, D.D.S., Ph.D.)

.....Thesis Advisor

(Professor Pitt Supaphol, Ph.D.)

.....Thesis Co-Advisor

(Assistant Professor Kumpanart Soontornvipart, DVM, Ph.D.)

.....Examiner

(Assistant Professor Tanom Bunaprasert, M.D.)

.....Examiner

(Assistant Professor Sorada Kanokpanont, Ph.D.)

.....External Examiner

(Angkana Tanvatanagul, M.D.)

นุชนันท์ เลียวหิรัญ : การเตรียมและการศึกษาลักษณะสมบัติของไฮโดรเจลเจลาติน/พีวีเอ ที่มีอนุภาคนาโนของเงินที่ได้จากการฉายรังสีแกมมา (PREPARATION AND CHARACTERIZATION OF GAMMA-RAY IRRADIATED GELATIN/PVA HYDROGEL CONTAINING SILVER NANOPARTICLES) อ.ที่ปรึกษาวิทยานิพนธ์หลัก: ศ. ดร.พิชญ์ ศุภผล, อ.ที่ปรึกษาวิทยานิพนธ์ร่วม: ผศ. น.สพ. ดร.กัมปนาท สุนทรวิภาต, 131 หน้า.

แผ่นปิดแผลเป็นผลิตภัณฑ์ทางการแพทย์ที่สำคัญ แผ่นปิดแผลต้านแบคทีเรียมีบทบาทสำคัญในการดูแลแผลที่มีการติดเชื้อแต่แผ่นปิดแผลต้านแบคทีเรียมีราคาแพง และผลิตได้น้อยในประเทศ การศึกษานี้มุ่งเตรียมแผ่นปิดแผลไฮโดรเจลต้านแบคทีเรียจากเจลาตินและพอลิไวนิลแอลกอฮอล์ (พีวีเอ) ไฮโดรเจลเจลาตินและไฮโดรเจลเจลาติน/พีวีเอสังเคราะห์โดยการฉายรังสีแกมมา โดยเตรียมไฮโดรเจลจากสารละลายเจลาตินร้อยละ 15 โดยน้ำหนักผสมกับสารละลายพีวีเอร้อยละ 15 โดยน้ำหนักที่อัตราส่วนต่างกัน ได้แก่ 100:0, 80:20 และ 60:40 น้ำหนักต่อน้ำหนัก และฉายรังสีที่ 30, 40 และ 50 กิโลเกรย์ จากนั้นศึกษาไฮโดรเจลในด้านต่างๆ ผลการศึกษาแสดงให้เห็นว่าการเพิ่มพีวีเอสามารถปรับปรุงความทนทานและสมบัติเชิงกลให้ดีขึ้น ไฮโดรเจลที่อัตราส่วน 60:40 ที่ฉายรังสีที่ 30 กิโลเกรย์เป็นตัวเลือกที่เหมาะสมที่สุด ส่วนผสมนี้ได้รับเลือกที่จะเพิ่มซิลเวอร์ไนเตรท ($AgNO_3$) ร้อยละ 0.25, 0.50, 0.75, และ 1.00 โดยน้ำหนัก (ยึดตามส่วนประกอบที่เป็นของแข็ง) การก่อตัวของอนุภาคนาโนของเงินถูกตรวจพบภายหลังการฉายรังสี ศึกษาลักษณะเฉพาะของไฮโดรเจลเจลาติน/พีวีเอที่มีอนุภาคนาโนของเงินในด้านสมบัติทางกายภาพ, ความเป็นพิษต่อเซลล์ และฤทธิ์ต้านแบคทีเรียต่อ *Escherichia coli* (*E. coli*), *Staphylococcus aureus* (*S. aureus*) และ Methicillin-resistant *S. aureus* (MRSA) ผลการศึกษาบ่งชี้ว่าไฮโดรเจลเจลาติน/พีวีเอที่มีอนุภาคนาโนของเงินสามารถใช้เป็นแผ่นปิดแผลต้านแบคทีเรีย ไฮโดรเจลในการศึกษาครั้งนี้มีสมบัติทางกายภาพที่เหมาะสม มีความเป็นพิษต่อเซลล์ต่ำ และสามารถยับยั้งการเจริญเติบโตของแบคทีเรีย

สาขาวิชา วิศวกรรมชีวเวช ลายมือชื่อนิสิต .....

ปีการศึกษา 2557 ลายมือชื่อ อ.ที่ปรึกษาหลัก .....

ลายมือชื่อ อ.ที่ปรึกษาร่วม .....

5287788921 : MAJOR BIOMEDICAL ENGINEERING

KEYWORDS: BIOMATERIAL / BIOMEDICAL APPLICATION / CROSSLINKING / HYDROGEL / IRRADIATION

NUCHANAN LEAWHIRAN: PREPARATION AND CHARACTERIZATION OF GAMMA-RAY IRRADIATED GELATIN/PVA HYDROGEL CONTAINING SILVER NANOPARTICLES. ADVISOR: PROF. PITT SUPAPHOL, Ph.D., CO-ADVISOR: ASST. PROF. KUMPANART SOONTORNVIPART, DVM, Ph.D., 131 pp.

Wound dressing is an important medical product. Antibacterial wound dressing has an important role in an infection wound care. However, antibacterial wound dressing is expensive and has a few domestic manufacturing. This study aimed to prepare a hydrogel antibacterial wound dressing from gelatin and polyvinyl alcohol (PVA). The gelatin hydrogels and gelatin/poly(vinyl alcohol)(PVA) hydrogels were prepared by gamma irradiation. A 15 wt% gelatin solution was mixed with a 15 wt% PVA solution at different weight ratios of 100:0, 80:20, and 60:40 w/w, and irradiated at 30, 40, or 50 kGy. The results showed that the addition of PVA can enhance both the durability and the mechanical integrity. The hydrogels made from the 60:40 composition at 30 kGy were the most appropriated selection. This condition was then chosen to add silver nitrate ($AgNO_3$) at 0.25, 0.50, 0.75, or 1.00 wt% (based on solid content). Formation of silver nanoparticles (AgNPs) was discovered after irradiation. The AgNP/gelatin/PVA hydrogels were characterized for their physical properties, cytotoxicity, and antibacterial activity against *Escherichia coli* (*E. coli*), *Staphylococcus aureus* (*S. aureus*), and Methicillin-resistant *S. aureus* (MRSA). The results indicated that the AgNP/gelatin/PVA hydrogels had a potential to used as an anti-bacterial wound dressing. The hydrogels in this study had appropriate physical properties, low-cytotoxicity, and antibacterial activity.

Field of Study: Biomedical Engineering Student's Signature .....

Academic Year: 2014 Advisor's Signature .....

Co-Advisor's Signature .....

ACKNOWLEDGEMENTS

This study was funded by THE 90TH ANNIVERSARY OF CHULALONGKORN UNIVERSITY FUND (Ratchadaphiseksomphot Endowment Fund) and the Integrated Innovation Academic Center IIAC (RES_01_54_63), Chulalongkorn University Centenary Academic Development Project, Chulalongkorn University. MRSA was kindly provided from Microbiology Laboratory, Pramongkutkao Hospital, Bangkok, Thailand. I would like to thank you my advisor, Prof. Dr.Pitt Supaphol, and my co-advisor, Assist. Prof. Dr.Kumpanart Soontornvipart. I am grateful to Prof. Dr.Prasit Pavasant and members in Research Unit of Mineral Tissue, Faculty of Dentistry for kind allowance to use the tissue culture laboratory. Gratitude is extended to Assoc. Prof. Dr.Mana Sriyudthsak, Prof. Dr.Suthiluk Patumraj, Asst. Prof. Dr.Sorada Kanokpanont, and Assoc. Prof. Dr.Siriporn Damrongsakkul for the feedback, guidance and kindness. I received generous support from all of professors, friends and staffs in BME. I am also grateful for the help from the professors, students and members in Faculty of Engineering, Faculty of Science, Faculty of Medicine, Faculty of Dentistry, Faculty of Veterinary Science, and The Petroleum and Petrochemical College. Special thanks to the members of PS, AS, RR, SWB, and SC groups at PPC. I am thankful for my mother and father who believed in me.

CONTENTS

Page

Page

Page

Page

LIST OF TABLES

Page

Page

LIST OF FIGURES

Page

Page

Page

LIST OF ABBREVIATIONS

Ag^+	silver ion
$AgNO_3$	silver nitrate
AgNP	silver nanoparticle
ASTM	American Society for Testing and Materials
ATP	adenosine triphosphate
cm	centimeter
°C	degrees Celsius
DMEM	Dulbecco's modified Eagle medium
DMSO	dimethyl sulfoxide
DNA	deoxyribonucleic acid
FBS	fetal bovine serum
FDA	Food and Drug Administration of the United States of America
FTIR	Fourier transform infrared
EDX	Energy-dispersive X-ray spectroscopy
EtO	ethylene oxide
h	hour
ISO	International Organization for Standardization
kg	kilogram
kGy	kilogray
M	molar
min	minute
mg	milligram
mm	millimeter
μm	micron
MTT	3-(4,5-dimethylthiazol-2-yl)-2,5-diphenyltetrazolium bromide
ml	milliliter
MS	mass spectrometry

MVTR	moisture vapor transmission rate
NB	nutrient broth
NHDF	normal human dermal fibroblasts
nm	nanometer
NMR	nuclear magnetic resonance
PBS	phosphate buffered saline
pI	isoelectric point
ppm	part per million
PVA	poly(vinyl alcohol)
PVP	poly(N-vinyl pyrrolidone)
RNA	ribonucleic acid
ROS	reactive oxygen species
rpm	rounds per minute
SEM	scanning electron microscope
SFM	serum-free medium
S.D.	standard deviation
SPR	surface plasmon resonance
TEM	transmission electron microscopy
UV	ultraviolet
w/w	weight/weight
wt%	weight percent
WVTR	water vapor transmission rate

CHAPTER 1
INTRODUCTION

1.1 Background and Rationale

Wounds are serious problems in global healthcare. Wounds can be caused by damage of tissue, accident, or injury. The prevalence of wounds among inhabitants of the EU 27 was estimated at 3-4 per 1,000 people (1.5-2.0 million from 491 million people). Patients with wounds were 25-50% of the patients of acute hospital beds *(1)*. In the United States, the National Center for the Prevention and Control of Injuries reported the numbers of injuries from burns were approximately 450,000 cases that required medical cares, and the number of death around 3,400 cases per year *(2)*. Illnesses, such as diabetes, can also cause wounds. In 2010, about 18.8 million people of the United States have diagnosed as diabetes *(3)*. Approximately 25% of the diabetes patients would progress diabetic foot ulcers *(4)*. The treatment of foot ulcers was very costly (around 7,439–20,622 US Dollars per episode) *(5)*. The total cost payment of the cure of diabetic foot ulcers in 2001 was 9 billion US Dollars *(6)*. In 2013, Medicinal and pharmaceutical imported products in Thailand worth 67,009 million baht *(7)*. Information from a database of medical supplies in Songkhlanagarind Hospital from November 2007 to March 2008 showed that the hydrocolloid wound dressings, size 4"×4" and 8"×8", were purchased about 109 and 47 sheets respectively per month *(8)*. Majority of commercial antibacterial wound dressings in Thailand are import products.

A traditional wound dressing, such as gauzes and bandages, can only protect wound from harm and dirt. Gauzes also cause pain during changing or removing *(9)*. A modern wound dressing has been improved to be able to moisten the wound area which stimulates the wound healing *(10)*. Modern wound dressings are divided into several categories which are semi-permeable films, foams, alginates, hydrocolloids, hydrogels, and hydroactive *(10, 11)*. Each category has its own disadvantages. For example, alginate dressings could disturb healing of dry wounds *(10)*. The characteristics of an ideal wound

dressing are providing moisture to wound area, vaporous exchange, prevention of infection, absorption of excess exudate, and low adherence *(12)*. Hydrogel could provide almost all characteristics of an ideal wound dressing *(13)*.

Hydrogels are polymeric network structures which contain water or fluid within their structure. Hydrogel can be applied in food industry *(14)*, biomedical application, tissue engineering, and pharmaceutics *(15)*. Gamma radiation is one of the crosslinking methods to prepare crosslinked hydrogels. Moreover, gamma radiation dose of 25 kGy has been suggested for a sterilization of medical products *(16)*. Therefore, hydrogels could be prepared and sterilized in one single step by using gamma irradiation.

Gelatin is a biopolymer, which is used in many applications such as food industry, adhesive glue, and pharmaceutical manufactures *(17, 18)*. It is a protein obtained by hydrolysis of collagen. A simple gelatin gelation can occur by heating a gelatin solution at a temperature over 40°C and then cooled down *(17)*. However, the gelatin hydrogels formed by this method are unstable and easily deforms when applied at body temperature (37°C). The gelatin hydrogel should then be crosslinked before used as biomedical materials at the body temperature *(19)*. A weak point of gelatin hydrogel is its poor mechanical property *(20)*. Addition of a synthetic polymer can improve the mechanical property. The outcome material, which is a mixture of both synthetic and natural polymers, could show improved mechanical property and proper biocompatibility *(21)*. Poly(vinyl alcohol) (PVA) is a water-soluble synthetic polymer which is usually mixed with other natural polymers. PVA has good water retention and film forming properties. It is used in biomedical applications such as wound dressing, artificial skin, and cardiovascular device *(22, 23)*. Both gelatin and PVA solutions can be crosslinked by gamma radiation *(17, 24)*. Although hydrogel can provide moisture to wound area, but the wet environment is also suitable for the growth of bacteria *(25)*. As a result, a use of antibacterial or antiseptic agent is needed.

Silver and silver compounds are effective antibacterial agents. It was known long time ago that the silver ions (Ag^+) can destroy or inhibit the growth of many bacterial species *(26)*. Franciscus Sylvius, a Dutch physician, first used silver nitrate ($AgNO_3$) in the treatment of wounds since the 17th century. Treatment with the use of 0.5% $AgNO_3$ solution is the standard treatment for burn wounds *(27)*. In recent years, the use of silver in the form of nanoparticles has significantly increased. The tiny size of the particles and huge surface area assist the faster dissolution of Ag^+ than bulk silver. The silver nanoparticles (AgNPs) can demonstrate antibacterial effect itself. AgNPs which can kill bacteria effectively have approximately 1-10 nm in diameter *(28)*. There are several synthesis methods of AgNPs such as chemical reduction by using sodium borohydride, heat treatment, and ultraviolet or gamma irradiation *(29)*. Gamma irradiation can reduce Ag^+ by the hydrated electron and secondary radicals which formed by water radiolysis in solution with water as solvent *(30)*.

This research then aims to prepare gelatin/PVA hydrogel sheets containing AgNPs. The hydrogels were crosslinked by gamma irradiation. AgNPs, which were used as antibacterial agents, were synthesized by gamma irradiation. The antibacterial agents were expected to prevent growth of bacteria on the hydrogel. AgNPs also expected to have an effective antibacterial activity and the least toxicity to human fibroblast cells. The hydrogels were tested for the necessary properties of wound dressing. This hydrogel sheet is expected to be used as an antibacterial wound dressing, which could reduce the cost of imported medical products.

1.2 Research Objectives

1.2.1 To prepare and characterize gamma-ray irradiated gelatin/PVA hydrogels incorporating with AgNPs

1.2.2 To determine the cytotoxicity and antibacterial effects of AgNP/gelatin/PVA hydrogels using fibroblast cells and bacteria (*in vitro* testing)

1.3 Scope of the Research

Part I: Preparation and Characterization of Gelatin/PVA Hydrogel

1. Prepare gelatin hydrogels and gelatin/PVA hydrogels by gamma irradiation. The variables are the ratios of the PVA and gelatin solutions, and doses of gamma radiation.

2. Characterize the properties of gelatin/PVA hydrogels

    2.1 Water holding capacity and swelling ratio

    2.2 Water vapor transmission rate (WVTR)

    2.3 Tensile test

    2.4 *In vitro* biodegradation

    2.5 Gel fraction

Part II: Preparation and Characterization of Gelatin/PVA Hydrogel Containing AgNPs

1. Prepare AgNP/gelatin/PVA hydrogels by gamma irradiation. The variables is ratios of the $AgNO_3$ to solid weight of hydrogel.

2. Characterize the properties of AgNP/gelatin/PVA hydrogels

    2.1 Water holding capacity and swelling ratio

    2.2 Water vapor transmission rate

    2.3 Tensile test

    2.4 *In vitro* biodegradation

    2.5 Gel fraction

    2.6 Morphology

    2.7 Chemical property

3. Characterize the AgNPs formation

    3.1 Surface plasmon resonance (SPR) phenomenon

    3.2 Size distribution of AgNPs

    3.3 Elemental analysis

    3.4 Silver-release

Part III: Determination of the Cytotoxicity of AgNP/gelatin/PVA Hydrogels on Fibroblast Cells and Antibacterial Effects (*In vitro* Testing)

1. *In vitro* cytotoxicity test of AgNP/gelatin/PVA hydrogels on human fibroblasts.
2. Antibacterial effects of the AgNP/gelatin/PVA hydrogels

CHAPTER 2
RELEVANT THEORY AND LITERATURE REVIEW

2.1 Wound

A definition of wound in Dorland's Illustrated Medical Dictionary is "an injury or damage, usually restricted to those caused by physical means with disruption of normal continuity of structures" *(31)*. Wound is an injury to the body tissues caused by a cut, hit, extreme heat, extreme cold, chemical, radiation, electricity, or other factor, which can harm the tissue *(32)*. An assortment of wound can be classified in many ways which depend on the criteria and objectives of classification.

2.1.1 Types of Wound

2.1.1.1 Based on the Duration of Wound Repair

(1) Acute wound

Acute wounds are the immediate wounds. They take a short time to heal completely, approximately 8-12 weeks *(33)*. There are several causes of acute wound such as surgical incisions, burns, abrasion, and rupture.

(2) Chronic wound

Chronic wounds heal slowly, that take time more than 12 weeks *(34)*. Chronic wounds often take step at any stage of the phases of wound healing, such as the inflammatory process, for long time *(35, 36)*. Diabetes, poor blood circulation, repeated trauma, and malignancy can conduce to chronic wounds.

2.1.1.2 Based on the Types of Injuries *(32, 37)*

(1) Non-penetrating wounds: This kind of wound does not pass through tissues.

- Abrasions

Abrasions (grazes or scrapes) are scrapings of the superficial skin layer. The damage occurs on epidermis only.

- Lacerated wound

Lacerated wounds (lacerations) are the open wound that induced by impact of a blunt object. Wound edges may be ragged.

- Contused wound

Contused wounds (contusion or bruises) also caused by an attack of a blunt object, but the outer layer of tissue dose not open. These closed wounds have the bleedings inside the wounds which are ecchymosis or hematoma.

- Concussion

Concussions are the injury of the underlying tissue or organs of head such as brain and spinal cord.

(2) Penetrating wounds: The injuries break through the tissues and organs

- Incised wound

Incised wounds (penetration, incisions, or cut wound) are caused by sharp objects such as a knife, blade, or glass. Wound edges are often smooth.

- Gunshot wound

Gunshot wounds (ballistic trauma) are the result from firearm shooting.

(3) Miscellaneous wounds

- Thermal and electrical wound

Very hot or cold temperature and electricity can damage the tissue and organs, for example, burn, scald wound, sunburn, and frostbite.

- Chemical wound

Chemical wound (chemical burn) is the result of exposure to corrosive chemical, acid, and base.

- Bites and stings

Wound can be caused by other organisms, for example, bites from humans and animals, and stings from insects.

Moreover, internal factors such as poor blood circulation, diabetes can also cause wound. For example, foot ulcers are problems in people with diabetes, and bedsores threaten the disabled patients.

2.1.2 Stages of Wound Healing

Wound healing is a biological process for repair itself. Definition of wound healing process is "a complex dynamic process that results in the restoration of anatomic continuity and function" *(38)*. The process is divided into 3 to 5 phases depend on the way of connecting between stages. Each reference has different numbers of steps. For example, Schultz (1999) *(39)* divides the wound healing process into 5 steps, which are haemostasis, inflammation, migration, proliferation and maturation phases. Robert F. Diegelmann and Melissa C. Evans (2004) divide the wound healing into 4 phases which are hemostasis, inflammation, proliferation and remodelling *(40)*. For this chapter, the three stages of wound healing process described by Gurtner, G. C., et. al. (2008) *(41)*, which is presented in Figure 2.1, are used.

2.1.2.1 Inflammation

After tissue injury, tearing of blood vessels and tissues are occurred. Bleeding flush the antigens and bacteria from the wound, and stimulate hemostasis. Vascular responses within a few seconds. Vasoconstriction helps to stop bleeding and decrease bacterial contamination. Hemostasis is the body reaction to prevent bleeding and loss of fluid. Platelets gather at the wound site to build a blood clot. The follow step is formation of fibrin matrix. Thrombin catalyzes the conversion of soluble fibrinogen into

insoluble fibrin which performs as the scaffold for immigrating cells move to the wound area.

While hemostasis is processed, the inflammation is occurred almost the same time. Inflammation is a response of the body against pathogens, trauma, or other factors that harm tissues. The inflammation can stay up to 3 days after tissue injury. The first type of white blood cell that comes out to ingest foreign agents is neutrophil. After a few days, usually 2-3 days, the next white blood cell that appears in the injury site is monocyte. Monocytes circulate in the blood circulation and then migrate into tissues. When monocyte moves into tissues, it differentiates into macrophage which recognizes and destroys antigen or damaged tissues. Macrophage is an important cell in correlation of inflammation and tissue repair *(42)*. There is other type of white blood cell in wound area, lymphocyte, which serves as phagocytes. Lymphocyte also destroys antigen.

2.1.2.2 New Tissue Formation

The second stage is new tissue formation. This stage includes migration and proliferation of cells. The migration process starts with the moving of keratinocytes to the injured dermis. Epithelial cells and fibroblasts also move to ruined area. The proliferative phase occurs nearly the same time as the migration phase about after the third day. The capillaries and lymphatic vessels grow into the wound. The vital growth factors that regulated the angiogenesis in this stage are vascular endothelial growth factor A and fibroblast growth factor 2 *(43)*. Fibroblasts and myofibroblasts create collagen which represented as extracellular matrix. Finally, this collagen can become a mature scar *(44)*.

2.1.2.3 Remodelling

The last stage is remodelling or maturation phase. The processes that occurred in the earlier stages are fewer and stop finally. The majority of cells in wound healing process, which are endothelial cells, macrophages, and myofibroblasts, enter into apoptosis or migrate from the wound area. Epithelial–mesenchymal interactions may

control skin integrity and homeostasis *(45)*. Within months or maybe two years, an acellular matrix is formed by changing of cellular granular tissue. Although many processes are happened, but the injured tissue can not recover the feature of uninjured skin *(46)*.

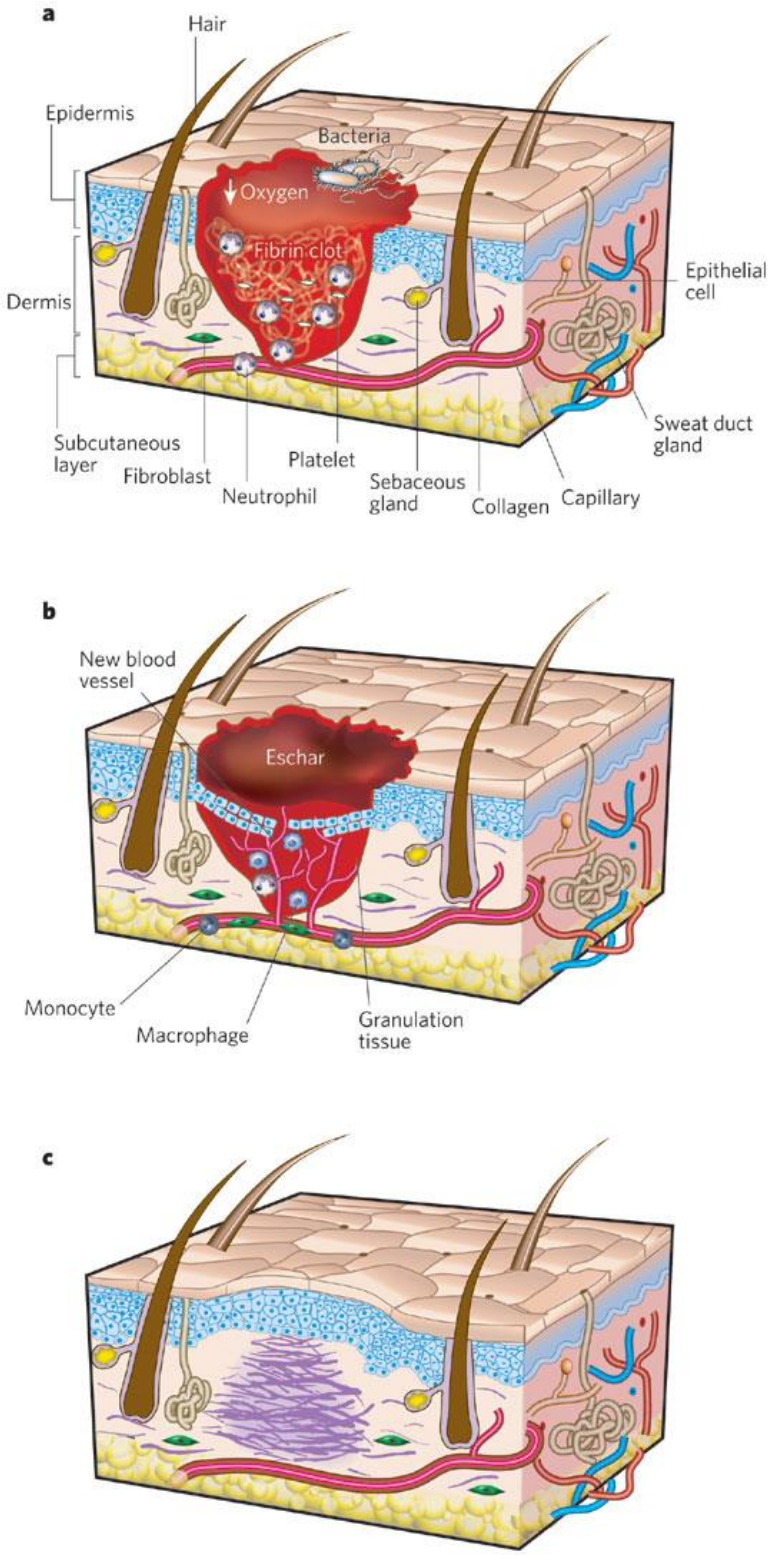

Figure 2.1 Three stages of wound healing: (a) inflammation, (b) new tissue formation, and (c) remodelling

Source: Gurtner, G. C., et. al. (2008) *(41)*

2.1.3 Factors Influencing Wound Healing

Many factors can affect wound healing process. The wound healing process can be interrupted or impaired by local factors (such as oxygenation) and systemic factors (such as nutrition or health condition) *(47)*. The factors influencing wound healing are listed as follow.

2.1.3.1 Oxygenation

Oxygen has an important role in cellular metabolism and all phases of wound healing. In inflammatory phase, oxygen helps to prevent infection. Oxygen increases cell production in proliferation phase. Collagen synthesis, collagen cross-linking, and maturation phase also needed oxygen *(48)*. After the tissue injury, the vascular breaks and the cellular activity requires high oxygen consumption. These events lead to depletion of oxygen in the microenvironment of wound *(49)*. Hypoxia plays a role to motivate the beginning step of wound healing process and induces cytokine, which are platelet-derived growth factor, transforming growth factor-β, vascular endothelial growth factor, tumor necrosis factor-α, and endothelin-1. These cytokine are significant in wound healing process. Hyperoxia also affects wound healing. Hypoxia and hyperoxia enhance reactive oxygen species (ROS) production *(50)*. However, a large quantity of ROS can lead oxidative damage *(51)*.

2.1.3.2 Infection

When a wound occurs, microorganism can enter the tissue in wound area. Microorganisms, especially bacteria, cause wound damage depend on three factors, which are immunity of patient, number and type of bacteria. An existence of bacteria is divided into contamination, colonization, and infection. The presence of bacteria that do not replicate or harm is called contamination. When the number of bacteria increases, but the injury does not occur. This event is called colonization. Bacterial infection, which is local, spreading, and systemic infection, can cause tissue damage *(52)*.

Wound infection could be identified by inflammation. Bacterial infection may delay inflammation process. Level of pro-inflammatory cytokines (interleukin-1 and tumor necrosis factor-α) can be increased by bacteria and endotoxins. This consequence may prolong the inflammatory phase and lead wound into chronic state and unsuccessful healing. Bacteria that generally isolated from clinically non-infected and infected wounds are *Staphylococcus aureus*, *Pseudomonas aeruginosa*, and β-haemolytic streptococci *(53)*.

2.1.3.3 Desiccation

In 1962, George D. Winter discovered that a dry scab can delay the epithelization of superficial wounds in porcine, but the epithelization process is quick in a moist surrounding *(54)*. Winter's study introduced a moist wound healing concept. Human wound fluid enhances fibroblast proliferation *(55)*. A moisture-retentive wound dressing decreases desiccation or dehydration and cell death, increases migration of epidermal and angiogenesis *(12)*. Autolytic debridement in wounds could be promoted by moist wound environment *(56)*. Moreover, wound healing under the environment of moisture is less painful than a dry wound.

2.1.3.4 Nutrition

Nutrition is an essential factor in wound healing process. Carbohydrates and fat are an energy reserve for wound healing. Glucose, which is a monosaccharide, is the important energy source for cellular adenosine triphosphate (ATP) synthesis. Angiogenesis and tissue deposition need energy from ATP *(57)*. A lack of protein influences synthesis of collagen, wound remodelling, and immune system. Leukocyte phagocytosis also declines. This event leads to more risk of infection *(58)*.

Vitamins and trace elements, which are micronutrients, also have an important role in wound healing process. The deficiencies of vitamins and trace elements have a number of effects on wound healing, such as decrease in immune response, and increase in infection susceptibility. The reduction of collagen synthesis, fibroblast

proliferation, angiogenesis, and capillary strength could be the result of the lack of vitamins C *(59, 60)*. Vitamin A has a role in anti-oxidant activity, cellular differentiation, fibroblast proliferation, and collagen and hyaluronate synthesis *(61)*. Advantages of vitamin E on wound healing are anti-oxidant property, anti-inflammatory properties, and reducing excess scar formation *(59, 61)*. A task of trace elements is being a co-factor for wound repairing. Synthesis of protein and collagen requires magnesium. Cytochrome oxidase and cytosolic anti-oxidant superoxide dismutase are emzymes that need copper for being a co-factor. Ribonucleic acid (RNA) and deoxyribonucleic acid (DNA) polymerase require zinc. Hydroxylation of proline and lysine is a process that requires iron *(57, 59, 60)*.

2.1.3.5 Health Conditions

Health and physical conditions influence wound healing process. An elderly age correlates with delayed wound healing. The inflammatory response changes in elderly people. T-cell migrates to wound area slowly and chemokine production changes. Macrophage phagocytic capacity also decrease *(62)*. Platelet aggregation and inflammatory mediator secretion increase. Processes and activities in proliferation and inflammation delay. Wound strength and collagen remodelling also decrease *(63)*. Many diseases can cause chronic wound, such as diabetes. The impact of diabetes is shown in Figure 2.2. Moreover, medications, especially glucocorticoid steroids, non-steroidal anti-inflammatory drugs, and chemotherapeutic drugs, affect wound healing process *(47)*.

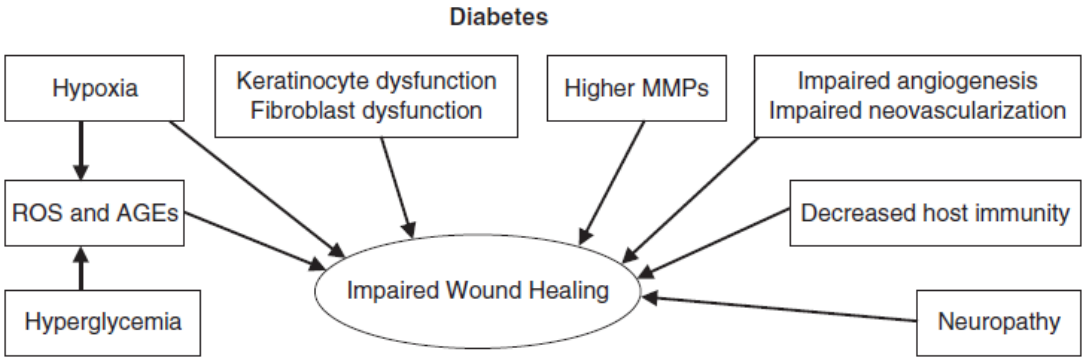

Figure 2.2 The potential effects of diabetes on wound healing.

MMPs, matrix metalloproteases; ROS, reactive oxygen species; AGEs, advanced glycation end-products.

Source: Guo & DiPietro (2010). *(47)*

2.2 Wound Dressing

2.2.1 Types and Properties of Wound Dressing

At present, wound dressings have developed greatly. The former wound dressing, which is a passive product, does not directly promote wound healing. It only covers wound area to prevent the wound from external environment, such as gauze dressings *(64)*. Nowadays, the concept of modern wound dressing has changed to be an active product that provides an optimal environment for wound healing *(54)*, especially moist wound environment and antibacterial activity.

Properties of ideal wound dressing are listed below *(12)*.

1) Provide a moist environment to the wound area

2) Absorb excess blood and exudates from wound

3) Allow gas and vapor exchange

4) Prevent wounds from bacterial infection

5) Be non-adherent to the wound surface and able to remove without trauma

The Food and Drug Administration of the United States of America (FDA) has classified the types of wound dressing into 5 categories *(65)*.

1) Non-resorbable gauze/sponge dressing for external use
2) Hydrophilic wound dressing
3) Occlusive wound dressing
4) Hydrogel wound and burn dressing
5) Interactive wound and burn dressing

According to its utilization, wound dressing can be classified into two classifications.

1) First-line interactive/bioactive dressings: interact with the wound surface and adjust the environment to optimize healing. The summary of first-line interactive/bioactive dressings is listed in Table 2.1.

2) Second-line dressings: promote and assist the healing process of first-line dressing. The summary of second-line dressings is listed in Table 2.2.

Table 2.1 First-line interactive/bioactive dressings

Dressing	Brand names	Indications
Semi-permeable films	Aqua protect film, Bioclusive, Cutifilm, Hydrofilm, Opsite (Flexigrid, Flexifix, Post-Op), Polyskin, Tegaderm	Non-absorbent; superficial burns, grazes, closed surgical incisions, small skin tears and IV sites; secondary dressing
Foams	Allevyn (adherent, non-adherent, wound cavity dressing), Cavi-care, Curafoam, Hydrosorb, Lyofoam (flat, extra, C, T, A), PermaFoam, Tegafoam, Truefoam	Moderate to heavily exudating, superficial and cavity wound, venous ulcers (with compression), pretibial lacerations, infected ulcers, skin tears, pressure ulcers, skin grafts or donor site, pilonidal sinuses.
Alginates	Algisite M, Algoderm, Comfeel SeaSorb, Curasorb, Kaltostat, Melgisorb, Sorbsan	Need exudate to function. Heavily exudating leg ulcers, pressure ulcers and dehisced abdominal wounds.
Hydrocolloids	Comfeel (ulcer dressing, transparent, contour dressing), CombiDERM, DuoDERM (extra thin, CGF, paste), Hydrocoll, RepliCare, Tegasorb	Light to moderately exudating wounds that would benefit from autolytic debridement. Leg ulcers, pressure ulcers, burns and donor sites. Thin sheets are useful over suture lines and IV sites.

Table 2.1 First-line interactive/bioactive dressings (continued)

Dressing	Brand names	Indications
Hydrogels	Aquaclear, Purilon Gel (amorphous), Curafil (amorphous), Curagel (sheet), DuoDERM Gel (amorphous unpreserved), Hypergel (hypertonic saline, amorphous), Intrasite Conformable (gauze impregnated), Intrasite Gel (amorphous unpreserved), Nu-gel, Second skin, SoloSite Gel (amorphous preserved), Solugel (amorphous preserved and unpreserved), Sterigel (amorphous)	Absorbency is limited; best for minimally exudating or dehydrated wounds such as minor burns, grazes, lacerations, donor sites and pressure ulcers. Indications for the thicker viscosity products include protection of exposed tendon and/or bone from dehydrating and rehydrating eschar prior to debridement. The thinner viscosity products are useful for soothing burns and acute lesions such as chicken pox.
Hydroactive	Allevyn Thin, Biatain, Cutinova Hydro, PloyMem, Tielle	Waterproof, expandable, non-residual and semi-permeable. Highly exudating surface and cavity wounds including leg ulcers, pressure wounds and minor burns. Useful over joints as they expand/contract without causing constriction. Not indicated for dry or lightly exudating wounds.

Source: C. Weller and G. Sussman (2006) *(11)*

Table 2.2 Second-line advanced interactive/bioactive dressings

Dressing	Brand names	Indication
Cadexomer iodine	Iodosorb (sheet, powder, paste)	Venous leg ulcers, foot ulcers, and diabetic foot ulcers. Contraindicated in patients sensitive to iodine products or with any thyroid pathology.
Capillary wicking	Vacutex	Heavily exudating and infected wounds. Contraindicated in low exudating wounds within close proximity to blood vessels.
Honey	Medihoney, B-Naturals, L-Mesitran. Medihoney is a blend that includes honey from the Leptospermum species of plants. Medihoney and Medihoney Wound Gels do not contain preservatives. BNatural's medicated honey is obtained from the Eucalyptus marginata and Santalum spicatum species of plants and does not contain preservatives. L-Mesitran contains 48% honey, aloe, calendula, zinc oxide, medilan and vitamins A, C and E.	May be useful in management of sloughy and septic wounds.
Hydrofibre	Aquacel, Aquacel Ag	Heavily exudating wounds such as dehisced abdominal or pelvic wounds, chronic leg ulcers and infected wounds. Dressing frequency may be reduced depending on level of exudate.
Hypertonic saline	Curasalt, Hypergel, Mesalt	Moist, necrotic, exudating infected wounds. May be effective in decreasing hypergranulation tissue.

Table 2.2 Second-line advanced interactive/bioactive dressings (continued)

Dressing	Brand names	Indication
Interactive wet	TenderWet	Infected, sloughy and diabetic wounds
Silicone	Mepitel (non-adherent), Mepilex (non-adherent, thin, absorbent, border, transfer), Mepitac (fixation tape) Silicone gel sheets: Cica-Care, Mepiform, Spenco	Painful wounds, skin tears, difficult wound. Mepitel can be reused, and is usually used under another dressing to reduce pain on dressing changes. They soften and flatten scar tissue and can be washed and reused. Large sizes are also useful under secondary dressings for cancer wounds.
Silver	Acticoat, Acticoat Absorbent (calcium alginate), Actisorb 220 (charcoal impregnated), Aquacel Ag (hydrofibre), Atrauman Ag (wound contact tulle), Avance, Contreet (hydroactive), Contreet-H (hydrocolloid), PolyMem Silver	Wounds with high microbial burden and moderate to high exudate. Useful in partial and full thickness wounds (burns, donor sites) and for complementary use in infected or contaminated partial thickness wounds.
Zinc paste	Flexidress, Gelopast, Steripaste, Tenderwrap, Viscopaste, Zincaband, Zipzoc	Chronic venous leg ulcers, particularly where venous eczema is present and when used in conjunction with appropriate compression bandaging.

Source: C. Weller and G. Sussman (2006) *(11)*

2.2.2 Hydrogel Wound Dressings

Hydrogel wound dressings have several properties of an ideal dressing *(13)*. They keep moist wound environment, absorb excess exudates, have low adherence, and allow water vapor and air exchange. Although there is a large amount of water in hydrogel structure, hydrogel can absorb further fluid. The additional absorption is caused by hydrophilic residues of hydrogel *(66)*.

Hydrogel dressings are divided into three types according to their forms *(67)*.

1) Amorphous hydrogels, which have unstable shape, are used to apply in a deep wound. A secondary wound dressing must be required to keep amorphous hydrogel in wound area. Packagings of amorphous hydrogels are tubes, spray bottles, and foil packets *(68)*.

Examples of commercial amorphous hydrogels include: *(69)*

- Anasept® Antimicrobial Skin & Wound Gel (Anacapa Technologies, Inc.)
- AquaSite® Amorphous Hydrogel Dressing (Derma Sciences, Inc.)
- Dermagran® Amorphous Hydrogel Dressing (Derma Sciences, Inc.)
- INTRASITE* Gel Hydrogel Wound Dressing (Smith & Nephew, Inc.)

2) Impregnated hydrogels or hydrogel-impregnated gauzes are used in necrosis wounds, tunneling wounds, and undermining wounds.

Examples of commercial impregnated hydrogels include: *(70)*

- AquaSite® Hydrogel Impregnated Gauze (Derma Sciences, Inc.)
- DermaGauze™ (DermaRite Industries, LLC)
- Gentell Hydrogel Impregnated Gauze (Gentell Wound and Skin Care)
- Kendall™ Hydrogel Impregnated Gauze (Covidien)

3) Sheet hydrogels, which can absorb liquid and retain the integrity of sheet *(71)*, are suitable for shallow or flat wounds.

Examples of commercial sheet hydrogels include: *(72)*

- AquaClear® (HARTMANN USA, Inc.)

- AquaDerm™ (DermaRite Industries, LLC)

- CoolMagic™ Gel Sheet (MPM Medical, Inc.)

- Derma-Gel® Hydrogel Sheet (Medline Industries, Inc.)

Hydrogel wound dressings are used in many types of wounds such as pressure ulcers, leg ulcers, surgical wounds, skin tears, burns. Hydrogels are also suitable for debridement of necrotic tissue *(73)* and healing diabetic foot ulcers *(74)*.

2.2.3 Silver Wound Dressings

Wound dressings containing silver are mainly used for management of infection wound. Examples of commercial silver wound dressings as follow:

1. Acticoat (Smith & Nephew) *(75, 76)*

Acticoat is a dressing coating with nanocrystalline silver used for partial and full-thickness wounds. Many types of wounds, such as burns, recipient graft sites, and ulcers, could be managed by Acticoat. This dressing has bactericidal effect and infection control. Components of Acticoat dressing are absorbent inner layer, silver coated layer (Silcryst technology), and low adherent polyethylene net. Types of Acticoat dressings are as follows.

- Acticoat and Acticoat7

Acticoat and Acticoat7 are high density dressing, which need water moistnees before used. The difference between Acticoat and Acticoat7 is duration of wound covering, three days for Acticoat and seven days for Acticoat7.

- Acticoat Absorbent

Acticoat Absorbent is a calcium alginate dressing with silver. Its function is absorbing exudates from wound area.

- Acticoat flex3 and Acticoat flex7

Acticoat flex3 (cover duration: three days) and Acticoat flex7 (cover duration: seven days) are dressings, which consist of polyester layer and Silcryst silver, for wounds with low to moderate exudate amount.

- Acticoat site

Acticoat site is a disc dressing consisting of silver contact layer, polyurethane foam layer, and waterproof polyurethane film layer. This disc with central opening could cover around vascular and non-vascular percutaneous device sites.

2. Allevyn Ag (Smith & Nephew) *(76)*

Allevyn Ag is an antimicrobial foam dressing. Its antimicrobial agent is silver sulfadiazine (SSD). Allevyn Ag keeps moist environment for wound area and absorbs excess exudates. This dressing could cover light to moderately exuding wounds. Allevyn Ag has different sizes and patterns, which are Allevyn Ag Heel, Allevyn Ag Sacrum, and Allevyn Ag Gentle Border.

3. Aquacel Ag (ConvaTec) *(77)*

Aquacel Ag is a dressing with Hydrofiber technology and 1.2% (w/w) silver. Aquacel Ag could absorb and remove exudates from wound area. The dressing has a wide range of antimicrobial activity and sustained silver release up to 14 days. There are three types of Aquacel Ag. First type is Aquacel Ag dressing, which is a sheet for infection, acute, chronic, and burn wounds. Second type is Aquacel Ag ribbon dressing, which is a ribbon that suitable for deep or cavity wounds. The last type is Aquacel Ag surgical cover dressing, which is a silver-saturated sheet with hydrocolloid adhesive layer and polyurethane film. This type is used for surgical incisions.

4. Urgotul SSD (Laboratoires Urgo) *(78)*

Urgotul SSD is a silver sulphadiazine-impregnated dressing for acute, chronic, and second-degree burn wounds. Components of Urgotul SSD are polyester mesh that composed of carboxymethylcellulose, Vaseline and 3.75% silver sulphadiazine. This

dressing prevents secondary infection, be easy removal, and give conformability to wound.

5. Atrauman Ag (Hartmann) *(79)*

Atrauman Ag is a non-adherent silver-containing dressing, which composed of neutral triglycerides, and polyamide textile with 1 mm-pores. This dressing has effective antimicrobial activity and low cytotoxicity.

6. Silvercel non-adherent (Systagenix) *(80)*

Silvercel non-adherent is an absorbent dressing with silver-coated fibers (X-STATIC) and outer porous film layer. There are two types of Silvercel non-adherent. First type is a flat dressing for superficial or exposed wounds. Second type is a rope dressing for deep or cavity wounds. Functions of Silvercel non-adherent are wound exudates absorption and wound infection control.

2.2.2.2 Price of Silver Wound Dressings

Price of wound dressing is an important part of the cost for medical treatment of wounds. Silver wound dressing product have quite high cost. Some products may not available in Thailand.

Table 2.3 Price list of primary wound management products

Source: Adlington, L., 2012 *(81)* (First-line choices products are bold letters, where suitable.)

Dressing	Product	Size	Cost per dressing
Alginates / Hydrofibres	**ActivHeal Aquafiber**	**5 × 5 cm^2**	**£0.76**
		10 × 10 cm^2	**£1.80**
		15 × 15 cm^2	**£3.40**
	Aquacel	5 × 5 cm^2	£0.98
		10 × 10 cm^2	£2.38
		15 × 15 cm^2	£4.38
		1 × 45 cm^2 (ribbon)	£1.76
	Suprasorb A	**5 × 5 cm^2**	**£0.59**
		10 × 10 cm^2	**£1.16**
	Sorbsan Plus SA	11.5 × 14 cm^2	£2.97
		14 × 24 cm^2	£5.23
Antimicrobial	**Inadine** (contains Iodine)	**5 × 5 cm^2**	**£0.32**
		9.5 × 9.5 cm^2	**£0.48**
	Iodoflex (contains Iodine)	5 g	£3.88
	Flamazine cream	50 g	£3.85
Honey	Medihoney Antibacterial medical honey	20 g	£3.96
	Medihoney Antibacterial Wound Gel	20 g	£4.02
	Medihoney Gel Sheet	5 × 5 cm^2	£1.75
		10 × 10 cm^2	£4.20
	Medihoney Tulle	10 × 10 cm^2	£2.98
Silver dressings – wound contact layer	**Atraumann Ag**	**5 × 5 cm^2**	**£0.49**
		10 × 10 cm^2	**£1.19**
		10 × 20 cm^2	**£2.32**
	Acticoat Flex 3	5 × 5 cm^2	£3.38
		10 × 10 cm^2	£8.24
		10 × 20 cm^2	£12.89

Table 2.3 Price list of primary wound management products. (continued)

Dressing	Product	Size	Cost per dressing
Silver - absorbent	Silvercel	5 × 5 cm^2	£1.68
		11 × 11 cm^2	£4.14
		10 × 20 cm^2	£7.68
Odour absorbant dressings	Clinisorb	10 × 10 cm^2	£1.81
		10 × 20 cm^2	£2.41
		15 × 25 cm^2	£3.88
Hydrogels / Hydrogel sheets	Activheal	15 g	£1.41
	Hydrosorb	5 × 7.5 cm^2	£1.49
		10 × 10 cm^2	£2.12
	Intrasite Conformable	10 × 10 cm^2	£1.73
		10 × 20 cm^2	£2.34
Fabric island adherent dressing	Primapore	6 × 8.3 cm^2	£0.17
		8 × 10 cm^2	£0.18
		8 × 15 cm^2	£0.32
		10 × 20 cm^2	£0.42
		10 × 35 cm^2	£0.92
Films	Hydrofilm	6 × 7 cm^2	£0.21
		10 × 12.5 cm^2	£0.41
		12 × 25 cm^2	£0.81
		15 × 20 cm^2	£0.92
Non-adherent dressings	Atrauman	5 × 5 cm^2	£0.25
		7.5 × 10 cm^2	£0.26
		10 × 20 cm^2	£0.59
		20 × 30 cm^2	£1.63
	Urgotul	5 × 5 cm^2	£1.50
		10 × 10 cm^2	£3.00
		15 × 20 cm^2	£8.49
Low adherent dressings	Telfa	7.5 × 5 cm^2	£0.12
		10 × 7.5 cm^2	£0.15
		15 × 7.5 cm^2	£0.17
		20 × 7.5 cm^2	£0.29

Table 2.4 Price list of dressings which are available in Thailand

Source: SROmedical Co., Ltd. (2014) *(82)* (June 2014)

Dressing	Product	Size	Cost per dressing
Hydrocolloid	Tegaderm	4" × 4"	151.6 baht (5 pieces 758 baht)
Dressing with silver	Tegaderm Ag mesh	4" × 5"	280 baht
Hydrocolloid	Tegaderm sacral hydrocolloid	6 3/4" × 6 3/8"	280 baht
Hydrofiber	Aquacel	4" × 4"	239.5 baht (10 pieces 2,395 baht)
Hydrofiber with silver	Aquacel Ag	4" × 4"	320 baht (10 pieces 3,200 baht)
Calcium alginate	Sorbsan flat	5 × 5 cm^2	79.5 baht (10 pieces 795 baht)
		10 × 10 cm^2	170 baht (10 pieces 1,750 baht)
Semi-permeable	Askina thinsite	10 × 10 cm^2	250 baht (10 pieces 2,500 baht)
Mesh/hydrocolloid with petroleum jelly and silver sulphadiazine	UrgoTul SSD	10 × 12 cm^2	175 baht (10 pieces 1,700 baht)
Mesh/hydrocolloid with petroleum jelly	UrgoTul	10 × 10 cm^2	43.5 baht (10 pieces 435 baht)
Mesh/hydrocolloid with petroleum jelly and absorbent pad	Urgotul duo	10 × 12 cm^2	87 baht (10 pieces 870 baht)
Multilayered hydrocellular dressing	Askina transorbent	10 × 10 cm^2	168.5 baht (10 pieces 1685 baht)
Polyurethane foam	Allevyn thin	4" × 4"	175 baht
Hydrocolloids	Duoderm CGF	4" × 4"	125 baht (5 pieces 625 baht)
		6" × 6"	230 baht (5 pieces 1,150 baht)

2.3 Biomaterials

2.3.1 Gelatin

Gelatin is a natural protein which is obtained by partial hydrolysis of collagen, a major protein in animal (such as bovine, porcine, and fish) skins, bones, ligaments and tendons. The appearances of gelatin are translucent, brittle in dry condition, flavorless and odorless. Preparative process for acidic and basic gelatins from collagen is presented in Figure 2.3. A largest number of amino acid in gelatin is glycine (approximately 30%), proline and 4-hydroxyproline residues. Amino acid composition of gelatins is listed in Table 2.5.

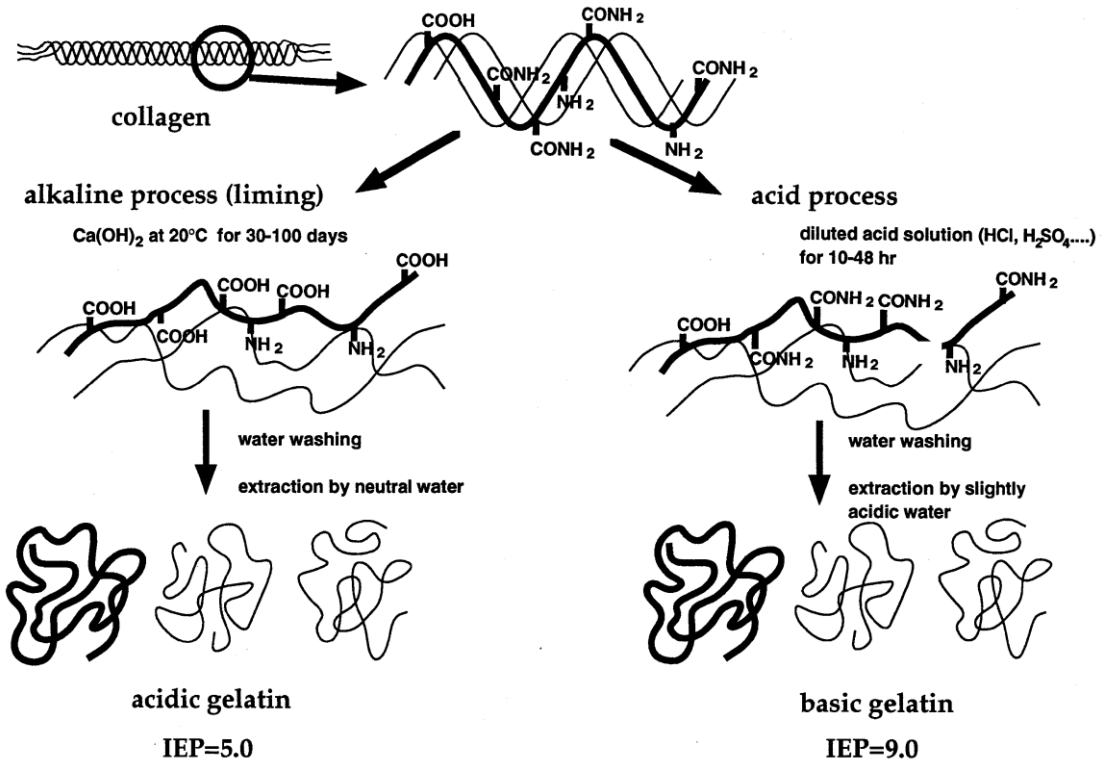

Figure 2.3 Preparative process for acidic and basic gelatins from collagen.

Source: Tabata, Y, and Ikada, Y. (1998) *(19)*

Table 2.5 Amino acid composition of gelatins

Amino acids	Type A (Pork skin)	Type B (Calf skin)	Type B (Bone)
Alanine	8.6-10.7	9.3-11.0	10.1-14.2
Arginine	8.3-9.1	8.55-8.8	5.0-9.0
Aspartic acid	6.2-6.7	6.6-6.9	4.6-6.7
Cystine	0.1	Trace	Trace
Glutamic acid	11.3-11.7	11.1-11.4	8.5-11.6
Glycine	26.4-30.5	26.9-27.5	24.5-28.8
Histidine	0.9-1.0	0.74-0.8	0.4-0.7
Hydroxylysine	1.0	0.91-1.2	0.7-0.9
Hydroxyproline	13.5	14.0-14.5	11.9-13.4
Isoleucine	1.4	1.7-1.8	1.3-1.5
Leucine	3.1-3.3	3.1-3.4	2.8-3.5
Lysine	4.1-5.2	4.5-4.6	2.1-4.4
Methionine	0.8-0.9	0.8-0.9	0.0-0.6
Phenylalanine	2.1-2.6	2.2-2.5	1.3-2.5
Proline	16.2-18.0	14.8-16.4	13.5-15.5
Serine	2.9-4.1	3.2-4.2	3.4-3.8
Threonine	2.2	2.2	2.0-2.4
Tyrosine	0.4-0.9	0.2-1.0	0.0-0.2
Valine	2.5-2.8	2.6-3.4	2.4-3.0

Source: Gelatin handbook, GMIA, 2012 *(83)*

There are two different types of gelatin, depending on the method of preparation process. Typical specifications for gelatin type A and B are listed in Table 2.6.

1) Basic gelatin (Type A gelatin) is produced from acid process. This process is typically used for porcine (pork) skin. The isoelectric point (pI) of type A gelatin is between 7 and 9. Because type A gelatin is usually made from pork skin, it is haram or forbidden by Islamic law *(84)*.

2) Acidic gelatin (Type B gelatin) is produced from alkaline process. Type B gelatin is made from cattle (cow) or calf skin. The pI of type B gelatin is between 4.7 and 5.4.

Table 2.6 Typical specifications for gelatin

Properties	Type A	Type B
pH	3.8-5.5	5-7.5
Isoelectric point	7-9	4.7-5.4
Gel strength (Bloom)	50-300	50-300
Viscosity (mps)	15-75	20-75
Ash	0.3-2	0.5-2

Source: Gelatin handbook, GMIA, 2012 *(83)*

Gelatin is one of biopolymers commonly used in biomedical engineering. It is an easily soluble substance. The unique property of gelatin in aqueous solution is a thermal reversible transition. It forms a gel when cooling down below the gel point of gelatin and recovers to viscous solutions when temperature increased. The gel point of gelatin from homeothermic animals is approximately between 30-35°C *(85)*. Simple gelatin hydrogel can be made by increasing temperature to above 40ºC and cooling down to room temperature. The hydrogel forming in this way is unstable and easily deformed when

applied to body temperature (37ºC). Therefore, gelatin hydrogel in medical application must be crosslinked to be maintained at the body temperature.

2.3.2 Poly(vinyl alcohol)

Poly(vinyl alcohol) (PVA) is a water-soluble synthetic polymer. It is colorless and odorless. PVA was first created in 1924 by Hermann and Haehnel by hydrolyzing polyvinyl acetate in ethanol with potassium hydroxide *(86)*. PVA is not prepared from a monomer in direct polymerization. Figure 2.4 present synthesis of PVA via alcoholysis of poly(vinyl acetate). Structure of PVA is presented in Figure 2.5.

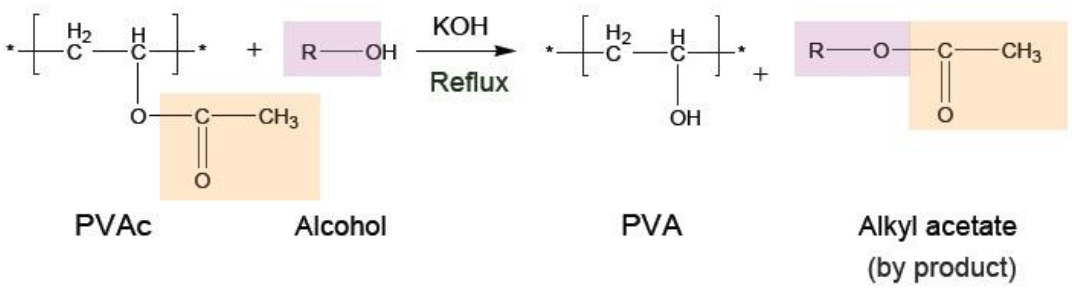

Figure 2.4 Synthesis of PVA via alcoholysis of poly(vinyl acetate)

Source: Prissanaroon-Ouajai, W. *(87)*

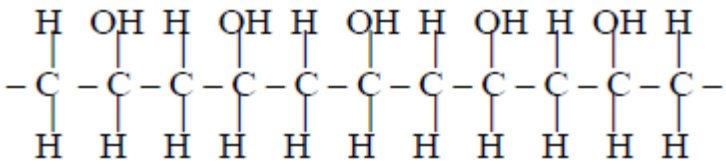

Figure 2.5 Structure of PVA

Source: Katz, D. A. *(88)*

PVA is the most important commercial water soluble plastic. Its advantages are biodegradability and biocompatibility. PVA can dissolve in ethanol slightly, but it is insoluble in other organic solvents. Outstanding properties of PVA are film forming,

emulsifying and adhesive properties. PVA has been developed for food industries, pharmaceutical and biomedical applications.

2.4 Gamma Irradiation

Radiation is an energy that emits from an original source and goes through space or medium *(89)*. Radiation can be divided into two categories. The first category is non-ionizing radiation such as visible light, infrared, and microwave. Another category is ionizing radiation, for example, x-ray, gamma radiation, alpha radiation, and beta radiation. Ionizing radiation can be used for many applications. (Table 2.7)

Table 2.7 Some typical radiation processing applications

Source: IAEA *(90)*

Product	Intended effect	Typical dose range (kGy)
Blood	Preventing TA-GVHD	0.020–0.040
Potatoes, onions, garlic	Inhibiting sprouting	0.05–0.15
Insects	Reproductive sterilization for pest management	0.1–0.5
Strawberries and some other fruits	Extending shelf life by delaying mould growth and retarding decay	1–4
Meat, poultry, fish	Delaying spoilage, killing certain pathogenic bacteria (e.g. salmonella)	1–7
Spices and other seasonings	Killing a variety of microorganisms and insects	1–30
Health care products	Sterilization	15–30
Polymers	Crosslinking Grafting	1-250 0.2-30

Gamma radiation, also recognized as gamma ray, was discovered by French scientist Paul Villard in 1900 and named by Ernest Rutherford in 1903. Gamma radiation is ionizing radiation that emitted from nucleus of radioactive atom. The wavelength of gamma radiation is less than 0.01 nm, which are the shortest wavelength in the electromagnetic spectrum. Because of its shortest wavelength, gamma radiation has the highest frequency that is approximately 10^{19} Hz. Moreover, gamma radiation is the highest energy among all different kinds of electromagnetic radiation.

The appropriate gamma radiation sources are cobalt-60 (^{60}Co) and caesium-137 (^{137}Cs). Both elements have high energy of gamma rays. Cobalt-60 has 5.27 years of half-life, while caesium-137 has 30.1 years of half-life. However, industries usually use cobalt-60 as the source of gamma radiation *(90)*. The radionuclide cobalt-60 can be created in a nuclear power reactor by irradiation of cobalt-59 with neutrons as displayed in Equation 1 *(91)*.

$$^{59}_{27}\mathrm{Co} + {}^{1}_{0}\mathrm{n} \rightarrow {}^{60}_{27}\mathrm{Co} \qquad (1)$$

Cobalt-60 atom is unstable because of the excess neutron. This unstable cobalt-60 will decay to a stable nickel-60 by emitting of photons of 1.17 and 1.33 MeV as demonstrated in Figure 2.6.

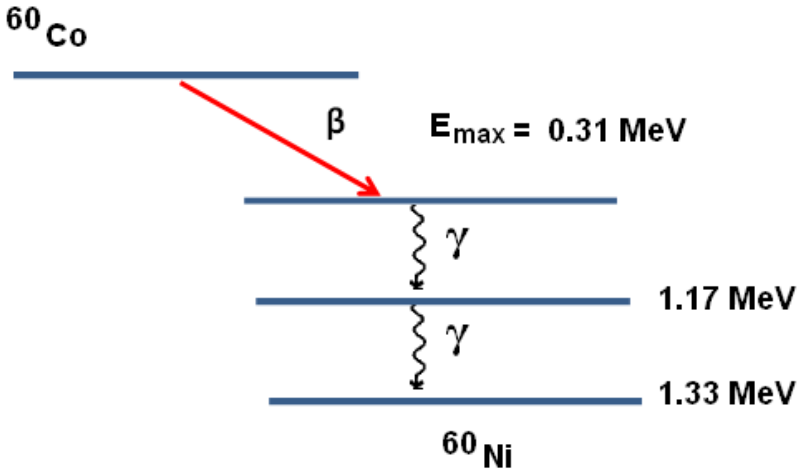

Figure 2.6 Disintegration of cobalt-60

Source: Kaplan, I. (1955) *(92)*

Radiation effects, which are chemical changes, on irradiated materials might be divided into two types which are direct and indirect effects *(93)*. The direct effect is the decomposition of chemical bonds which caused by radiation energy. Molecules might be activated to excited state or ionization. Another type is an indirect effect which is important to the total radiation action. Indirect effect occurs by the continuous reactions of radiolytic products which are hydroxyl radicals (OH·), e^-_{aq}, hydrogen radicals (H·), hydrogen peroxide (H_2O_2), and hydroperoxyl radicals (HO_2^o). Figure 2.7 (a) and 2.7 (b) show water radiolysis and free radical integration, respectively.

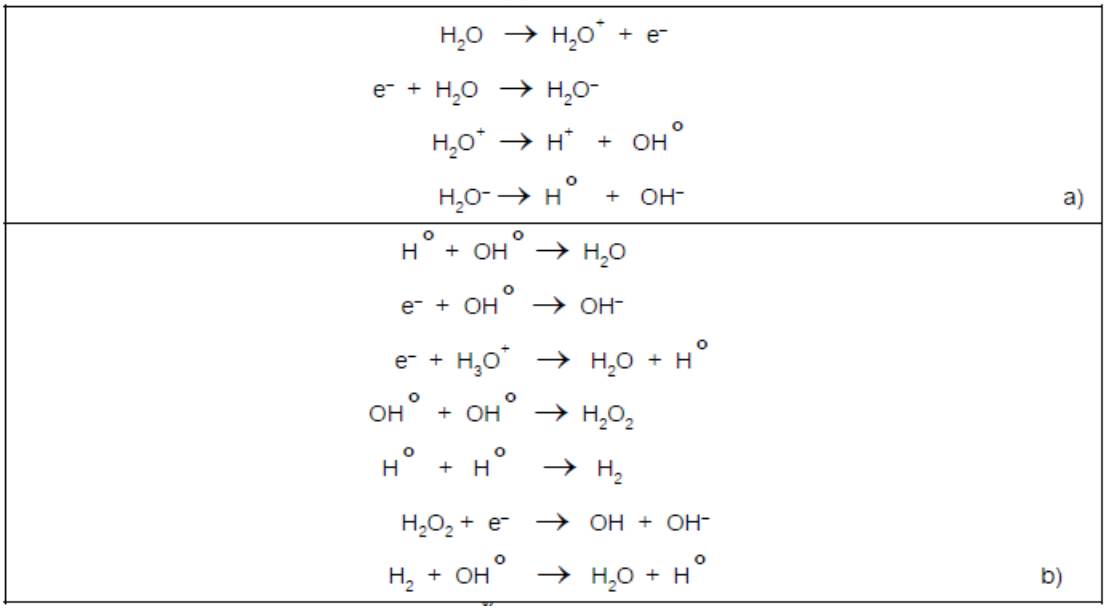

Figure 2.7 (a) water radiolysis, and (b) free radical integration.

Source: Fellows (2000) (a) *(94)*, and Saisanom (2540) (b) *(95)*

2.5 Mechanisms of Crosslinking by Irradiation Method

The hydrogel sheet was successfully synthesized by polymer crosslinking using ionizing radiation. Polymers that used in this research were gelatin and PVA. Both polymers could be crosslinked by irradiation method. Gelatin molecules can be reacted with hydroxyl radicals ($^{\bullet}OH$) in aqueous solution *(96)*. The gelatin carbon-centered radicals ($Gel^{\bullet}$) were created by the withdrawal of hydrogen atoms by $^{\bullet}OH$ as shown in Equation 2. The continuous reactions lead to the crosslinking of gelatin (Equation 3-4)

$$^{\bullet}OH + Gel \longrightarrow Gel^{\bullet} + H_2O \quad (2)$$

$$Gel^{\bullet} + Gel \longrightarrow Gel\text{-}Gel^{\bullet} \quad (3)$$

$$Gel\text{-}Gel^{\bullet} + Gel\text{-}Gel^{\bullet} \longrightarrow Crosslinked\ gelatin \quad (4)$$

PVA crosslinking mechanism also begins with $^{\bullet}OH$ *(97)* (Equation 5-6).

$$^{\bullet}OH + PVA(H) \longrightarrow PVA^{\bullet} + H_2O \quad (5)$$

$$PVA^{\bullet} + PVA^{\bullet} \longrightarrow PVA\text{-}PVA\ Crosslinked\ PVA \quad (6)$$

The crosslinked reaction between PVA and gelatin radicals was demonstrated in Equation 7.

$$PVA^{\bullet} + Gel^{\bullet} \longrightarrow PVA\text{-}Gel\ Crosslinked\ gelatin\ with\ PVA \quad (7)$$

2.6 Mechanisms of AgNP Formation by Irradiation Method

The AgNPs can be successfully in situ synthesized by direct photolysis and photosensitization of silver salt, such as silver nitrate ($AgNO_3$). The production from water radiolysis (Equation 8) reduced Ag^+, which came from $AgNO_3$ in solution, to become the neutral Ag^0 atoms *(30, 98-100)* (Equation 9) and finally form AgNPs *(100-102)* (Equation 10-12).

$$H_2O \longrightarrow OH^{\bullet}, e^-_{aq}, H^{\bullet}, H_2O_2, H_2, H^+, \ldots \quad (8)$$

$$Ag^+ + e^-_{aq} \longrightarrow Ag^0 \quad (9)$$

$$Ag^0 + Ag^+ \longrightarrow Ag_2^+ \quad (10)$$

$$Ag_2^+ + Ag^+ \longrightarrow Ag_3^+ \quad (11)$$

$$Ag_n^+ + Ag^+ \longrightarrow Ag_{n+1}^+ \quad (12)$$

Moreover, the radicals from PVA ($PVA^{\bullet}$) and the functional groups of gelatin, which are amino groups ($-NH_2$), and hydroxyl groups (-OH), also reduced Ag^{+} to AgNPs *(103-105)*.

2.7 Gamma Sterilization

Definition of sterilization is a process or method that eliminates all forms of life, especially microorganisms such as viruses, bacteria, and fungi. There are several methods to sterilize material depending on the goals and types of material. Sterilization can be performed using sunlight, heat, radiation, pressured vapor, ethylene oxide (EtO), formaldehyde, gas plasma (H_2O_2), and peracetic acid. A gamma irradiation dose of 25 kGy can sterilize devices and materials and it is recommended for medical purpose *(16)*.

Advantages of gamma sterilization are *(106)*

1) Good certainty of product sterilization, which is better than filtration and aseptic processing.

2) No waste or residue, which is better than chemical process such as EtO.

3) More penetrating, which is better than e-beam.

4) Ability to process at low-temperature.

5) Simple validation process.

Radiation affect on microorganisms or bacteria. The main reaction occurs at DNA in chromosomes. DNA damage from irradiation might inhibit cell division and lead to cell death. Factors that affect the amount of survived microorganisms are the components in microorganisms, developmental stage of microorganisms, amount of radiation, ability to repair, and species or strain of microorganisms. In micrology, microorganism's radiation resistance can be determined by D_{10} value or decimal reduction dose. D_{10} value is the radiation dose (kGy) required to kill 90% of total microorganisms or reduce the total number of microorganism by 10-fold (one log cycle) *(107)*. D_{10} values of some microorganisms are shown in Table 2.8.

Table 2.8 D_{10} values of some microorganisms

Microorganism	D_{10} value (kGy)
Aeromonas hydrophila	0.04 – 3.40
Bacillus cereus (vegetative cells)	0.02 – 0.58
B. cereus (spores)	1.25 – 4.00
Campylobacter jejuni	0.08 – 0.32
Clostridium botulinum (vegetative cells)	0.41 – 3.20
C. perfringens (spores)	0.29 – 0.85
Escherichia coli	0.23 – 0.45
E. coli O157 : H 7	0.24 – 0.47
Listeria monocytogenes	0.25 – 0.77
Salmonella	0.37 – 0.80
Staphylococcus aureus	0.26 – 0.45
Yersinia enterocolitica	0.04 – 0.39
Vibrio	0.08 – 0.44
Clostridium sporogenes	2.30 – 10.90
Micrococcus radiodurans	12.70 – 14.10
Moraxella phenylpyruvica	0.63 – 0.88
Pseudomonas putida	0.08 – 0.11
Sporolactobacillus inulinus (spores)	2.10 – 2.58
S. inulinus (vegetative cells)	0.35 – 0.53
Streptococcus faecalis	0.65 – 0.70
Viruses	2.02 – 8.10

Source: Barbosa-Canovas et al. (1998) *(108)*

2.8 Silver Nanoparticles

2.8.1 Nanometer

Nanometer (nm, 10^{-9} m) is one billionth of a meter. United States National Nanotechnology Initiative defines nanotechnology as “science, engineering, and technology conducted at the nanoscale, which is about 1 to 100 nanometers” *(109)*. A concept of nanotechnology originated from a lecture “There’s Plenty of Room at the Bottom" by Richard Feynman in 1959. Atoms and molecules could be investigated in nanoscale. The lower limit of the range of 1-100 nm is the size of the atom. The size of hydrogen atom, which is the smallest atom, is 0.24 nm. *(110)* In organism, many functional components, such as DNA and ATP synthase, have nanoscale diameter as shown in Figure 2.8.

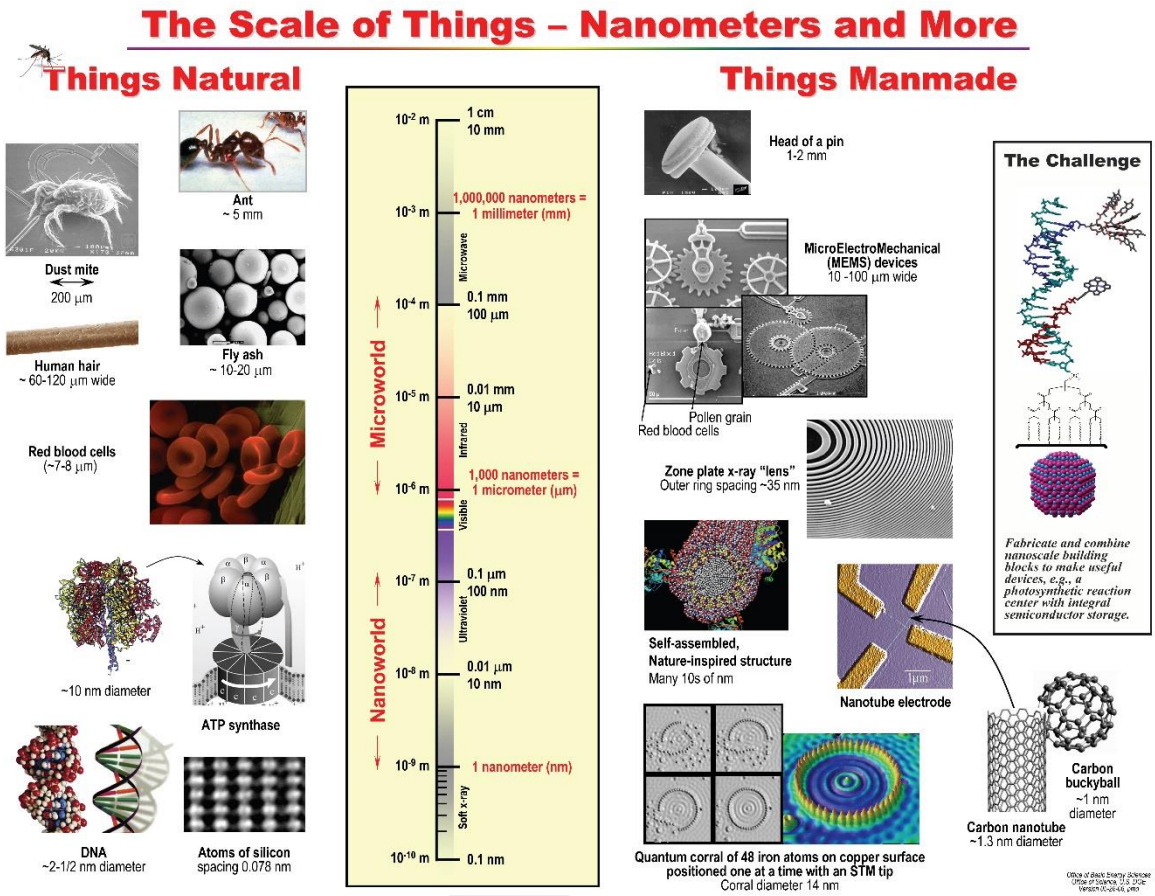

Figure 2.8 Scale of things chart

Source: BES (2006) *(111)*

2.8.2 Synthesis of AgNPs

Nanomaterials or nanoparticles (NPs) have unique properties that are different from their properties of bulk components. Silver (Ag) is a metal that can usually be processed to nanoparticle. General processes to synthesize AgNPs are chemical, physical, photochemical (irradiation), and biological methods.

2.8.2.1 Chemical Synthesis

Chemical methods are the most common ways to produce stable AgNPs, which are colloidally dispersed in water or organic solvents *(112)*. Several reducing agents were used in this synthesis, for example, polyols, sodium borohydride ($NaBH_4$), hydrazine (N_2H_4), sodium citrate, and N,N-dimethyformamide *(113)*. The chemical

synthesis methods usually consist of three compositions, which are precursors of metal, reducing agents chemical, and stabilizing agents *(114).* The process of chemical reduction starts with Ag complexes provide neutral atom of silver (Ag^0). Next step is agglomeration, that leads to the construction of colloidal Ag particles in the end *(115)*. However, for environmental issue, toxicity, and biological hazards of chemical usages should be concerned *(116)*.

2.8.2.2 Physical Method

The nanoparticles could be created by evaporation-condensation, which is a physical approach. This method can be applied by using a furnace at atmospheric pressure. At a definite temperature and pressure, the metal precursor is vaporized into a carrier gas. After that, nanoparticles are synthesized by evaporation-condensation procedure *(117, 118)*. However, this method has many disadvantages such as a large consumption of energy, large space of tube furnace, very long time to achieve thermal stability *(114)*.

2.8.2.3 Photochemical or Irradiation Method

AgNPs could be produced by using several irradiation methods. Both ionizing and non-ionizing radiation can be used such as laser *(112)*, X-ray *(119)*, ultraviolet (UV) light *(120)*, microwave *(112)*, and gamma radiation *(121)*. A zero-valent metal (M^0) could be formed by two processes (Figure 2.9). The first process is direct photolysis of a metal source such as metal salt or complex. The second process is photosensitization, which using sensitizers or photochemically generated intermediates. The obvious advantages of irradiation method are cleanness and convenience.

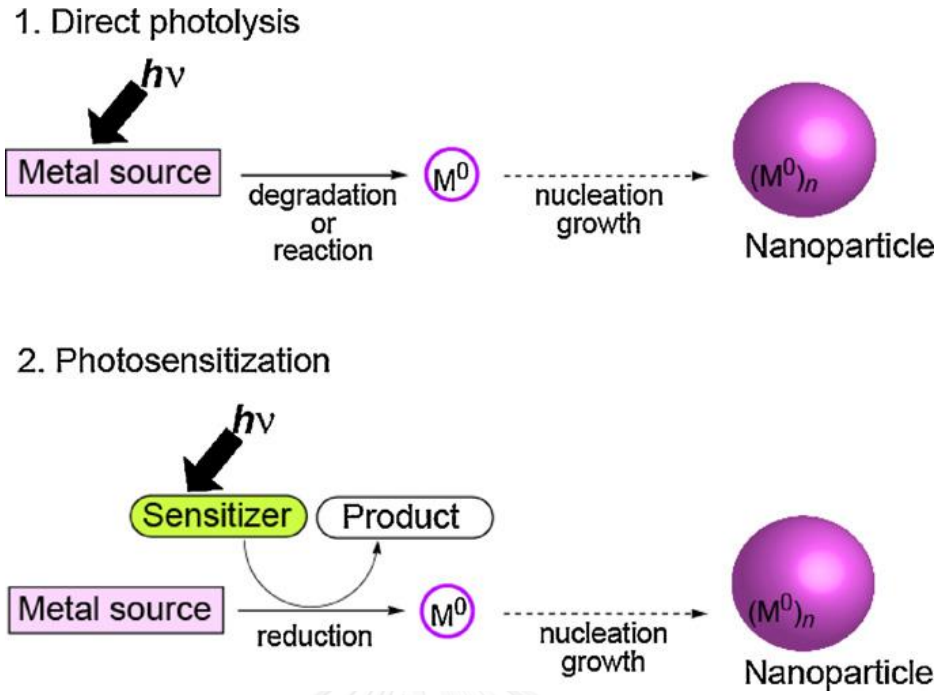

Figure 2.9 Systematic scheme of photochemical synthesis

Source: Sakamoto, M., et. al. (2009) *(122)*

2.8.2.4 Biological Synthesis

Several types of living organisms can produce metal nanoparticles. The reducing agent and stabilizer, which are essential for AgNPs synthesis, could be replaced by biological molecules in living organisms, which are microorganisms (such as bacteria, fungi, algae, and yeasts) and plants *(123)*. Example of AgNPs biological synthesis is a study of *Bacillus licheniformis* in 2008 *(124)*. Possible mechanism for AgNPs production in *B. licheniformis* is shown in Figure 2.10. Ag^{+} from solution of $AgNO_3$ may be converted to Ag^{0} by the electron shuttle enzymatic metal reduction process.

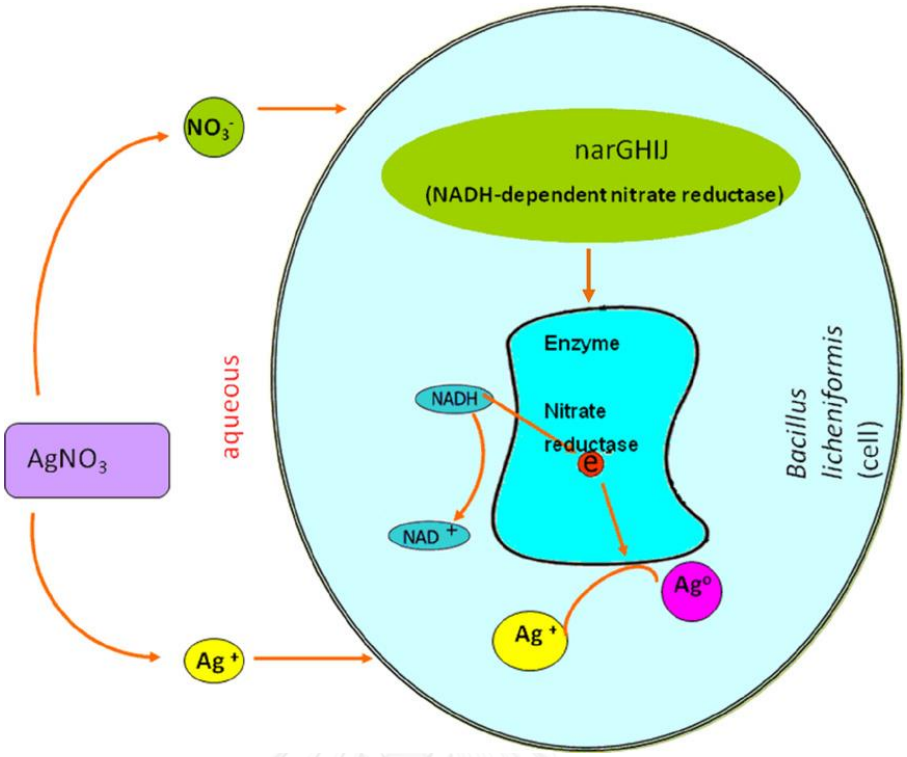

Figure 2.10 Possible mechanism for AgNP synthesis in *B. licheniformis*
Source: Kalimuthu, K., et. al. (2008) *(124)*

2.8.3 Optical Properties of AgNPs

The properties of nanoparticles are different from bulk material because of their extremely tiny size. The nanoparticles of noble metal have unique optical properties that depend on size and shape. The important optical property of AgNPs is surface plasmon resonance. Surface plasmon resonance is a type of plasmon band associated with the light phenomena of the conduction electrons on the nanoparticle surface *(125)*. Surface plasmons have at least three types which are

(1) Propagating surface plasmons take place on metal surfaces as shown in Figure 2.11 A.

(2) Localized surface plasmons are associated with small sized particles.

(3) Acoustic surface plasmons are probably exist on some metal surfaces.

The surface plasmon resonance can be explained by electron gas theory. The atomic nucleus is a local habitat of the inner-shell electrons. But the outer-shell electrons have free movement within particle. Because the nanoparticle size is much smaller than the wavelength of light, the motion of electron induces the presentation of dipole as shown in Figure 2.11 B. The coincidence between the frequency of light oscillations and electrons close to the surface of particle cause the surface plasmon resonance. This phenomenon is the absorption and scattering of the resonance light *(126).* The AgNPs have different color from bulk silver. Huang T. and Xu X.-H. (2010) *(127)* demonstrated the synthesis method of AgNPs, which are different in sizes and shapes, and showed the rainbow colors of AgNPs (Figure 2.12).

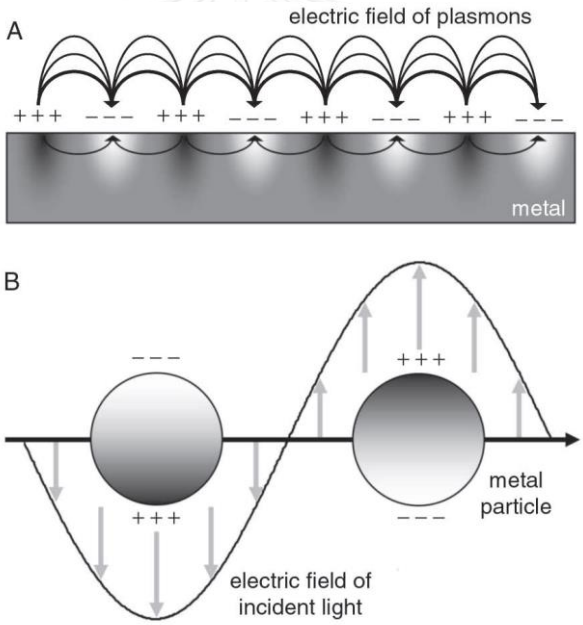

Figure 2.11 (A) Reproductive surface plasmons, (B) Localized surface plasmons.
Source: Campbell, D. J., and Xia, Y. (2007) *(125)*

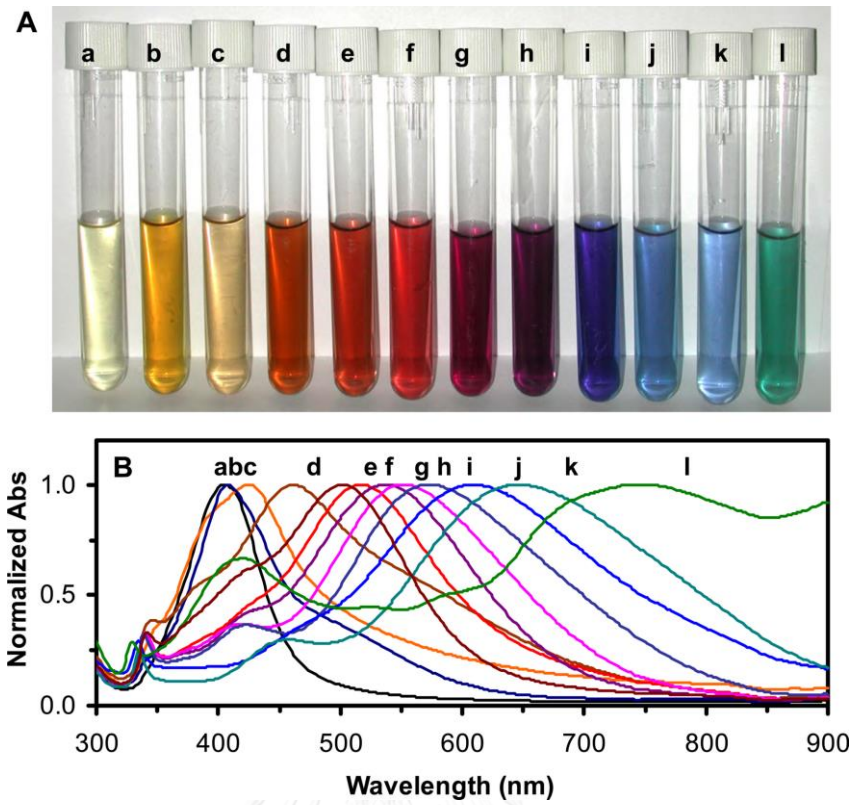

Figure 2.12 (A) Photos of rainbow colored colloidal AgNPs (B) Normalized absorbance of UV-vis absorption spectra of the colloidal AgNPs in (A).

Source: Huang, T., and Xu, X.-H.N. (2010) *(127)*

2.8.4 Antibacterial Properties of AgNPs

Colloidal AgNPs have been used for more than a century. United States registered colloidal silver as a biocidal material since 1954 *(128)*. Nanoparticles have huge surface area when compared with bulk material. Their large surface leads to rapid dissolution and enlarged toxicity. The antibacterial properties of AgNPs have been used in several utilizations. Nowadays, the full antibacterial mechanisms of AgNPs are still unknown. The possible mechanisms could be divided into three mechanisms *(129)* (Figure 2.13). The first mechanism is associated with bacteria membrane. AgNPs attached to the surface of bacteria, changed properties of membrane, degraded lipopolysaccharide, constructed “pits” to amass inside the membrane, and made the membrane permeability increases *(130)*. The next mechanism is a penetration into bacteria cell, which causes DNA damage. The last one is the dissolution of AgNPs, which could release the antibacterial Ag^{+} *(28)*.

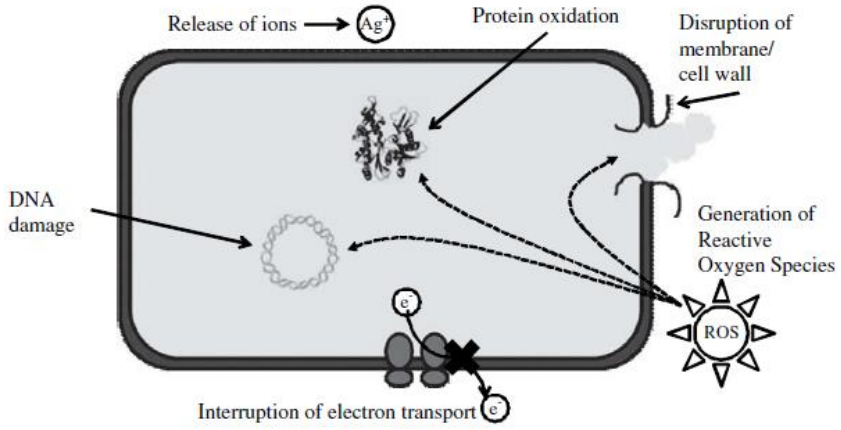

Figure 2.13 Mechanisms of antimicrobial activities of nanomaterials

Source: Li, Q., et. al. (2008) *(129)*

2.9 Literature Review

2.9.1 The Properties of Wound Dressings

The wound dressings have a variety of thickness. In 1995, Wu, P., et al. *(131)* investigated commercial wound dressings, which are hydrocolloid, hydrogel, and film. The thickness of these wound dressings was approximately 0.077-2.92 mm (Table 2.9). Wokalek, H. (1991) suggested in his patent *(132)* about the thickness of hydrogel sheet wound dressings. General thickness is between 2–10 mm, especially in the range of 3-5 mm. The size of dressing could be modified later (such as by cutting). Uzun, M., Anand, S. C., and Shah, T. (2013) *(133)* evaluated and characterized thirteen commercial wound dressings, which are available in United Kingdom. These thirteen wound dressings can be categorized into three types, which are nonwoven, foam and hydroactive dressings. Thickness and fluid handling properties of wound dressing product were shown in Table 2.10.

Table 2.9 Dressings evaluated and the results of WVTR

(mean ± 1 s.d., n = 7)

Dressing type	Trade name	Manufacturer	Thickness (mm)	WVTR (g m^{-2} d^{-1}) (at 24 h)	
				0.4 m s^{-1}	Static
Hydrocolloid	Biofilm®	CliniMed Ltd	1.79 ± 0.09	6512 ± 445	2892 ± 337
	Comfeel®	Coloplast A/S	1.27 ± 0.11	285 ± 8	308 ± 16
	Dermiflex®	Johnson & Johnson	2.41 ± 0.05	76 ± 5	90 ± 10
	Duoderm®	ConvaTec Ltd	1.93 ± 0.10	889 ± 49	886 ± 60
	Duoderm CGF®	ConvaTec Ltd	2.27 ± 0.08	120 ± 19	*
	Granuflex E® Extra Thin	ConvaTec Ltd	0.50 ± 0.05	216 ± 6	205 ± 10
	IntraSite®	Smith & Nephew	1.29 ± 0.08	357 ± 29	354 ± 42
	Metoderm®	ConvaTec Ltd	2.92 ± 0.20	809 ± 19	823 ± 45
	Restore Cx®	Hollister Inc.	1.19 ± 0.08	476 ± 18	482 ± 69
	Tegasorb®	ConvaTec Ltd	2.10 ± 0.15	136 ± 15	*
	Ultec®	Sherwood Med	1.10 ± 0.02	534 ± 63	*
Hydrogel	Geliperm®	Geistlich Ltd	1.13 ± 0.19	9009 ± 319	*
	Vigilon® (no films)	Bard	1.13 ± 0.17	9360 ± 34	*
	Vigilon® (+1 film)	Bard	1.16 ± 0.17	50 ± 19	*
Film	Bioclusive®	Johnson & Johnson	0.077 ± 0.01	394 ± 12	*

*Not selected for test under static condition.

Source: Wu, P., et al. (1995) *(131)*

Table 2.10 Thickness and fluid handling properties of commercial wound dressing

Product	Manufacturer	Dressing Type	Thickness (mm)	Fluid Handling (g per g)
Aquacel®	ConvaTec	Nonwoven	1.6	19.07±2.1
Kaltostat®	ConvaTec	Nonwoven	2.0	18.44±1.3
CarboFlex™	ConvaTec	Nonwoven	3.9	11.11±0.5
Melolin*	Smith&Nephew	Nonwoven	3.4	13.56±0.6
CliniSorb®	CliniMed	Nonwoven	1.2	3.54±0.2
Versiva® XC®	ConvaTec	Foam	2.5	4.16±0.4
Mepilex®Border	Molnlycke	Foam	4.2	7.71±1.0
Allevyn Gentle Border	Smith&Nephew	Foam	4.2	7.85±0.1
Mepilex®	Molnlycke	Foam	5.9	11.87±0.2
Mepilex® lite	Molnlycke	Foam	1.6	4.08±0.3
Aquacel® Surgical	ConvaTec	Hydroactive	4.2	3.82±0.7
CombiDERM®	ConvaTec	Hydroactive	1.8	6.80±0.4
Biatain	Coloplast	Hydroactive	3.4	7.42±0.2

Source: Uzun, M., Anand, S. C., and Shah, T. (2013) *(133)*

Water holding is the outstanding property of hydrogels, but the wetness could lead to the accumulation of exudates. Kim, I. Y., et al. (2007) *(134)* studied the chitosan/poloxamer semi-interpenetrating polymer network which performed water holding capacity of 90-96% and found that it prevented the collection of exudates. An *in situ* forming hydrogel in the study of Balakrishnan, B., et al. (2005) *(135)*, which is prepared from oxidized alginate and gelatin, had an equilibrium fluid content approximately 90%.

Water vapor transmission rate (WVTR), which referred as moisture vapor transmission rate (MVTR), could estimate potential of wound dressings to maintain moisture. *(136, 137)* The range of WVTR values of commercial wound dressings is 76-

9360 g/m^2/day *(131)*. Queen et al. *(138)* exhibited that dressings with WVTR of 2000-2500 g/m^2/day were appropriate because of their suitable moisture level. From Table 2.9, Wu, P., et al. *(131)* also investigated WVTR of commercial hydrogel wound dressings. A method in their study was ASTM standard method (ASTM E96-90) with modification.

Wound dressings should be flexible for comfortable to follow any dimensional changes. Suitable net-like adhesive layer having elongation at break of 100-800%, range of 200-750% is desirable *(139)*. Erizal, E. and Wikanta, T. (2011) *(140)* prepared polyethylene oxide-chitosan hydrogel by gamma irradiation. Elongation at break of hydrogels is ranged between approximately 90-145%. Another research about hydrogel wound dressing containing chitosan is the work of Sung, J. H. and colleague (2010) *(141)* PVA-chitosan hydrogel with minocycline prepared by freeze-thawing method had elongation at break about 120-170%. The elongation at break of hydrogel without minocycline was higher than that of hydrogel with minocycline.

In vitro biodegradation was tested to evaluate the stability of hydrogels. The available dressings should have weight remaining after *in vitro* biodegradation more than 80% *(134)*. Kamoun, E. A., et al. (2015) *(142)* immersed the PVA-sodium alginate physically crosslinked hydrogel membranes in phosphate buffer saline (PBS). At 24 h of degrading time, weight loss of hydrogel was vary from approximately 20-60% depend on sodium alginate content. Shi, L., et al. (2015) *(143)* investigated *in vitro* degradation of poly(γ-glutamic acid)/silk sericin hydrogels by papain solution immersion. Papain is a papaya proteinase. At 24 h, the remaining weight of hydrogel was about 80%.

2.9.2 Gelatin and PVA-containing Hydrogels for Wound Dressing

Balakrishnan, B., et al. (2005) *(135)* prepared alginate diadehyde cross-linked gelatin hydrogels. They mixed the polymer solutions to prepare *in situ* forming hydrogels. From equilibrium swelling testing, the hydrogels had fluid content about 90%. The

hydrogels were applied on the full thickness wounds in rat model. After 15 days of observation, the wounds were completed with new epithelium.

Yu, H., et al. (2007) *(144)* prepared PVA/poly(N-vinyl pyrrolidone) (PVP) hydrogels containing AgNPs by a freezing-thawing method. AgNPs in their research were created by sodium citrate reduction of $AgNO_3$. The hydrogels had three-dimensional structures. The average size of AgNPs was approximately 100 nm. Their hydrogels had excellent antibacterial effects against *E. coli* and *S. aureus*.

Sung, J. H., et al. (2010) *(141)* developed PVA/chitosan hydrogel films by a freeze-thawing method. Minocycline, which is an antibiotic drug, was loaded in hydrogel preparation process. An addition of chitosan affects the mechanical properties of hydrogels. The cross-linking density of the hydrogel with chitosan was decreased. Results from the *in vivo* wound healing test in rats revealed that the hydrogels can heal the wound effectively.

2.9.3 Hydrogel Wound Dressings Prepared by Gamma Irradiation

Investigations of hydrogel prepared by gamma irradiation have been increased in recent year. Hydrogel wound dressings, which made from both natural and synthetic polymers, were listed in Table 2.11.

El-Mohdy (2013) *(145)* prepared hydrogels by radiation synthesis. PVA, cellulose acetate, and gelatin were dissolved and irradiated at 15, 20 and 25 kGy. After that, the crosslinked polymer was swollen with $AgNO_3$ and 2-propanol solutions in water. The polymer was irradiated again to reduce Ag^+. AgNPs were successfully created. The diameters of AgNPs were approximately 39-60 nm. The hydrogels had antimicrobial activity for fungus and bacteria.

Zhou and colleagues (2012) *(104)* created nanosilver/gelatin/carboxymethyl chitosan hydrogels by gamma irradiation (30 kGy). The hydrogels had porous structure, good water retention capacity, suitable mechanical property, and antibacterial ability.

Singh and Singh (2012) *(146)* used gamma radiation of 25 and 40 kGy dose to create the hydrogels. The compositions of hydrogels were polyvinyl pyrrolidone, alginate, and silver nitrate. These hydrogels had proper absorption capacity and permeability. They also inhibited the microbial growth.

Singh and Pal (2011) *(147)* selected PVA and PVP as main compositions of hydrogels, and sterculia gum as antimicrobial agent. From this study, the mechanism of drug release could be explained by non-Fickian diffusion mechanism.

Erizal and Wikanta (2011) *(140)* prepared polyethylene oxide/chitosan hydrogels by gamma irradiation (20-40 kGy). Hydrogels with 1% chitosan, which were irradiated at 20 kGy, had high gel fraction, swelling ratio, and elongation at break. The hydrogels also had antibacterial property.

Table 2.11 Related researches in hydrogel wound dressings prepared by gamma irradiation

Components	Significant Results	References
PVA / CA / gelatin / $AgNO_3$	Well-dispersed, spherical AgNPS / AgNPs inhibit the crystallization of PVA-based gel / antibacterial ability	El-Mohdy, H. L. A., *J. Polym. Res.* 2013 *(145)*
Gelatin / CM-chitosan / $AgNO_3$	Interconnected porous structure / good swelling behavior / antibacterial ability	Zhou, Y., Zhao, Y., Wang, L., Xu, L., Zhai, M. and Wei, S. *Radiat. Phys. Chem.* 2012 *(104)*
PVP / alginate / $AgNO_3$	MVTR 278.44 g/(m^2h) / 70 ppm nanosilver dressings completly inhibit microbial growth	Singh, R., Singh, D. *J. Mater. Sci. Mater. Med.* 2012 *(146)*
Sterculia gum / PVA / PVP	Swelling increased with increasing sterculia and NVP / release of drug through non-Fickian diffusion mechanism	Singh, B. and Pal, L. *Int. J. Biol. Macromol.* 2011 *(147)*
PEO / chitosan	Gel fraction (85%) at chitosan 1%, swelling ratio 10 g/g, elongation at break (145%) / antibacterial activities	Erizal, E., Wikanta, T. *Indo. J. Chem*. 2011 *(140)*

CHAPTER 3
MATERIALS AND METHODS

3.1 Material, Reagents, and Equipments

3.1.1 Materials and Reagents

(1) Gelatin powder (Type A; porcine skin; 170-190 g Bloom; Fluka, Switzerland)

(2) PVA (Average Mw 89,000-98,000, 99+% hydrolyzed; ALDRICH, USA)

(3) $AgNO_3$ (Fisher Scientific, UK)

(4) Dulbecco's modified Eagle medium (DMEM, Hyclone, USA)

(5) Ethanol 95%

(6) Fetal bovine serum (FBS, Hyclone, USA)

(7) Dimethylsulfoxide (DMSO, Sigma-Aldrich, Germany)

(8) MTT [3-(4,5-dimethylthiazol-2-yl)-2,5-diphenyltetrazolium bromide]

(9) Phosphate buffer saline (PBS, OmniPur, Germany)

(10) Trypsin-EDTA (0.25% trypsin with EDTA · 4Na, Hyclone, USA)

(11) Lysozyme from hen egg white (62971, Fluka, USA)

3.1.2 Equipments

(1) Auto-pipettes (200, 1000 µl)

(2) Laboratory glassware (Pyrex, USA; Duran, Germany)

(3) Franz cell (Custom-made, Scientific and Technological Research Equipment Centre)

(4) Energy-dispersive X-ray spectroscopy (Hitachi/S-4800, Japan)

(5) Freezer (-40°C, Heto HLLF-205, Denmark)

(6) Laminar flow hood (Lab Service Ltd., Part., Thailand)

(7) Lyophilization machine (Labconco, USA)

(8) Nylon bag (purchase from Rachawong Packaging Co., Ltd.)

(9) Scanning electron microscope (Hitachi/S-4800, Japan)

(10) Ultrasonic cleaning unit (Elmasonic S 70/(H), Germany)

(11) Ultraviolet–visible spectrophotometer (Shimadzu UV-2550, USA)

(12) Universal Testing Machine (Lloyd/LRX, UK)

3.2 Experimental Procedures

Experimental procedures are divided into three parts. Part I is the preparation and characterization of gelatin/PVA hydrogel. The ratios of gelatin and PVA solutions and the irradiation doses were varied and the characteristics of gelatin/PVA hydrogels were studied in order to use as wound dressing hydrogel sheet. Part II is the preparation and characterization of gelatin/PVA hydrogel containing AgNPs. The physical, mechanical, and chemical properties of the gelatin/PVA hydrogels with various $AgNO_3$ concentrations were tested. The formation of AgNPs was also investigated. Part III is the determination of the cytotoxicity and antibacterial effects of AgNP/gelatin/PVA hydrogels using fibroblast cells and bacteria (*in vitro*). The procedures of each part were summarized in the flow chart in Figure 3.1, Figure 3.2, and Figure 3.3.

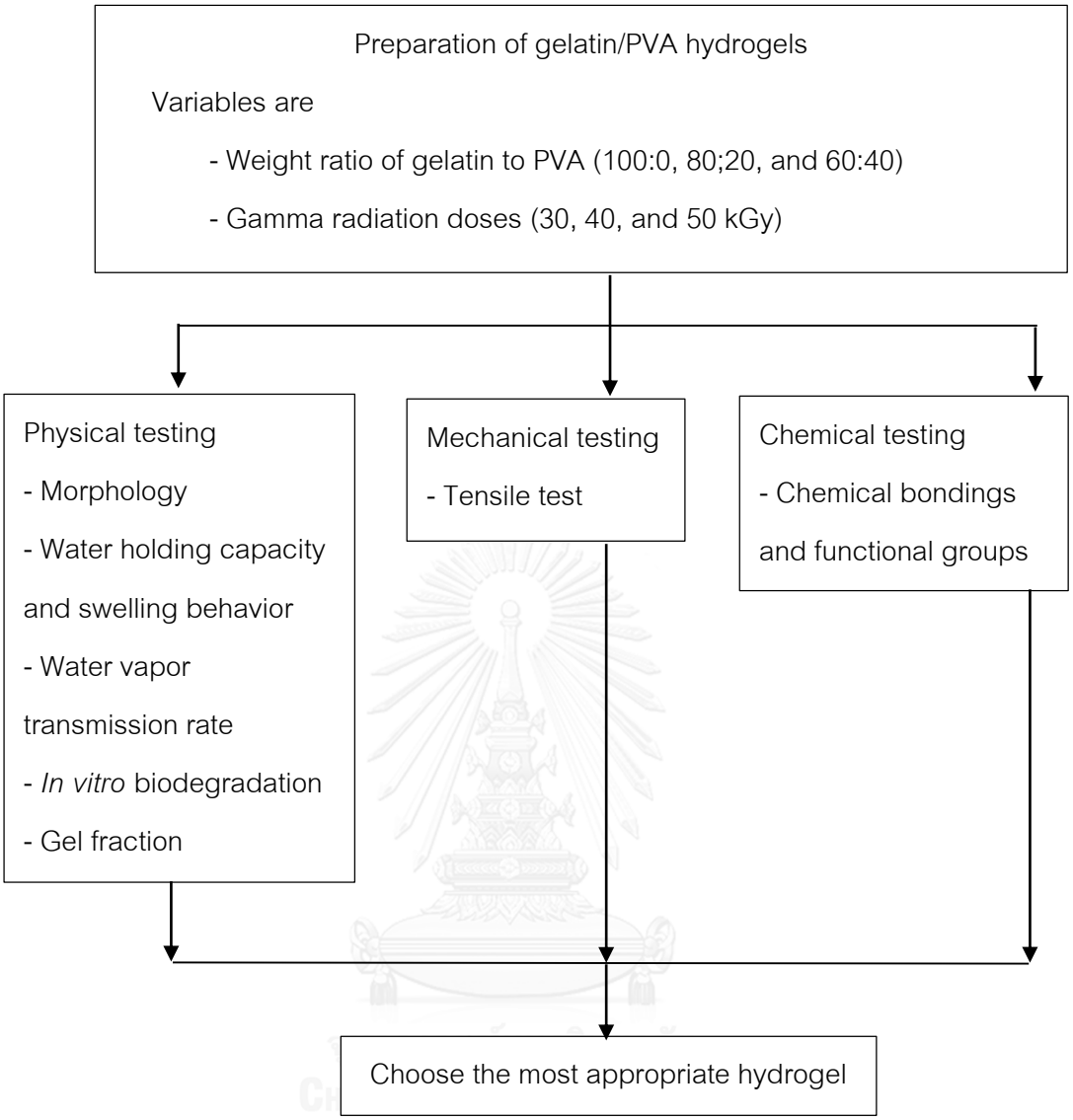

Figure 3.1 Diagram of experimental procedures of part I

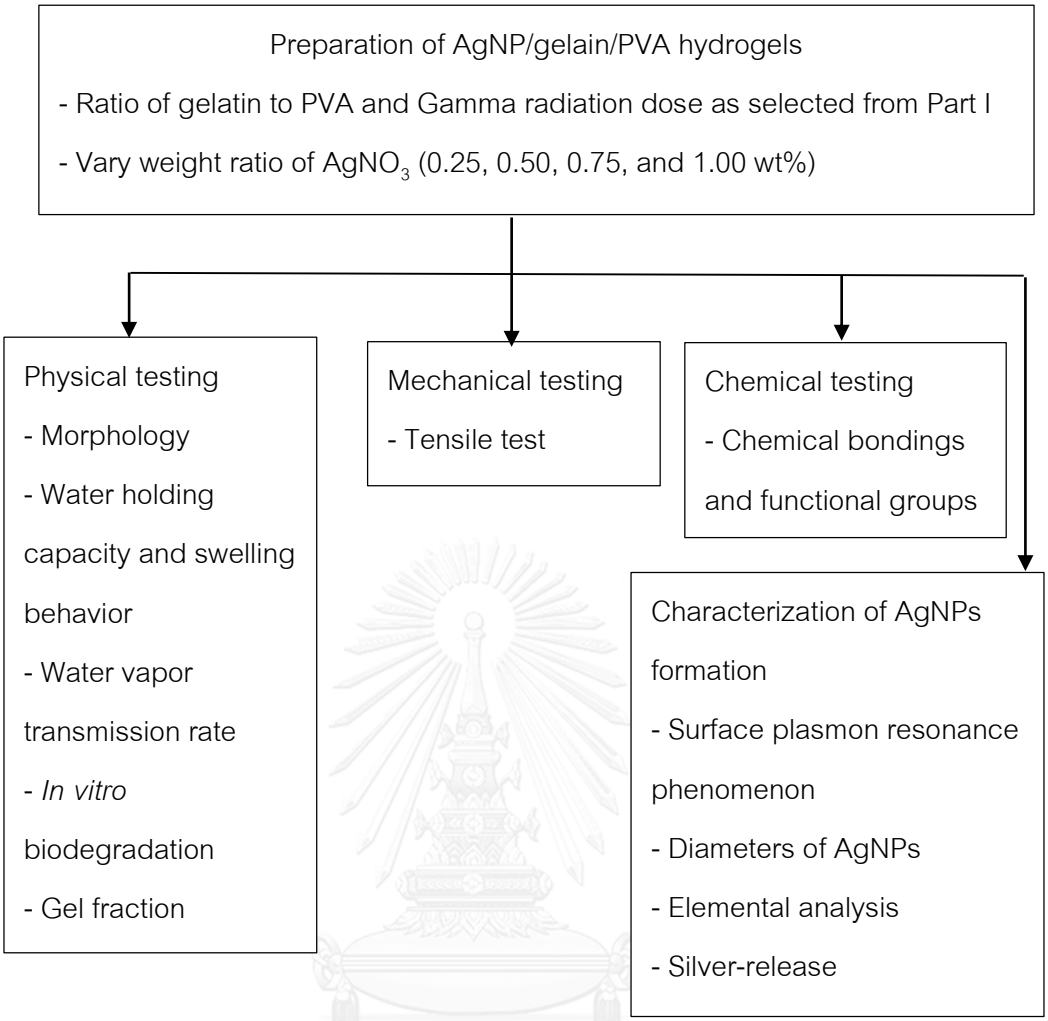

Figure 3.2 Diagram of experimental procedures of part II

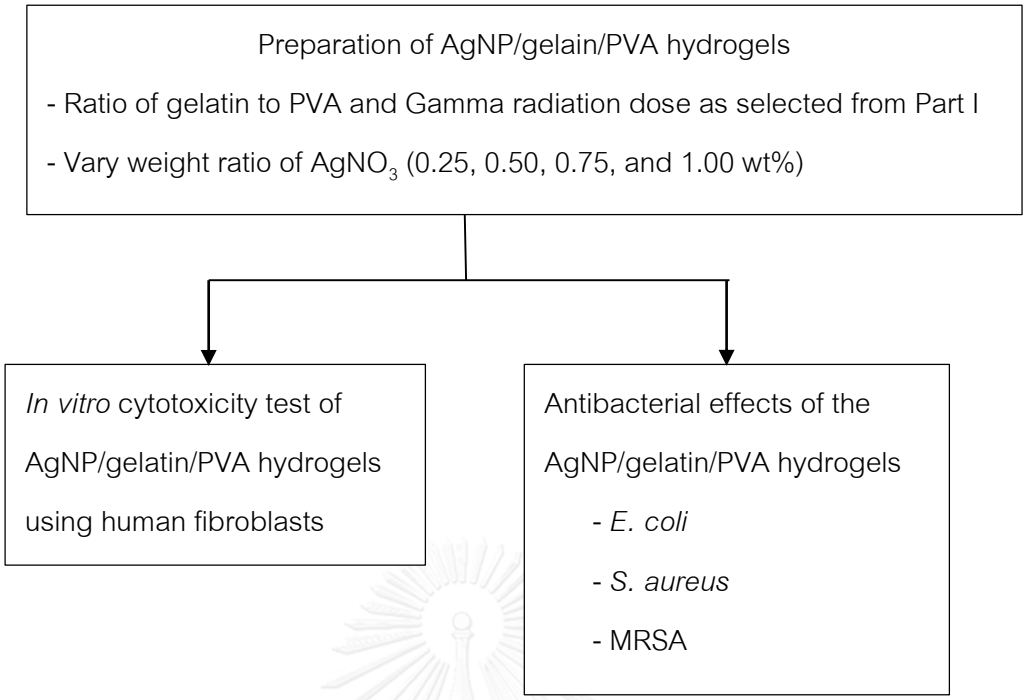

Figure 3.3 Diagram of experimental procedures of part III

3.2.1 Part I: Preparation and Characterization of Gelatin/PVA Hydrogel

3.2.1.1 Preparation of the Gelatin/PVA Hydrogels

Gelatin solution was prepared by dissolving type A gelatin powder in 45°C distilled water to produce 15 wt% gelatin solution and stirring at 300 rpm for 40 min. PVA solution was prepared by dissolving PVA powder in 95°C distilled water to produce 15 wt% PVA solution and stirring at 300 rpm for 40 min. The gelatin/PVA solution was prepared by pouring the gelatin solution into the PVA solution. The weight ratios of gelatin to PVA solutions were 100:0, 80:20 and 60:40 (15 wt% solid). The gelatin/PVA solution was stirred at 80°C, 300 rpm for 30 min. The solution was degassed by an ultrasonic cleaning unit (Elmasonic S 70/(H), Germany) for 15 min to remove air bubbles. When the homogeneous solution was obtained, it was packed into nylon bag and sealed by an impulse sealer. Two plates, such as glass plates or acrylic plates, were compressed on two opposite sides of nylon bag for overnight. The plastic sheet with the same thickness

was inserted between the glass sheets on both sides to control the thickness of the nylon bag. The sides of the plates were clamped with paper clips, shown in Figure 3.4.

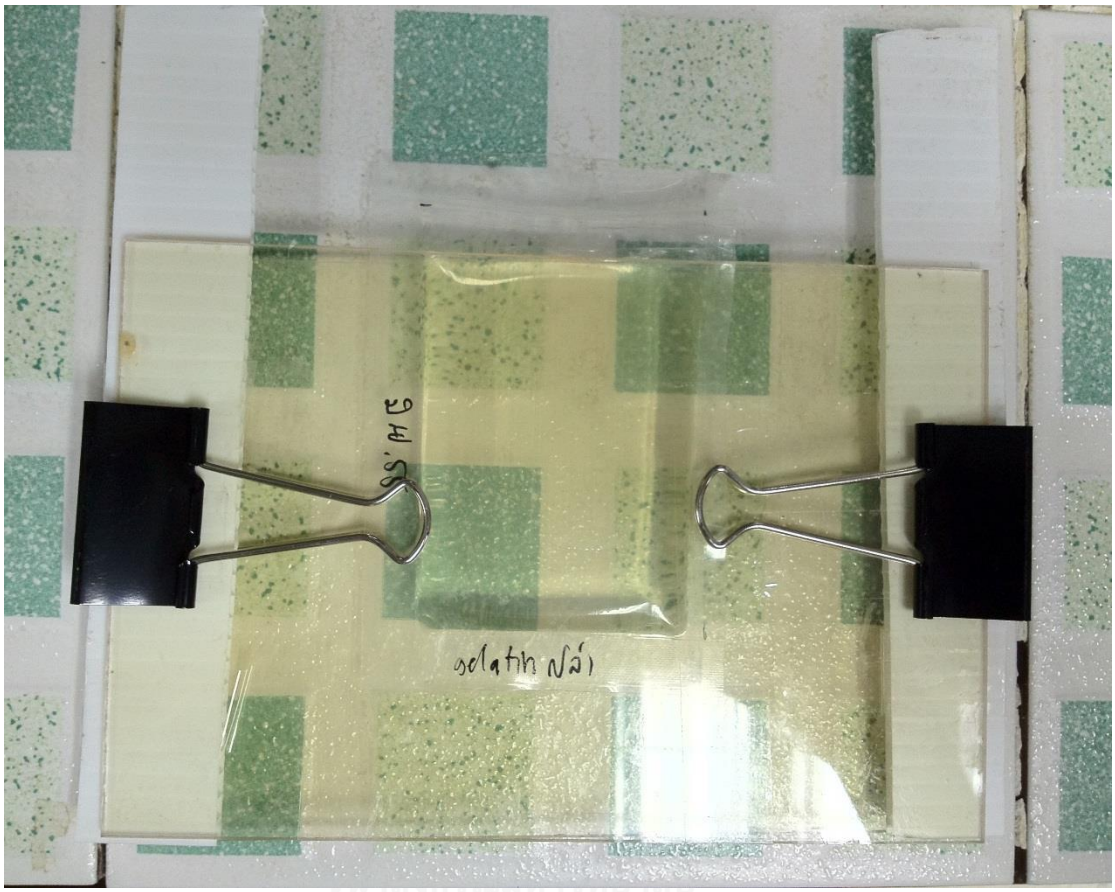

Figure 3.4 Demonstration of hydrogel preparation. Two plates were compressed on nylon bag by using paper clips.

The samples were irradiated with gamma ray generated from cobalt-60 at Synergy Health (Thailand) Ltd. At the dose rates of 5 kGy/h, gamma radiation doses were targeted at 30, 40, and 50 kGy. The solution was gelled after irradiation. The obtained hydrogels were stored at room temperature prior to testing. The summary of hydrogel type and doses of gamma radiation were shown in Table 3.1.

Table 3.1 Hydrogel compositions and doses of gamma radiation used in the experiment

Hydrogel	Gelatin 100%	Gelatin 80% + PVA 20%	Gelatin 60% + PVA 40%
Doses of gamma radiation (kGy)	30	30	30
	40	40	40
	50	50	50

3.2.1.2 Physical Testing

(1) Morphology

Scanning electron microscope (SEM; Hitachi/S-4800, Japan) at The Petroleum and Petrochemical College was used to investigate the morphology of the freeze-dried hydrogels. SEM specimens were coated with Platinum. SEM images of hydrogel were maximized the histogram distribution by SemAfore program (JEOL SemAfore Software, Germany). This program was also used to determine pore size of hydrogel.

(2) Water Holding Capacity and Swelling Ratio

The circular discs of hydrogel with the thickness of 3.6-4.1 mm and the diameter of 15 mm were immersed in 50 ml of PBS (pH 7.4) at 37°C and shaken at 50 rpm for 24 h. The immersed samples were removed from the solution and the apparent solution on the surface was gently absorbed by tissue paper. After that, the swelled samples were dried in an oven at 70°C for 48 h until reaching constant weight. The water holding capacity and swelling ratio were calculated by following formulas.

$$\text{Water holding capacity (\%)} = (W_s - W_d) / W_s \times 100 \quad (13)$$

$$\text{Swelling ratio (\%)} = (W_s - W_i) / W_i \times 100 \quad (14)$$

Where W_s was the weights of swollen hydrogel after immersion, W_d was the weights of dried hydrogel, and W_i was the weights of initial hydrogels which did not immerse in PBS.

(3) Water Vapor Transmission Rate (WVTR)

WVTR across the hydrogels was determined as specified by ASTM standard *(148)* with some modifications. The circular discs of hydrogel with the thickness of 3.6-4.1 mm and the diameter of 35 mm were placed on the mouth of the laboratory bottle (100 ml) which contained 10 ml of distilled water. The samples were attached across the edges of the cup by binding with paraffin film strip. The assembly was incubated at 37°C and 35% relative humidity. Saturated solution of magnesium chloride was used to retain relative humidity. The assembly was weighted at constant time interval. The graph of weight loss versus time was plotted to find out the slope, representing average weight loss per hour. WVTR was calculated by the following formula. Slope was multiplied by 24 to dertermine WVTR in $g/m^2/day$.

$$\text{WVTR} = (\text{slope} \times 24) / \text{area of hydrogel in } m^2 \quad (15)$$

(4) *In vitro* Biodegradation

The hydrogels were cut into small pieces (100 mg/piece). Each sample was immersed in 5 ml PBS with 1×10^4 U/ml of lysozyme concentration *(149)* at 37°C. The incubation times of hydrogels in the media were 6, 12, 18, and 24 h. After that, the degraded hydrogels were taken out from the media and washed by distilled water to remove residual lysozyme. The remaining hydrogels were then freezed at -40°C for 24 h, dried for another 24 h, and weighed. The weights of the dried sample after degradation were calculated as percentage compared with the initial weight.

(5) Gel Fraction

Gel fraction testing was adapted from the report by Rita Singh (2012) *(146)*. The circular disc of hydrogel with diameter of 15 mm was incubated in an oven at 50°C for 24 h until reaching a constant weight. Next, the dried sample was immersed in

50 ml distilled water (50°C), shaken at 50 rpm for 2 h and dried again in an oven at 50°C. The percentage of gel fraction was calculated using the following formula.

$$\text{Gel fraction (\%)} = (W_d / W_i) \times 100 \quad (16)$$

Where W_d represented the weight of dried hydrogel after extraction. W_i represented the initial weight of dried hydrogel before extraction.

3.2.1.3 Mechanical Testing

(1) Tensile Test

The hydrogels were prepared according to D638-03 ASTM standard *(150)* with adaptation (n=5 per group). The samples were cut in a dumbbell shape (total length:115 mm, total width: 25 mm, narrow section width:10 mm) using shape-plastic sheet (Figure 3.5) as a model. The universal testing machine (Lloyd/LRX, UK) was used for tensile test at the speed of 22 mm/min with pre-load of 0.01 N.

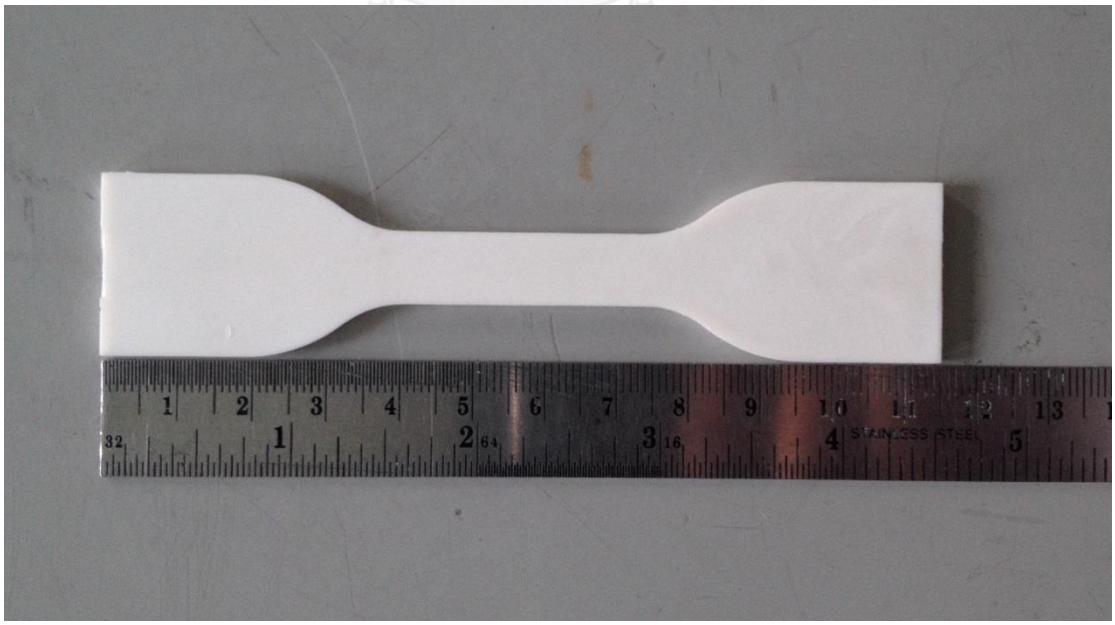

Figure 3.5 A dumbbell shape-plastic sheet

3.2.1.4 Chemical Testing

(1) Chemical Bondings and Functional Groups

Fourier transform infrared (FTIR) spectroscopy (Perkin Elmer, Spectrum One, United States) at Scientific and Technological Research Equiment Centre was used to investigate the chemical bondings and functional groups of the hydrogels. Pieces of hydrogel were freezed at -40°C for 24 h and then were dried in lyophilization machine (Labconco, USA) for another 24 h. The freeze-dried hydrogels were used for FTIR analysis in attenuated total reflection (ATR) mode. The wavenumber range was 4000-515 cm^{-1}.

3.2.2 Part II Preparation and Characterization of Gelatin/PVA Hydrogel Containing AgNPs

Gelatin/PVA solution was prepared as described above. Silver nitrate ($AgNO_3$) was added into gelatin/PVA solution. The concentrations of $AgNO_3$ were 0.25, 0.50, 0.75, and 1.00 wt% based on the solid part of the solution. The mixing solution was blended at 80°C, and stirred at 300 rpm for 30 min. The mixing solution was vibrated by an ultrasonic cleaning unit for 15 min to remove air bubbles in the solution. Packing and irradiation method were prepared as described in the previous section.

Characterization of AgNPs Formation

3.2.2.1 Surface Plasmon Resonance (SPR) Phenomenon

The UV-vis absorption spectra of AgNPs in the AgNP/gelatin/PVA hydrogels were investigated by a Shimadzu UV-2550 Ultraviolet–visible (UV-vis) spectrophotometer (USA). The appearance of the surface plasmon resonance (SPR) band was performed in the range of 200-900 nm.

3.2.2.2 Diameters of AgNPs

The AgNP/gelatin/PVA hydrogel was cut into a cube with 5 mm in width. The cube was freezed at -40°C for 24 h. After freezing, the cube was dried in lyophilization

machine (Labconco, USA) for another 24 h. The freeze-dired cubes of hydrogel were ground and immersed in 1 ml of ethanol for 30 min. The 10 µL of solution was dropped on the copper grid and left to air-dry overnight. The grids were examined by a JEOL JEM-2100 transmission electron microscope (TEM; Japan) at Scientific and Technological Research Equiment Centre operated at 120 kV, Magnification 100–250 K. The diameters of 50 pieces of AgNPs in the TEM images were sized by SemAfore program.

3.2.2.3 Elemental Analysis

The freeze-dried AgNP/gelatin/PVA hydrogels were investigated by Energy-dispersive X-ray spectroscopy (EDX; Hitachi/S-4800; Japan) to analyze the element in hydrogels.

3.2.2.4 Silver-release

The circular disc of hydrogel with diameter of 15 mm were placed on the cellulose acetate (CA) membrane (diameter 25 mm, poresize 0.45 µm, VERTICAL®). This assembly was placed on the top of the cell body of Franz cell (15 ml) which full of PBS at 37°C. PBS was collected at a specific diffusion time point of 1, 3, 6, 12, and 24 h. The release of silver in the PBS was investigated by Atomic Absorption Spectrophotometer (Varian Model AA280FS) at Scientific and Technological Research Equiment Centre. A new hydrogel sample set was investigated for each time point.

3.2.3 Part III: Determination of the Cytotoxicity and Antibacterial Effects of AgNP/gelatin/PVA Hydrogels Using Fibroblast Cells and Bacteria (*In vitro* Test)

3.2.3.1 Indirect Cytotoxicity

The indirect cytotoxicity of the AgNP/gelatin/PVA hydrogels was implemented by an adaptation from the ISO10993-5 standard test method. The normal human dermal fibroblasts (NHDF; 11^{th}-15^{th} passage) were cultured in tissue-culture plate in serum-containing Dulbecco's modified Eagle's medium (DMEM). Numbers of cell were counting by Hemocytometer. The 10,000 cells were seeded in each well by using auto pipette.

NHDF were cultured for 24 h to make cell attachment. After the cell attachment, DMEM was replaced by serum-free medium (SFM). NHDF were starved with SFM for 24 h.

At the same time, an extraction media of hydrogel was prepared. The gelatin/PVA hydrogels and AgNP/Gelatin/PVA hydrogels were cut into tiny cubes. These cubes were immersed in SFM to obtain the extraction media for 24 and 72 h. The extraction ratio was 10 $mg \cdot mL^{-1}$ SFM in the wells with NHDF was replaced with the 24 h and 72 h extraction media. NHDF were incubated with the extraction media for 24 h. The viability of NHDF was determined by MTT assay (3-(4,5-dimethylthiazol-2-yl)-2,5-diphenyltetrazolium bromide) at the absorbance wavelength of 570 nm *(151)*. The absorbance [A] was measured by a Microplate Reader. Cell viability was determined by the following formula:

$$\text{Cell viability (\%)} = ([A]\ \text{test} / [A]\ \text{control}) \times 100 \quad (17)$$

Where "[A] test" represented the absorbance of solution in the well with hydrogels. "[A] control" represented the absorbance of solution in a blank well.

3.2.3.2 Antibacterial Testing

Three types of bacteria were selected for antibacterial testing of AgNP/gelatin/PVA hydrogels. There were *Staphylococcus aureus* (*S. aureus*; Gram-positive; ATCC 25023), Methicillin-resistant *S. aureus* (MRSA; Gram-positive; ATCC 43300), and *Escherichia coli* (*E. coli*; Gram-negative; ATCC 25922). The gelatin/PVA hydrogels with no AgNPs were used as the control group. MRSA was kindly provided from Microbiology Laboratory, Pramongkutkao Hospital, Bangkok, Thailand.

(1) Antimicrobial Activity Assays

This assay was adapted from the report of Siriporn Theapsak (2012) *(152)*. A broth solution was prepared by mixing Nutrient Broth (NB), pH 6.9 without NaCl (Sisco Research Laboratories) with 100 ml of sterile deionized water. Two colonies of bacteria were put into broth solutions and cultured at 37°C in a shaking incubator at a speed of

150 rpm for 24 h. The bacterial suspensions of *E. coli*, *S. aureus*, and MRSA were diluted by 0.85% sterile NaCl aqueous solution at dilution factor of 10^5, 10^6, and 10^3 respectively. The circular disc of hydrogel with diameter of 15 mm (approximately 0.65 g) were immersed in the diluted bacterial suspensions and incubated at 37°C in a shaking incubator at a speed of 150 rpm for 3 h. Each hydrogel disc (one disc for each $AgNO_3$ concentration) was immersed in 10 ml of the diluted bacterial suspensions in a test tube. Next, 100 µL of the suspension from each test tube was spread on NB agar plate (in triplicate) and incubated at 37°C for 24 h. The bacteria colonies on agar plate were counted. The anti-bacterial efficacy (ABE in %) of the hydrogels was calculated by the following formula:

$$ABE\ (\%) = (V_c - V_t)/V_c \times 100 \quad (18)$$

where V_c is the numbers of viable bacterial colonies of the control group and V_t is the numbers of viable bacterial colonies from the plate of AgNP/Gelatin/PVA hydrogels.

(2) Zone of Inhibition Test

This test was performed according to US Clinical and Laboratory Standards Institute (CLSI) disc diffusion method. The bacterial suspension was spread on the NB agar in a petri dish. The circular disc of hydrogel with a diameter of 15 mm, vancomycin and gentamicin, which were used as control antibacterial drugs for gram-positive bacteria and gram-negative bacteria, were placed on the NB agar and then incubated at 37°C for 24 h. After that, the clear zones which the area on NB agar had no growth of bacteria were measured.

3.2.4 Statistical Analysis

Data was presented in the form of means ± standard deviation (S.D.). A t-test was used as statistical analysis (Data Analysis; Excel 2007; Microsoft). The statistical significance was accepted at 0.05 confidence level ($p < 0.05$).

CHAPTER 4
RESULTS

This chapter was divided into three parts. First part described results from preparation and characterization of gelatin hydrogel and gelatin/PVA hydrogel. Second part demonstrated the results of gelatin/PVA hydrogel containing AgNPs testing. The last part was the effects of gelatin/PVA hydrogels containing AgNPs on fibroblast cells and bacteria.

Part I: Preparation and Characterization of Gelatin Hydrogel and Gelatin/PVA Hydrogel

After gamma irradiation, cross-linked hydrogel was successfully obtained as shown in Figure 4.1. The appearance of gelatin hydrogel and gelatin/PVA hydrogel was quite transparent. A neat gelatin hydrogels were pale yellow and the gelatin/PVA hydrogels showed slightly white opaqueness. The hydrogels in this research were prepared in a sheet form with an approximate thickness of 3.6-4.1 mm. Table A.1 (APPENDIX A) shows the thickness of gelatin and gelatin/PVA hydrogels.

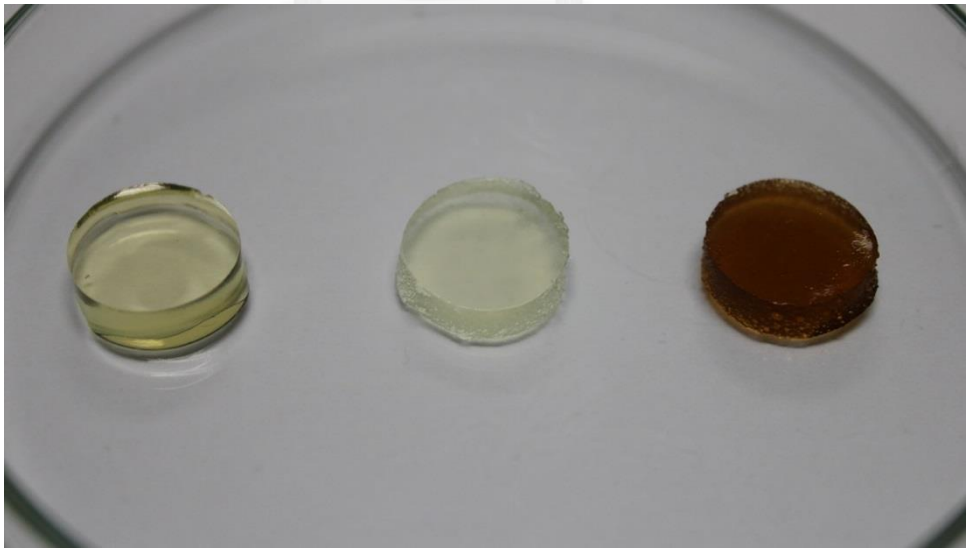

Figure 4.1 As-prepared hydrogels Left: neat gelatin, middle: gelatin/PVA, and right: gelatin/PVA with $AgNO_3$.

4.1 Water Holding Capacity and Swelling Ratio

Liquid absorption is the important property of hydrogels. Table 4.1 shows water holding capacity of gelatin and gelatin/PVA hydrogels. All hydrogels showed similar water holding capacities, which were approximately 94-96%. It was noticed that water holding capacity tended to be decreased when irradiation dose was increased. Water holding capacity of 100:0 hydrogel irradiated at 30 kGy was greater than 100:0 hydrogel irradiated at 40 and 50 kGy. There was a significant difference between water holding capacity of 80:20 hydrogel which irradiated at 30 kGy and 80:20 hydrogel which irradiated at 50 kGy. Water holding capacity of 60:40 hydrogel which irradiated at 30 kGy was greater than 60:40 hydrogel which irradiated at 50 kGy. The result revealed that water holding capacity was decreased when the amount of PVA was highest. There were significant differences between water holding capacity of 60:40 hydrogels and 100:0 hydrogels at every irradiation doses.

Table 4.1 Water holding capacity (%) of gelatin/PVA hydrogels

Gelatin:PVA hydrogels	Irradiation dose (kGy)		
	30	40	50
100:0	96.64 ± 0.25 ^{a,b}	95.51 ± 0.03 ^{a}	95.07 ± 0.40 ^{b}
80:20	96.69 ± 0.44 ^{c}	95.79 ± 0.90	94.34 ± 0.44 ^{c}
60:40	95.46 ± 0.65 ^{*,d}	94.71 ± 0.47 *	94.12 ± 0.24 ^{*,d}

A significant difference ($p < 0.05$) among the same hydrogel type is denoted by the same letter. An asterisk (*) represented a significant difference at $p < 0.05$ between gelatin/PVA and neat gelatin hydrogels in the same irradiation dose.

In this experiment, water holding capacity and swelling ratio were calculated. Water holding capacity was calculated from the weight of dried hydrogel to determine the hydrogel's ability to hold or retain water. Swelling behavior of hydrogels was determined by swelling ratio testing. Swelling ratio was calculated from the weight of initial hydrogels. Figure 4.2 shows swelling ratio of gelatin/PVA hydrogels. It was seen that swelling ratio was decreased when the irradiation dose was increased. Swelling ratio was in the range

of approximately 115-230 %. Swelling ratio of 100:0 hydrogel which irradiated at 30 kGy was greater than 100:0 hydrogel which irradiated at 40 and 50 kGy. There was also a significant difference between swelling ratio of 100:0 hydrogel which irradiated at 40 kGy and 100:0 hydrogel which irradiated at 50 kGy. A significant difference among swelling ratio of 80:20 hydrogels was not found. Swelling ratio of 60:40 hydrogel which irradiated at 30 kGy was greater than 60:40 hydrogel which irradiated at 50 kGy. A significant difference between swelling ratio of neat gelatin hydrogels and gelatin/PVA hydrogels was not found.

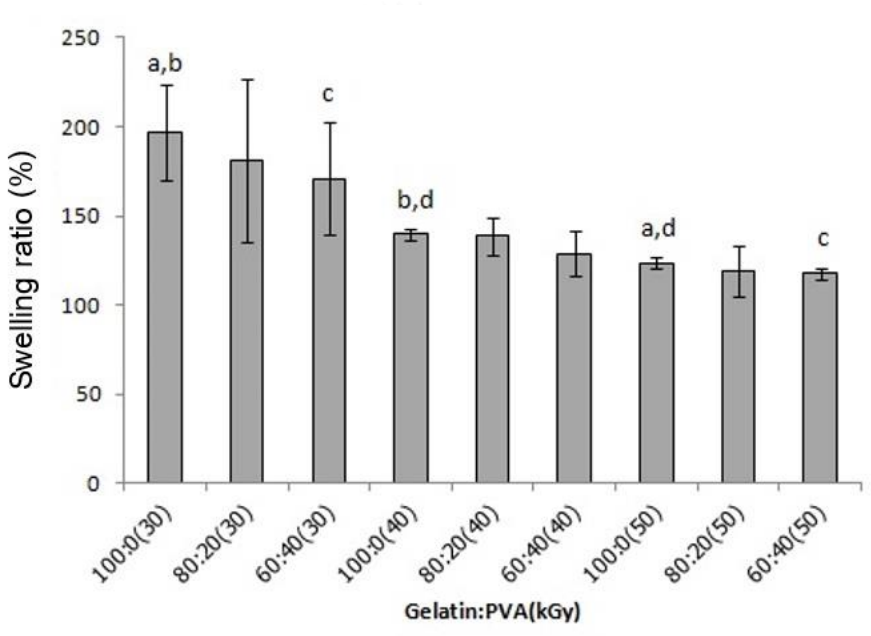

Figure 4.2 Swelling ratio of gelatin/PVA hydrogels.

A significant difference ($p < 0.05$) among the same hydrogel type is denoted by the same letter. An asterisk (*) represented a significant difference at $p < 0.05$ between gelatin/PVA and neat gelatin hydrogels in the same irradiation dose.

4.2 Water Vapor Transmission Rate (WVTR)

Figure 4.3 shows WVTR of gelatin/PVA hydrogels. Range of WVTR was about 3,000-5,400 g/m^2/day. It was seen that WVTR was decreased when the amount of PVA was increased or irradiation dose was increased. WVTR of 100:0 hydrogel which irradiated at 30 kGy was greater than 100:0 hydrogel which irradiated at 50 kGy. A

significant difference among WVTR of 80:20 hydrogels was not found. WVTR of 60:40 hydrogel which irradiated at 30 kGy was greater than 60:40 hydrogel which irradiated at 40 and 50 kGy. Moreover, there were significant differences between WVTR of 60:40 hydrogels and 100:0 hydrogels at every irradiation doses.

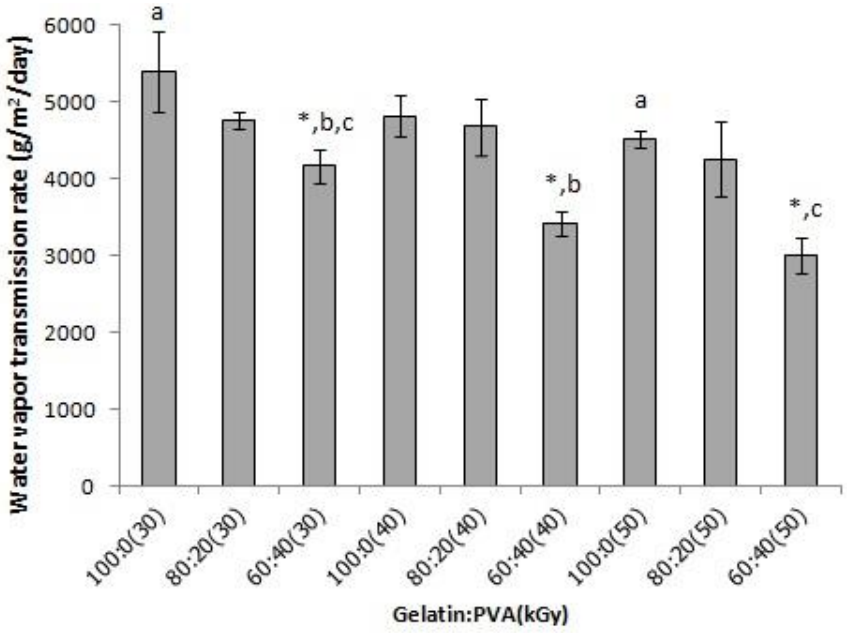

Figure 4.3 Water vapor transmission rate of gelatin/PVA hydrogels.

A significant difference ($p < 0.05$) among the same hydrogel type is denoted by the same letter. An asterisk (*) represented a significant difference at $p < 0.05$ between gelatin/PVA and neat gelatin hydrogels in the same irradiation dose.

4.3 Percentage Strain at Maximum Load and Stress at Maximum Load (Mechanical Strength)

The tensile properties of gelatin/PVA hydrogels were tested. Figure 4.4 shows percentage strain at maximum load of gelatin/PVA hydrogels. Percentage strain at maximum load of hydrogels varied between 50-180 %. It was seen that percentage strain at maximum load was increased when the amount of PVA was increased or irradiation dose was increased. Percentage strain at maximum load of 100:0 hydrogel which irradiated at 30 kGy was greater than 100:0 hydrogel which irradiated at 40 and 50 kGy.

A significant difference among percentage strain at maximum load of 80:20 hydrogels was not found. Percentage strain at maximum load of 60:40 hydrogel which irradiated at 30 kGy was greater than 60:40 hydrogel which irradiated at 50 kGy. There were significant differences between percentage strain at maximum load of neat gelatin hydrogels and gelatin/PVA hydrogels at every irradiation doses.

Figure 4.5 shows stress at maximum load of gelatin/PVA hydrogels. Stress at maximum load of gelatin/PVA hydrogels were about 0.028-0.043 N/mm^2. It was observed that stress at maximum load of 100:0 hydrogel was decreased when irradiation dose was increased. Stress at maximum load of 100:0 hydrogel which irradiated at 30 kGy was greater than 100:0 hydrogel which irradiated at 40 and 50 kGy. There was also a significant difference between stress at maximum load of 100:0 hydrogel which irradiated at 40 kGy and 100:0 hydrogel which irradiated at 50 kGy. A significant difference among stress at maximum load of 80:20 hydrogels was not found. There was a significant difference between stress at maximum load of 60:40 hydrogels which were irradiated at 30 and 40 kGy. Moreover, there was a significant difference between stress at maximum load of 100:0 hydrogel which irradiated at 50 kGy and 80:20 hydrogel which irradiated at 50 kGy.

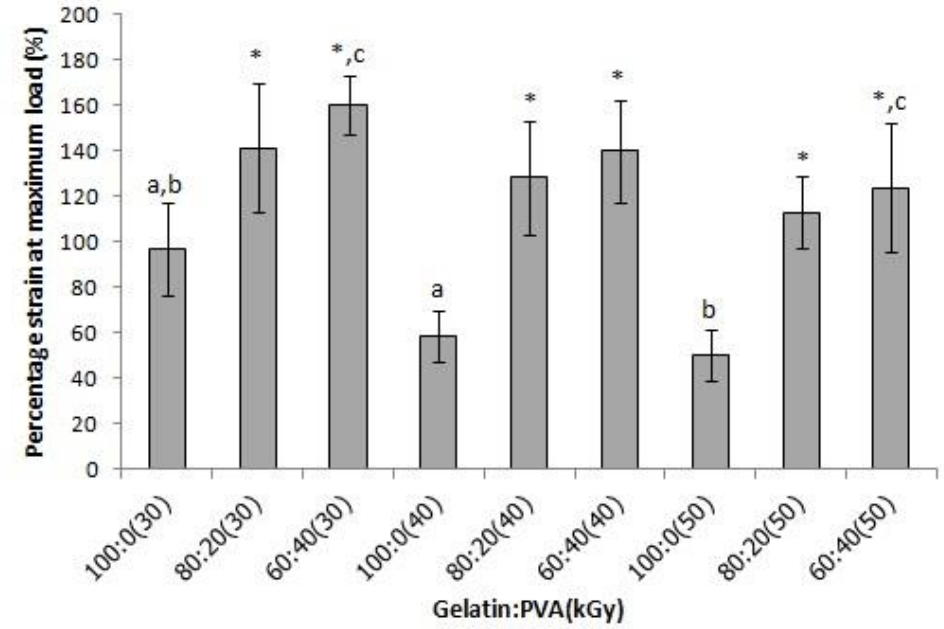

Figure 4.4 Percentage strain at maximum load of gelatin/PVA hydrogels.

A significant difference ($p < 0.05$) among the same hydrogel type is denoted by the same letter. An asterisk (*) represented a significant difference at $p < 0.05$ between gelatin/PVA and neat gelatin hydrogels in the same irradiation dose.

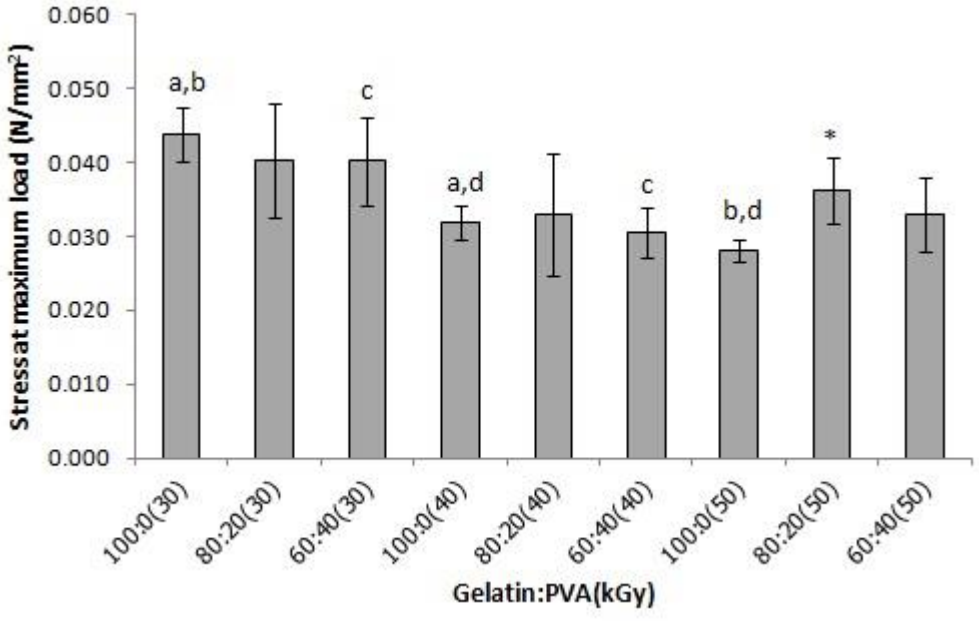

Figure 4.5 Stress at maximum load of gelatin/PVA hydrogels.

A significant difference ($p < 0.05$) among the same hydrogel type is denoted by the same letter. An asterisk (*) represented a significant difference at $p < 0.05$ between gelatin/PVA and neat gelatin hydrogels in the same irradiation dose.

4.4 Gel fraction

Gel fraction of hydrogels was tested and used to indirectly evaluate the degree of crosslinking. From Figure 4.6, range of gel fractions of hydrogel was 64 and 89%. The gelatin/PVA hydrogels with higher irradiation dose or more PVA contents had increasing gel fractions. A significant difference was not found among the 100:0 hydrogels which irradiated at 30, 40, and 50 kGy. Gel fraction of 80:20 hydrogel which irradiated at 50 kGy was greater than 80:20 hydrogel which irradiated at 30 and 40 kGy. Gel fraction of 60:40 hydrogel which irradiated at 30 kGy was lower than 60:40 hydrogel which irradiated at 40 and 50 kGy. There was a significant difference between gel fraction of 60:40 hydrogel which irradiated at 40 kGy and 100:0 hydrogel which irradiated at the same irradiation dose. Gel fraction of 80:20 hydrogel which irradiated at 50 kGy was significantly different compared to 100:0 hydrogel which irradiated at the same irradiation dose. Moreover, there was significant difference between gel fraction of 60:40 hydrogel which irradiated at 50 kGy and 100:0 hydrogel which irradiated at the same irradiation dose.

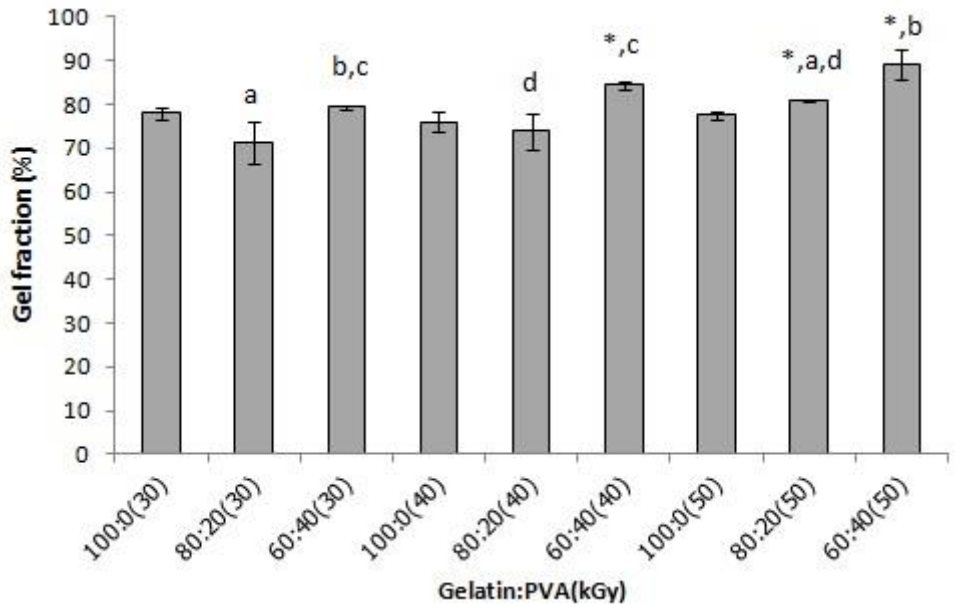

Figure 4.6 Gel fraction of gelatin/PVA hydrogels.

A significant difference ($p < 0.05$) among the same hydrogel type is denoted by the same letter. An asterisk (*) represented a significant difference at $p < 0.05$ between gelatin/PVA and neat gelatin hydrogels in the same irradiation dose.

4.5 *In vitro* Biodegradation

The hydrogel samples were incubated in PBS with 1 × 10^4 U/ml of lysozyme concentration. Lysozyme can be found in wound and blister fluid *(153)*. Figure 4.7 shows the remaining weight after biodegradation of the gelatin/PVA hydrogels for 24 h. Range of remaining weight was around 40-75 %. The hydrogels with higher irradiation dose or more PVA contents showed quite higher remaining weight. A significant difference among remaining weight of gelatin/PVA hydrogels was not found.

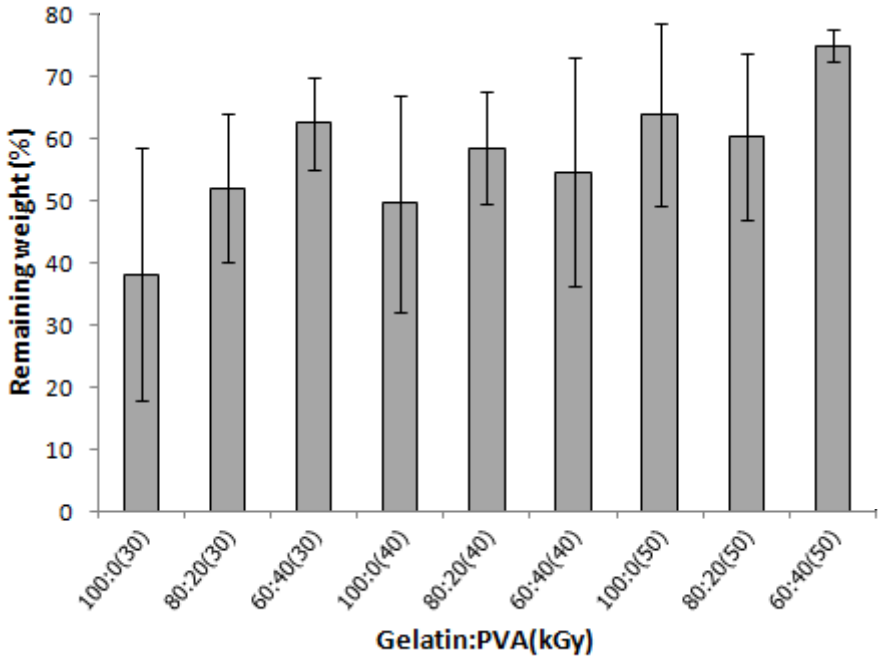

Figure 4.7 Remaining weight after 24 h *in vitro* biodegradation of gelatin/PVA hydrogels without AgNPs

A significant difference ($p < 0.05$) among the same hydrogel type is denoted by the same letter. An asterisk (*) represented a significant difference at $p < 0.05$ between gelatin/PVA and neat gelatin hydrogels in the same irradiation dose.

Part II: Preparation and Characterization of Gelatin/PVA Hydrogel Containing AgNPs

From the results of hydrogel property in Part I, the 60:40 gelatin/PVA hydrogel with 30 kGy irradiation dose was chosen for further study of AgNPs addition since it had highest percentage strain at maximum load, appropriate water holding capacity, and acceptable remaining weight after biodegradation testing. After irradiation, the gelatin/PVA hydrogels with $AgNO_3$ was brown as shown in Figure 4.1. The appearance of brown color, which is a result from surface plasmon excitation, indicates the occurrence of AgNPs in hydrogel structure *(154, 155)*. Table A.2 (APPENDIX A) shows the thickness of AgNP/gelatin/PVA hydrogels compared with gelatin/PVA hydrogel without AgNPs. The thicknesses of AgNP/gelatin/PVA hydrogels were approximately 3.6-4.1 mm, which is similar to the thickness of gelatin/PVA hydrogel without AgNPs (3.7 mm). In this part, results of 60:40 hydrogel with $AgNO_3$ at 30 kGy irradiation dose were shown, comparing to the ones without $AgNO_3$ at the same irradiation dose.

4.6 Water Holding Capacity and Swelling Ratio

Table 4.2 shows the percentage of water holding capacity of AgNP/gelatin/PVA hydrogels compared with gelatin/PVA hydrogel without $AgNO_3$. Range of water holding capacity percentages of hydrogels with $AgNO_3$ were approximately 95-98 %. A significant difference was found between the water holding capacity of 60:40 hydrogels without $AgNO_3$ and hydrogels with $AgNO_3$ 0.75 wt%.

Table 4.2 Water holding capacity of AgNP/gelatin/PVA hydrogels compared with gelatin/PVA hydrogel without $AgNO_3$.

Hydrogels	$AgNo_3$ wt%				
Gelatin:PVA	0.00	0.25	0.50	0.75	1.00
60:40 (30 kGy)	95.46 ± 0.65	95.86 ± 0.16	96.11 ± 0.03	98.06 ± 0.26 #	96.78 ± 0.14

A hash (#) represented a significant difference at $p < 0.05$ relative to 60:40 hydrogels (30 kGy) without $AgNO_3$.

Figure 4.8 shows swelling ratio of AgNP/gelatin/PVA hydrogels compared with gelatin/PVA hydrogel without $AgNO_3$. Swelling ratio of AgNP/gelatin/PVA hydrogels were about 166-231 %. Swelling ratios of hydrogels with $AgNO_3$ 0.25 and 0.50 wt% were significantly different compared with swelling ratio of 60:40 hydrogels without $AgNO_3$.

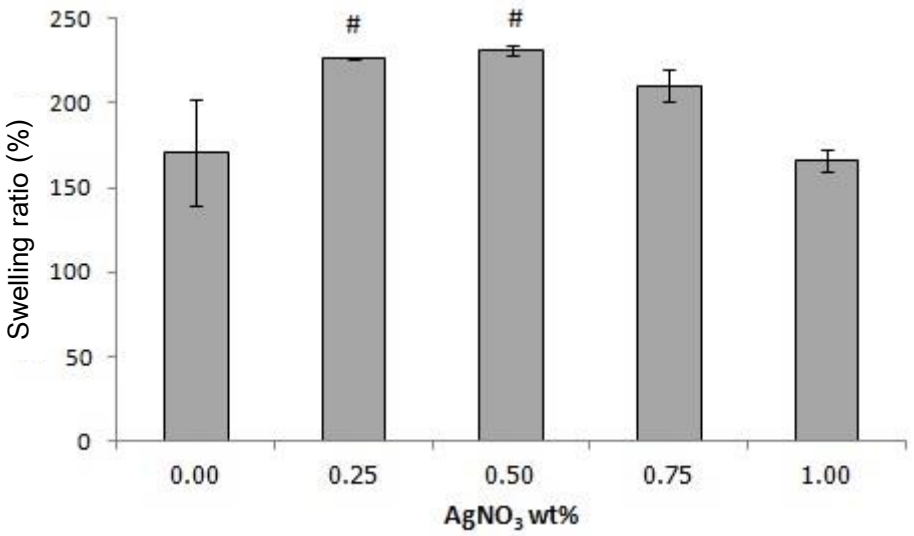

Figure 4.8 Percentages of swelling ratio of AgNP/gelatin/PVA hydrogels compared with gelatin/PVA hydrogel without $AgNO_3$.

A hash (#) represented a significant difference at $p < 0.05$ relative to 60:40 hydrogels (30 kGy) without $AgNO_3$.

4.7 Water Vapor Transmission Rate (WVTR)

Figure 4.9 shows WVTR of AgNP/gelatin/PVA hydrogels compared with gelatin/PVA hydrogel without $AgNO_3$. WVTR of AgNP/gelatin/PVA hydrogels was approximately 4250-4645 g/m^2/day. The significant difference was not found among all samples.

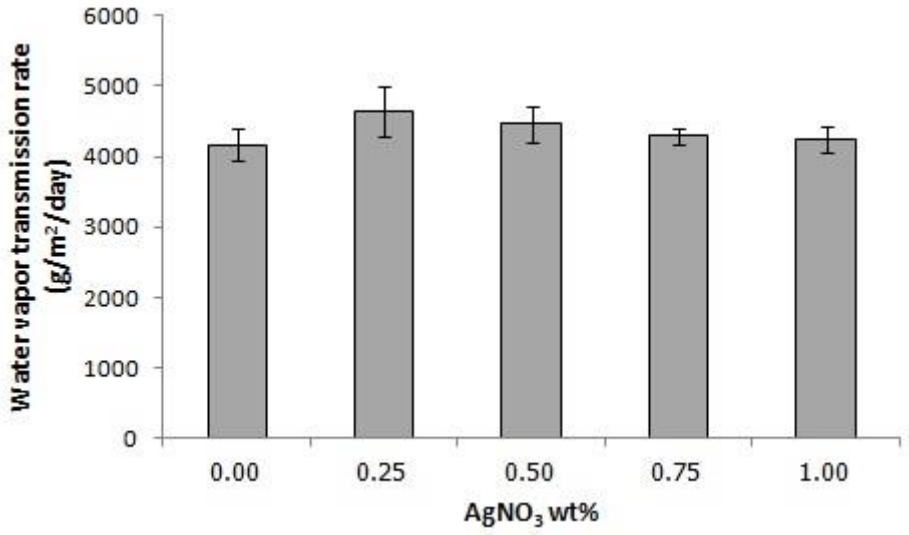

Figure 4.9 Water vapor transmission rate of AgNP/gelatin/PVA hydrogels compared with gelatin/PVA hydrogel without $AgNO_3$

A hash (#) represented a significant difference at $p < 0.05$ relative to 60:40 hydrogels (30 kGy) without $AgNO_3$.

4.8 Percentage Strain at Maximum Load and Stress at Maximum Load (Mechanical Strength)

Figure 4.10 shows percentage strain at maximum load of AgNP/gelatin/PVA hydrogels compared with gelatin/PVA hydrogel without $AgNO_3$. Percentage strain at maximum load of AgNP/gelatin/PVA hydrogels were approximately 99-179%. There were significant differences between percentage strain at maximum load of hydrogels with $AgNO_3$ 0.75 and 1.00 wt% compared with 60:40 hydrogels without $AgNO_3$. Percentage strain at maximum load was significantly decreased when the amount of $AgNO_3$ was greater or equal 0.75 wt%.

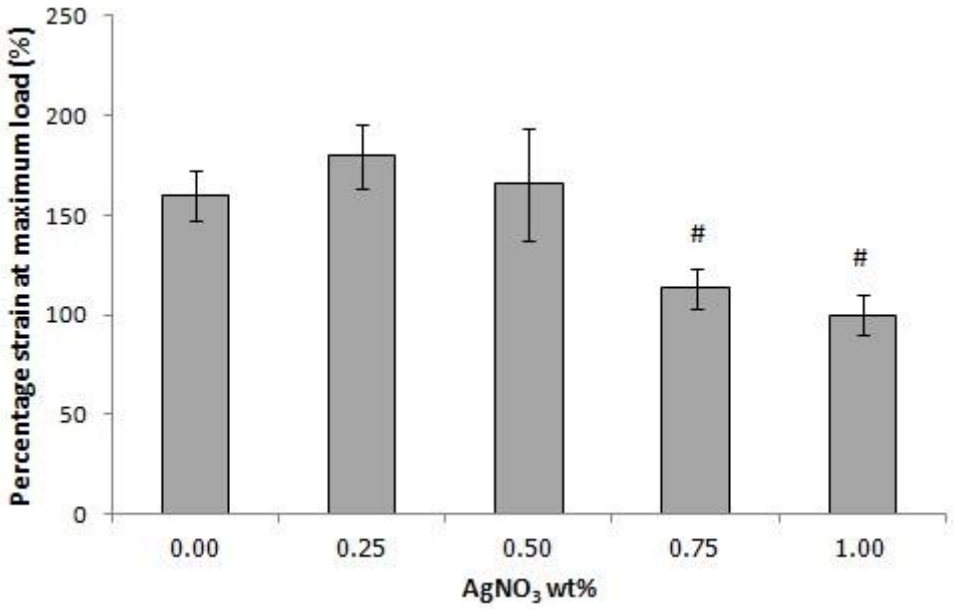

Figure 4.10 Percentage strain at maximum load of AgNP/gelatin/PVA hydrogels compared with gelatin/PVA hydrogel without AgNPs.

A hash (#) represented a significant difference at $p < 0.05$ relative to 60:40 hydrogels (30 kGy) without $AgNO_3$.

Figure 4.11 shows stress at maximum load of AgNP/gelatin/PVA hydrogels compared with gelatin/PVA hydrogel without $AgNO_3$. Stress at maximum load of hydrogels with $AgNO_3$ was about 0.012-0.025 N/mm^2. There were significant differences between stress at maximum load of all AgNP/gelatin/PVA hydrogels compared with gelatin/PVA hydrogel without $AgNO_3$. Stress at maximum load of AgNP/gelatin/PVA hydrogels was compare with each other. There were significant differences between stress at maximum load of hydrogels with $AgNO_3$ 0.25, 0.50, 0.75 and 1.00 wt%. However, there was no significant difference between stress at maximum load of hydrogel with $AgNO_3$ 0.75 wt% compared with hydrogel with $AgNO_3$ 1.0 wt%. It was found that percentage strain at maximum load and stress at maximum load was decreased when the amount of $AgNO_3$ was increased.

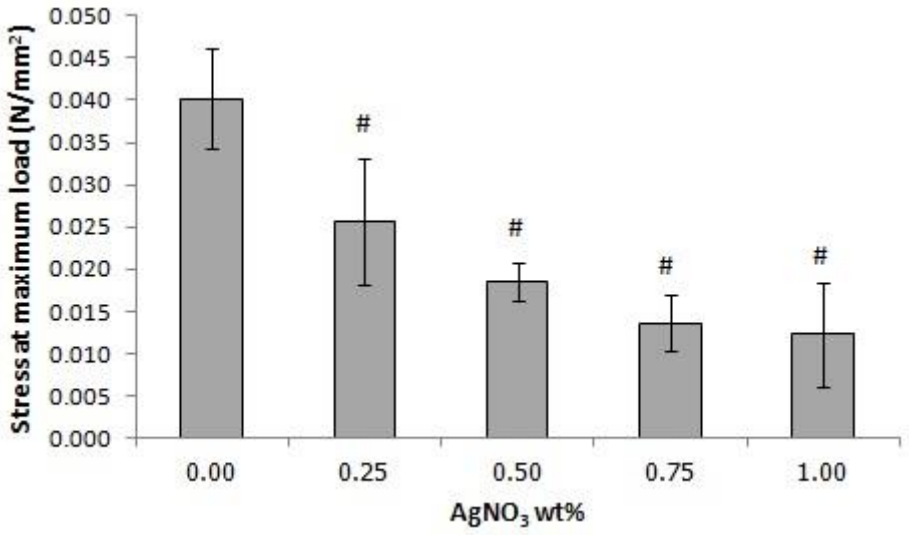

Figure 4.11 Stress at maximum load of AgNP/gelatin/PVA hydrogels compared with gelatin/PVA hydrogel without AgNPs.

A hash (#) represented a significant difference at $p < 0.05$ relative to 60:40 hydrogels (30 kGy) without $AgNO_3$.

4.9 Gel fraction

Figure 4.12 shows gel fraction of AgNP/gelatin/PVA hydrogels compared with gelatin/PVA hydrogel without AgNPs. Percentages of gel fraction of AgNP/gelatin/PVA hydrogels were in the range of 64-77 %, approximately. Gel fraction was decreased when the amount of $AgNO_3$ was increased. There were significant differences between gel fractions of hydrogels with $AgNO_3$ 0.50, 0.75 and 1.00 wt% compared with 60:40 hydrogels without $AgNO_3$. There were significant differences between gel fraction of hydrogels with $AgNO_3$ 0.25, 0.50, 0.75 and 1.00 wt%. However, there was no significant difference between gel fraction of hydrogel with $AgNO_3$ 0.75 wt% compared with hydrogel with $AgNO_3$ 1.0 wt%.

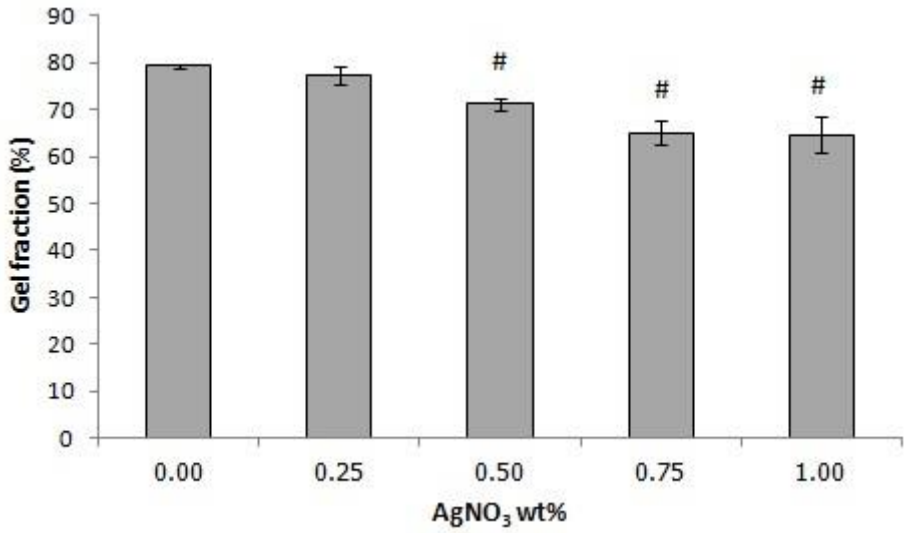

Figure 4.12 Gel fraction of AgNP/gelatin/PVA hydrogels compared with gelatin/PVA hydrogel without AgNPs.

A hash (#) represented a significant difference at $p < 0.05$ relative to 60:40 hydrogels (30 kGy) without $AgNO_3$.

4.10 *In vitro* biodegradation

In the previous part, the biodegradation of gelatin/PVA hydrogels was tested for 24 h. In this part, we tested the *in vitro* biodegradation of hydrogels for 6, 12, 18, and 24 h. Figure 4.13 showed the degradation of the hydrogels with and without $AgNO_3$ for 6, 12, 18, and 24 h. Remaining weights were in the range of 36-91 %. There were significant differences between remaining weights of hydrogels with and without $AgNO_3$ in the same duration of time. However, there was no significant difference between remaining weights of hydrogels without $AgNO_3$ and hydrogels with $AgNO_3$ 0.25 wt% at 24 h. There was no significant difference between remaining weights of hydrogels without $AgNO_3$ and hydrogels with $AgNO_3$ 0.50 wt% at 12 h.

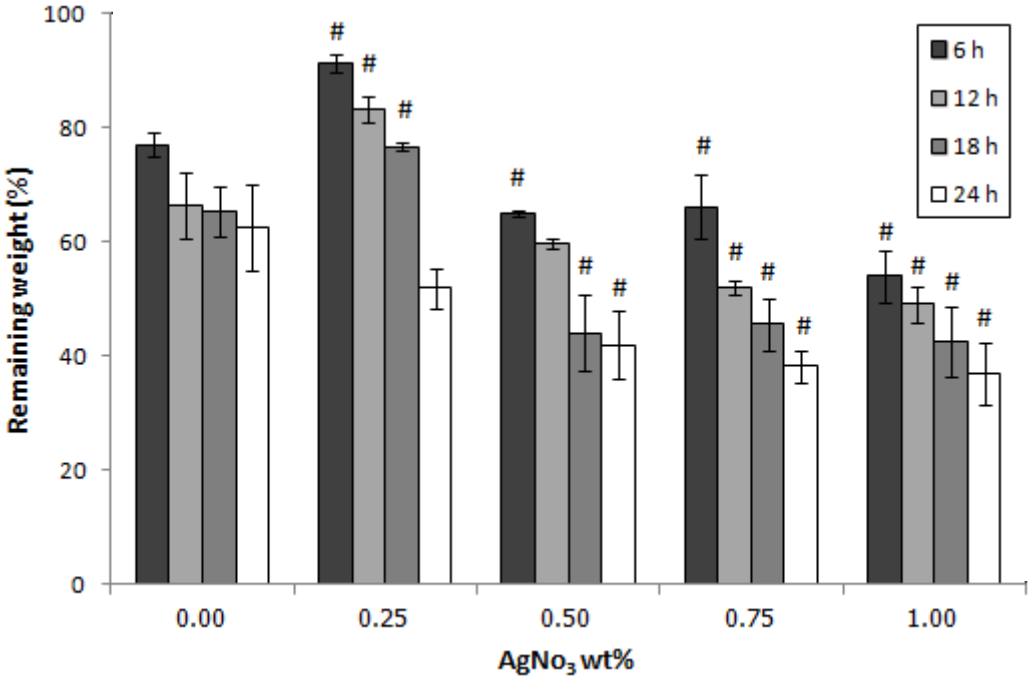

Figure 4.13 Remaining weight after *in vitro* biodegradation of AgNP/gelatin/PVA hydrogels compared with gelatin/PVA hydrogel without AgNPs in PBS with lysozyme for various incubation time.

A hash (#) represented a significant difference at $p < 0.05$ relative to the remaining weight of 60:40 hydrogels (30 kGy) without $AgNO_3$ at the same incubation time.

4.11 Morphology

SEM images of hydrogels were shown in Figure 4.14. The hydrogels showed porous network structures. The appearances of pores were elliptical and irregular shapes. The pore diameter was approximately 1-5 μm. However, the nanoparticles in the structures of hydrogels were not observed in the SEM images.

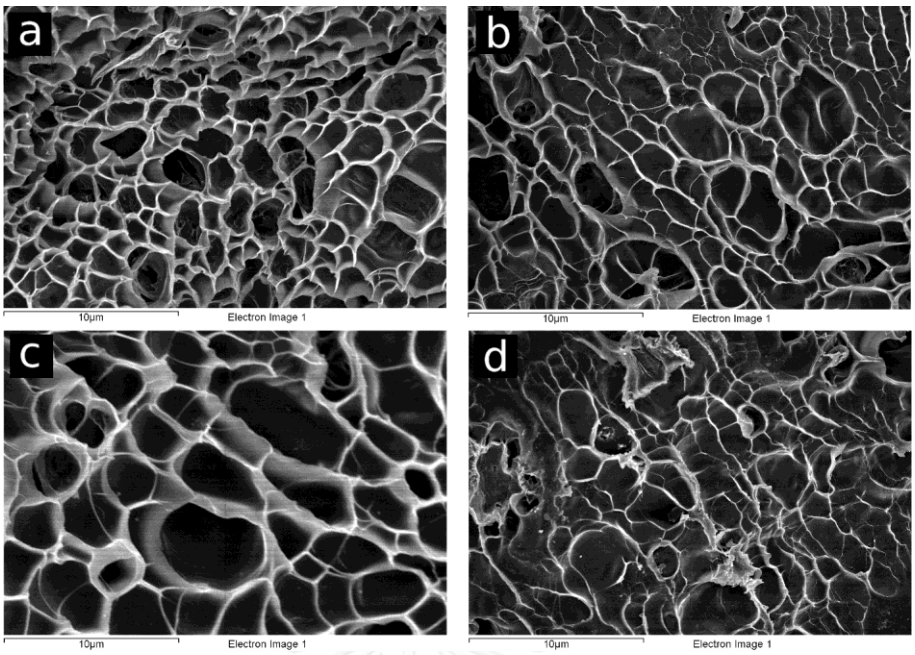

Figure 4.14 Representative SEM images (scale bar = 10 µm) of AgNP/gelatin/PVA (60:40) hydrogels with (a) $AgNO_3$ 0.25 wt%, (b) $AgNO_3$ 0.50 wt%, (c) $AgNO_3$ 0.75 wt%, and (d) $AgNO_3$ 1.00 wt%.

4.12 Chemical Bondings and Functional Groups

FTIR spectra of the hydrogels at 100:0, 60:40, and 60:40 with $AgNO_3$ 1.00 wt%, which were irradiated at 30 kGy, are shown in Figure 4.15. According to the characteristic of IR absorption bands in Table 4.3, FTIR spectrum of neat gelatin hydrogel showed a peak at 3289, 2920, 1630, and 1528 cm^{-1} corresponding to –NH stretching of the secondary amide, C-H stretching, C=O stretching, and N-H bending, respectively.

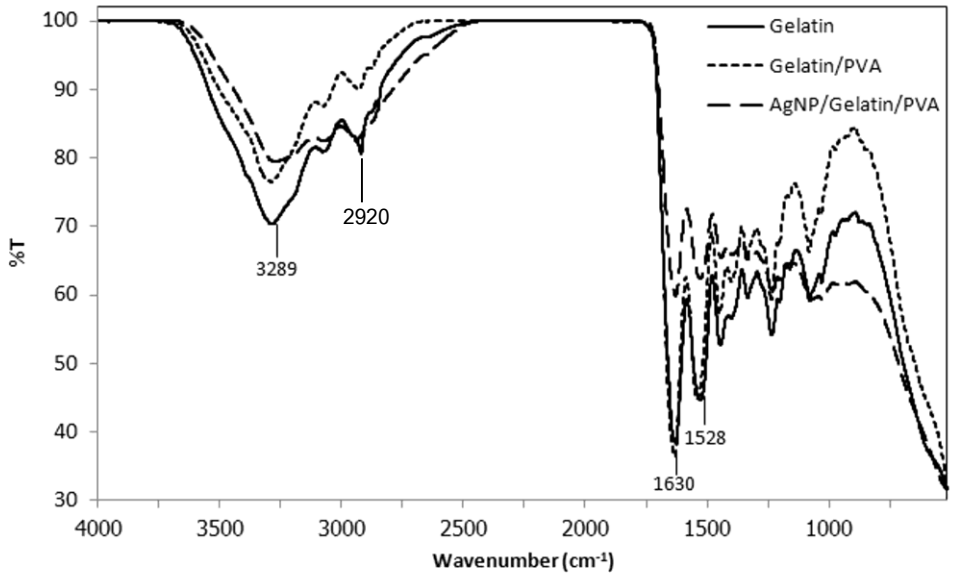

Figure 4.15 FTIR spectra of gelatin, gelatin/PVA, and AgNP/gelatin/PVA hydrogels.

Table 4.3 Characteristic of IR absorption bands

Frequency (cm^{-1})	Functional group
3400-3200	N-H stretching band
3100-2800	C-H stretching band
1660-1600	C=O stretching band
1565-1500	C-N-H bending band
1480-1300	C-H bending band

Reference: Derrick, M. R., 1999. *(156)*

Characterization of AgNPs Formation

4.13 SPR Phenomenon

An optical property of AgNPs is one of the property to be used to confirm the formation of AgNPs. A characteristic peak of surface plasmon resonance (SPR) band of AgNPs is around 410-430 nm *(104, 157-160)*. As seen in Figure 4.16, there was no sign of peak or shoulder of spectra of hydrogels without $AgNO_3$. The spectra of gelatin/PVA hydrogel with $AgNO_3$ 0.25 wt% showed a shoulder between approximately 372 nm and

439 nm. The gradual declines were found in the spectrum of gelatin/PVA hydrogel with $AgNO_3$ 0.50, 0.75, and 1.00 wt%.

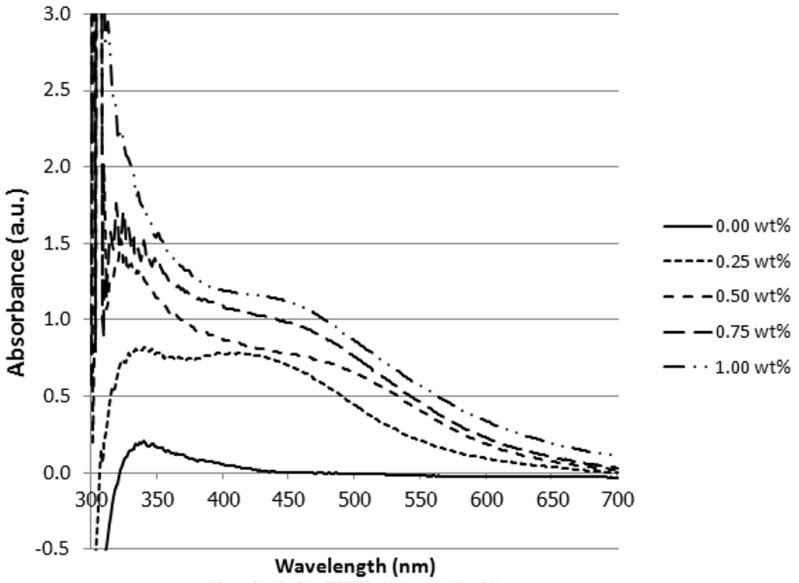

Figure 4.16 UV-vis absorption spectra of gelatin/PVA hydrogel and gelatin/PVA hydrogels with $AgNO_3$ 0.25, 0.50, 0.75, and 1.00 wt%.

4.14 Diameters of AgNPs and Elemental Analysis

The TEM micrographs of the AgNPs are shown in Figure 4.17. The sizes of the AgNPs in this study are quite small. The sizes, which represent as mean ± SD, of AgNPs in gelatin/PVA hydrogel with $AgNO_3$ 0.25, 0.50, 0.75, and 1.00 wt% are 4 ± 1, 3 ±1, 4 ± 1, and 4 ± 1 nm, respectively. The size distributions of AgNPs are shown in Figure 4.18. The largest particles have a diameter of 8 nm which are good for antibacterial performance. The nanoparticles with diameters less than 10 nm have high efficiency for antibacterial activity. These small particles can attach bacteria directly *(126)*. Moreover, the TEM images in Figure 4.17 demonstrated that the hydrogel structure can prevent the aggregation of AgNPs.

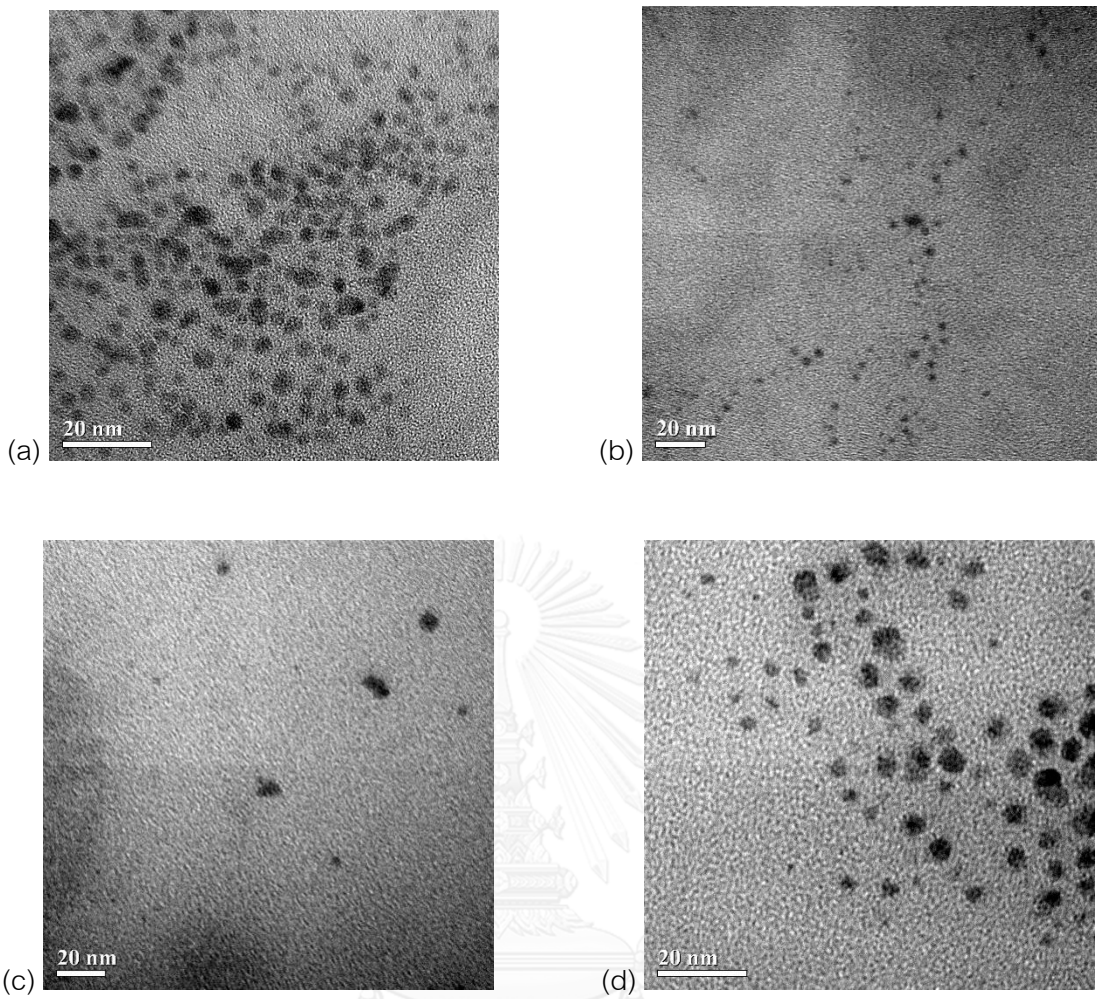

Figure 4.17 TEM images (scale bar = 20 nm) of AgNPs in AgNP/gelatin/PVA hydrogels (a) 0.25 wt%, (b) 0.50 wt%, (c) 0.75 wt%, (d) 1.00 wt%

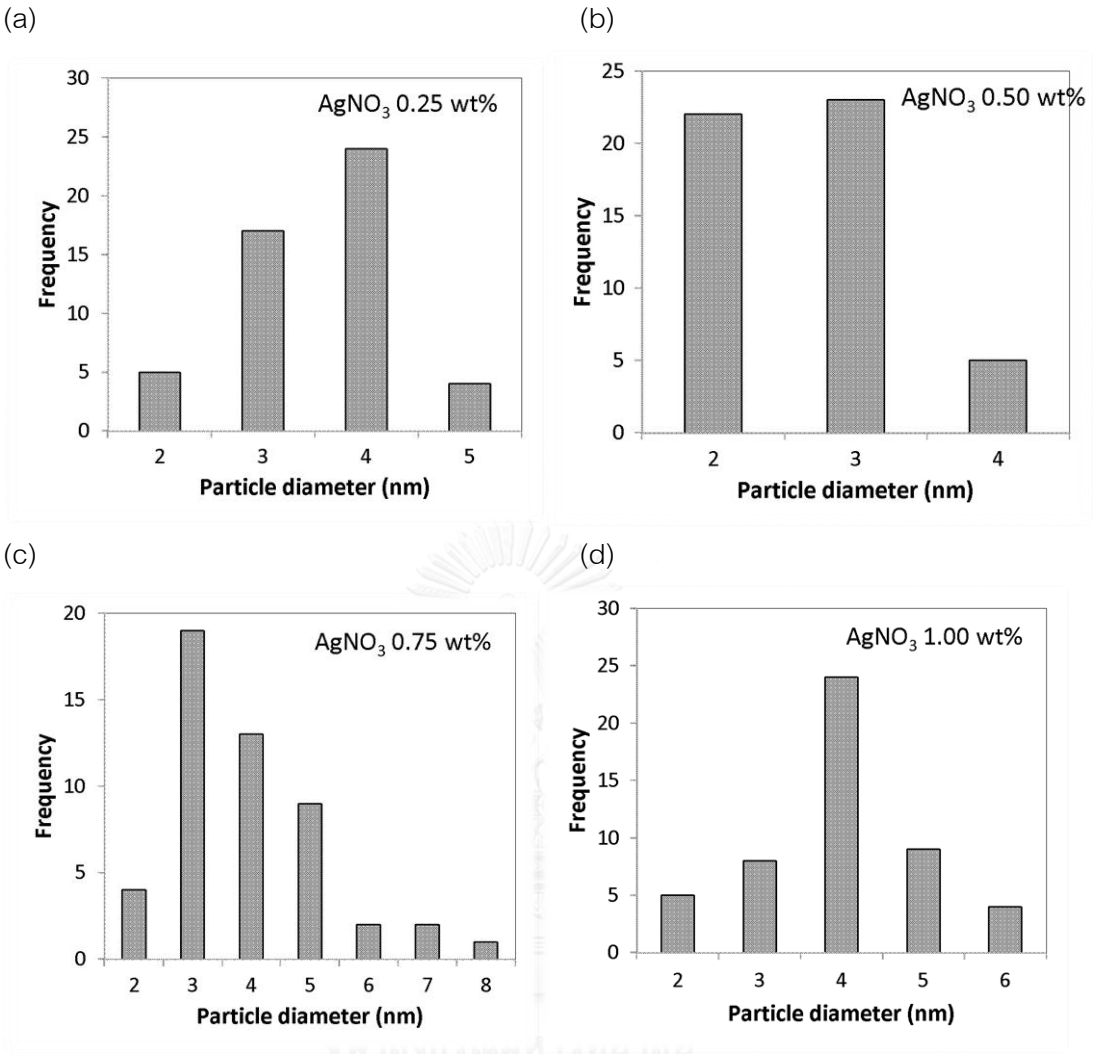

Figure 4.18 Size distribution of AgNPs in gelatin/PVA hydrogel with $AgNO_3$ (The diameters of particles in the TEM images were sized by SemAfore program.) (a) $AgNO_3$ 0.25 wt%, (b) $AgNO_3$ 0.50 wt%, (c) $AgNO_3$ 0.75 wt%, and (d) $AgNO_3$ 1.00 wt%.

Figure 4.19 shows the results of EDX analysis which confirm the persistence of silver element in the hydrogel structure. In Figure 4.19, the EDX spectrum displays characteristic L-series peaks of silver which located between 2.63 to 3.82 keV *(161)*. EDX peaks of silver (Ag) were observed in all hydrogels. Table 4.4 shows the proportion of carbon, oxygen, and silver element in hydrogels with $AgNO_3$ by EDX. The weight percentage of silver was increased when the amount of $AgNO_3$ was increased. The weight percentage of silver was higher than the amount of $AgNO_3$ added.

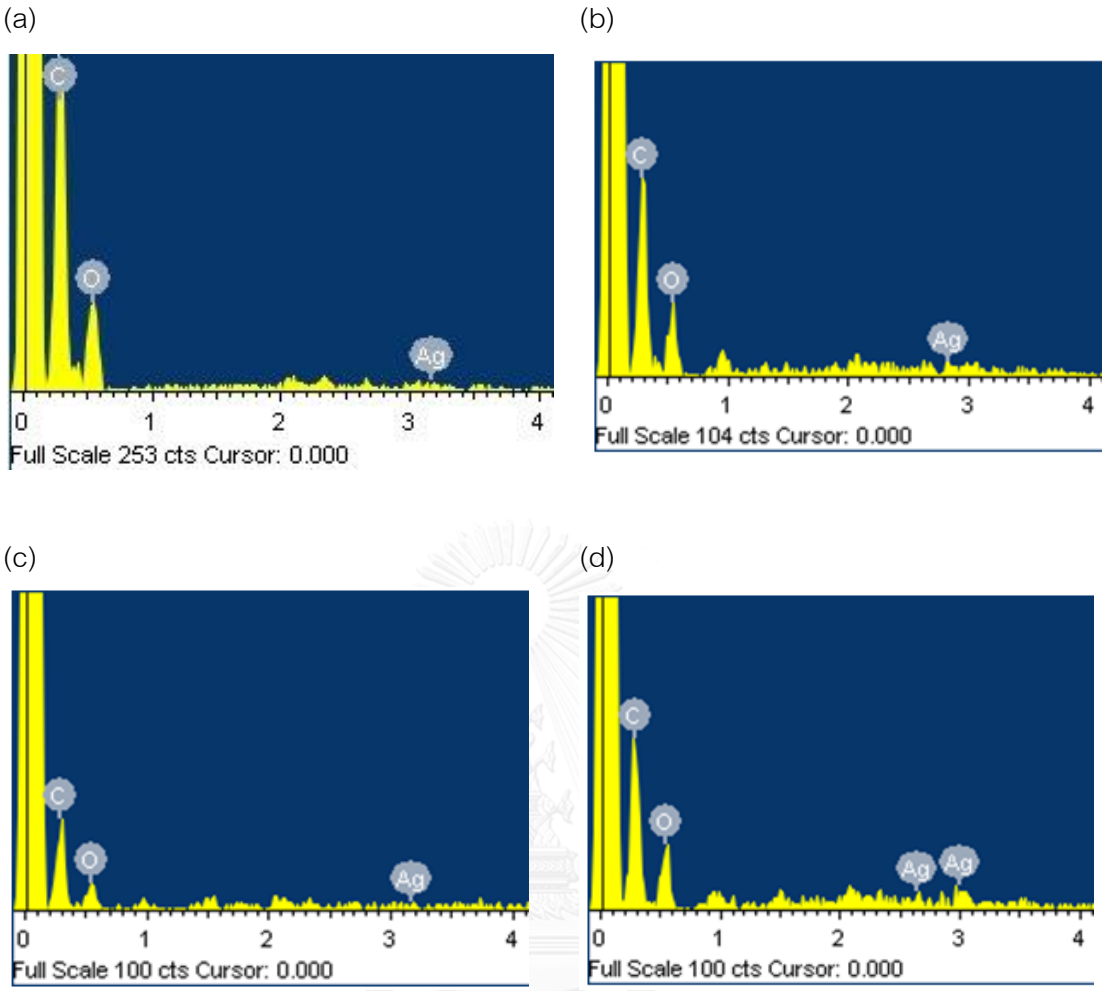

Figure 4.19 EDX analysis of AgNP/gelatin/PVA hydrogels (a) $AgNO_3$ 0.25 wt%, (b) $AgNO_3$ 0.50 wt%, (c) $AgNO_3$ 0.75 wt%, and (d) $AgNO_3$ 1.00 wt%.

Table 4.4 Weight% of element in hydrogels with $AgNO_3$ by EDX.

$AgNO_3$ wt%	Carbon (C)	Oxygen (O)	Silver (Ag)
0.25	64.78	32.95	2.27
0.50	64.90	30.34	4.77
0.75	67.80	23.00	9.21
1.00	57.56	29.90	12.53

4.15 Silver-release

Figure 4.20 (a) shows the release profiles of silver from AgNP/gelatin/PVA hydrogels. Figure 4.20 (b) shows the release profiles of silver, which represent as percent. A fresh hydrogel was investigated at each time duration. It was seen that the amount of released silver was increased when the amount of $AgNO_3$ was increased. The rapid release was shown at the initial part of the release profile. The slow release was shown after 6 h.

(a)

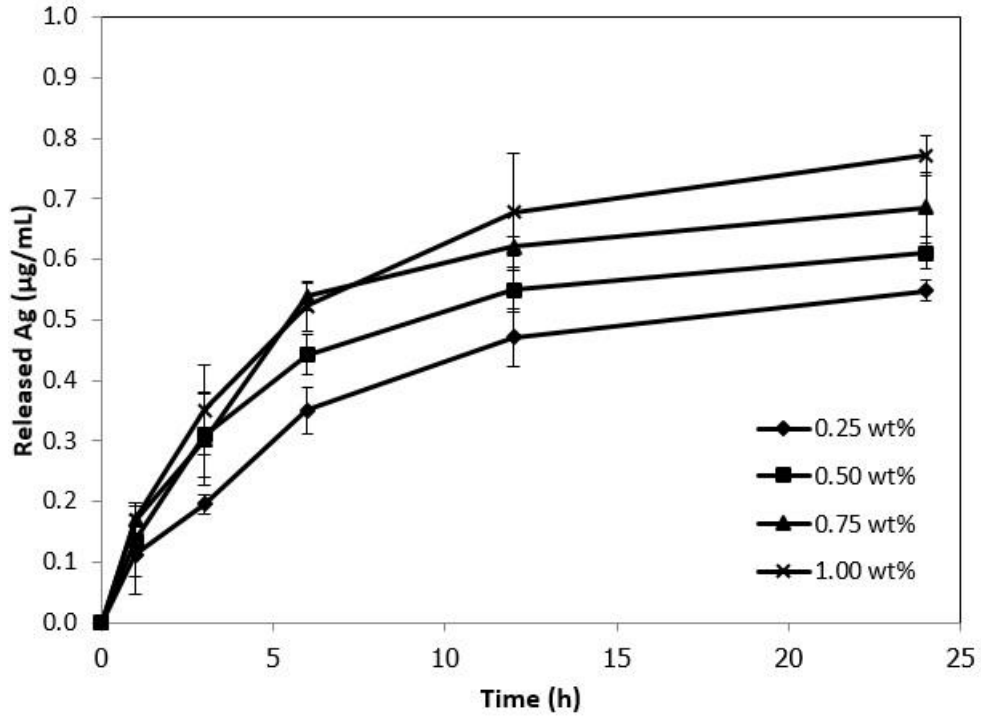

(b)

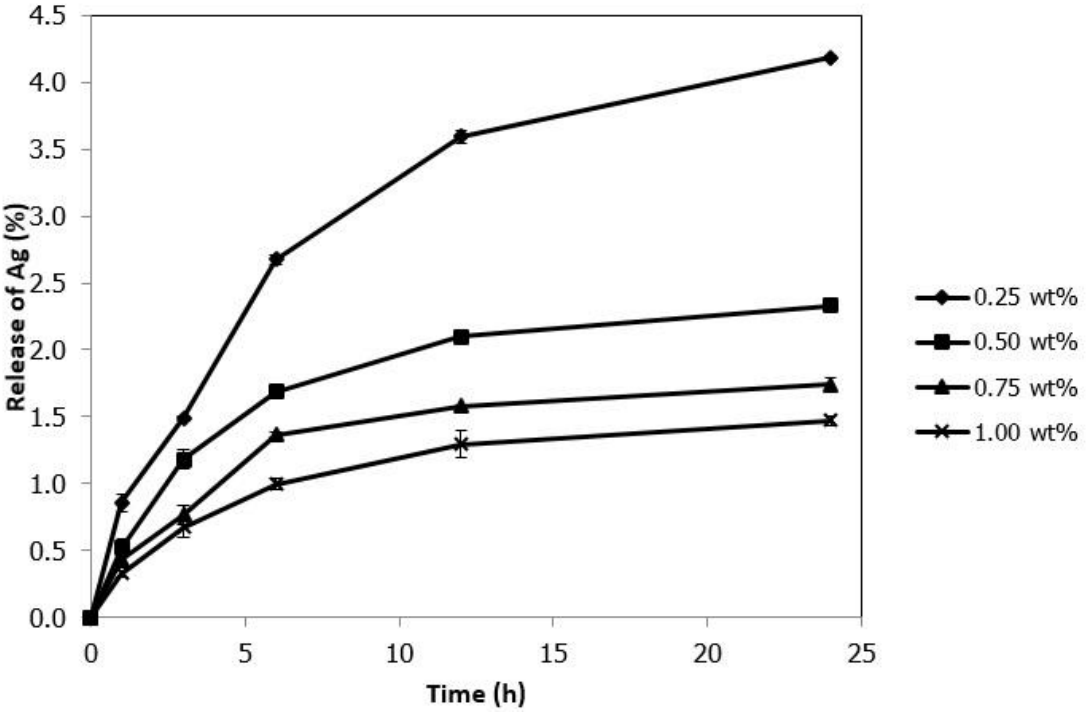

Figure 4.20 Release profiles of silver from AgNP/gelatin/PVA hydrogels.

(a) amount of silver (b) percent.

Part III: Determination of the Effects of AgNP/gelatin/PVA Hydrogels on Fibroblast Cells and Bacteria

4.16 Indirect Cytotoxicity Testing

The ability to kill bacteria is an outstanding characteristic of the wound dressing with antibacterial agent. But the cytotoxicity to human cells is also important. Therefore, we investigated the indirect cytotoxicity of AgNP/gelatin/PVA hydrogels on normal human dermal fibroblasts. Figure 4.21 presents the viability of normal human dermal fibroblasts that was cultured with extraction media of gelatin/PVA hydrogels with and without $AgNO_3$ for 1 d (24 h) and 3 d (72 h). The solution from blank well was used as control. The cell viability of all hydrogels was greater than 80%. There was no significant difference between cell viability of control and gelatin/PVA without AgNPs. There was significant difference between cell viability of hydrogels with $AgNO_3$ and control group. However, at 3 d, cell viability of hydrogels with $AgNO_3$ 0.25 wt% was not significantly different compared to the control group. Results from indirect cytotoxicity testing revealed that cell viability of hydrogels with $AgNO_3$ was decreased when the amount of $AgNO_3$ was increased.

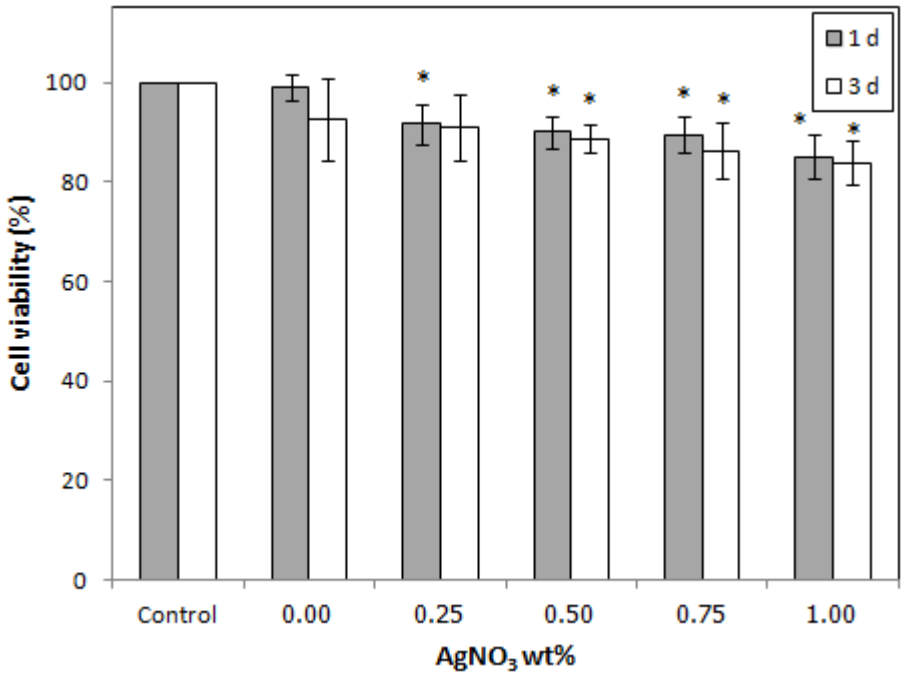

Figure 4.21 Viability of normal human dermal fibroblasts that was cultured with extraction media of gelatin/PVA hydrogels with and without $AgNO_3$ for 1 d (24 h) and 3 d (72 h). The solution from blank well was used as control.

An asterisk (*) represented a significant difference at $p < 0.05$ relative to cell viability of control group at the same time duration.

4.17 Antibacterial Activity

Counting the colonies of bacteria is an effective way to determine the number of viable and productive bacteria. As seen in Figure 4.22, the anti-bacterial efficacy of gelatin/PVA hydrogels with $AgNO_3$ was quite similar (almost 100%). Figure 4.23 shows a diagram of sample and clear zone observed after the test. Table 4.5 shows the results of the diameter of the hydrogel sample after testing and the length of the clear zone. The gelatin/PVA hydrogels without $AgNO_3$ and the antibiotic discs of Gentamicin 10 µg and Vancomycin 30 µg were used as the negative control and the positive control, respectively. There were slightly clear zones around the AgNP/gelatin/PVA hydrogels, but there was no clear zone around the $AgNO_3$ 1.00 wt% hydrogels. Many AgNP/gelatin/PVA hydrogels were soft after the test. There was no bacterial growth in area of soft hydrogels.

The NB agar under the gelatin/PVA hydrogels without $AgNO_3$ showed opaque appearance, indicating the growth of bacteria.

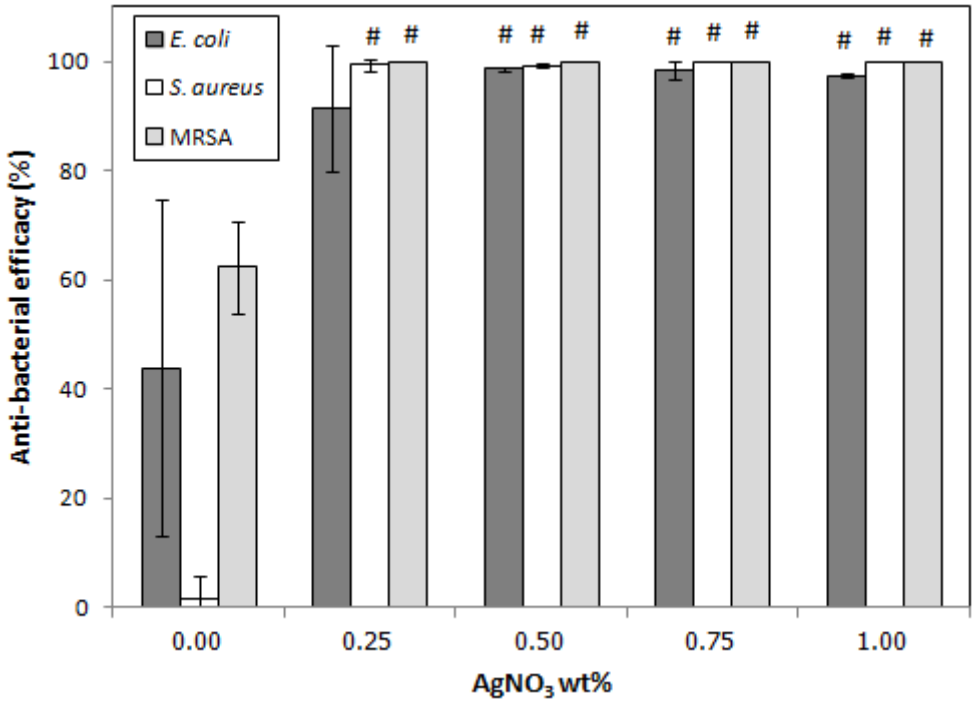

Figure 4.22 Antibacterial efficacy of AgNP/gelatin/PVA hydrogels compared with gelatin/PVA hydrogel without AgNPs.

A hash (#) represented a significant difference at $p < 0.05$ relative to antibacterial efficacy of gelatin/PVA hydrogel without AgNPs at the same type of bacteria.

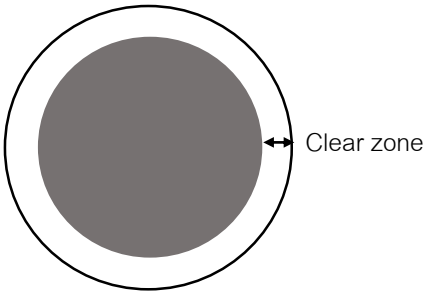

Figure 4.23 Diagram of sample and clear zone.

Gray circle represents sample. White ring represents clear zone.

Table 4.5 Average diameter of the gelatin/PVA hydrogel samples and antibiotic discs before and after antibacterial activity test, and clear zone after zone of inhibition test.

Samples	Diameter of the sample before test (mm)	Diameter of the sample after test (mm)			Clear zone (mm)		
		E. coli	*S. aureus*	MRSA	*E. coli*	*S. aureus*	MRSA
Gelatin/PVA	15 ± 0	15 ± 0	15 ± 0	15 ± 0	0 ± 0	0 ± 0	0 ± 0
Gelatin/PVA $AgNO_3$ 0.25 wt%	15 ± 0	15 ± 0	15 ± 0	16 ± 0	1 ± 0	1 ± 0	1 ± 0
Gelatin/PVA $AgNO_3$ 0.50 wt%	15 ± 0	18 ± 0	18 ± 0	19 ± 0	0 ± 0	1 ± 0	0 ± 0
Gelatin/PVA $AgNO_3$ 0.75 wt%	15 ± 0	27 ± 2*	20 ± 0	24 ± 0*	0 ± 0	2 ± 0	0 ± 0
Gelatin/PVA $AgNO_3$ 1.00 wt%	15 ± 0	24 ± 3*	26 ± 2*	26 ± 1*	0 ± 0	0 ± 0	0 ± 0
Gentamicin 10 µg	7 ± 0	7 ± 0	7 ± 0	7 ± 0	5 ± 0	5 ± 1	1 ± 0
Vancomycin 30 µg	7 ± 0	-	-	7 ± 0	-	-	6 ± 1

An asterisk (*) mean that the samples were soft.

CHAPTER 5
DISCUSSIONS AND CONCLUSIONS

5.1 Discussions

Part I: Preparation and Characterization of Gelatin/PVA Hydrogel

An appropriate wound dressing contributes a suitable wound environment, which could promote wound healing. Since the first study of moist wound healing by Winter in 1962 *(54)*, the interest in moisture-retentive wound dressing was increased. The modern wound dressings have moisture-retaining ability. Hydrogel is one of the modern wound dressings.

To develop wound dressing hydrogel, gelatin/PVA hydrogel was prepared by gamma-ray irradiation. In the first part, the proportions of hydrogel component and doses of gamma radiation were varied to find out suitable conditions for preparing hydrogels for wound dressing application. Gelatin, a natural material, was the major component in this study. The weight ratios of gelatin and PVA solution were 100:0, 80:20, and 60:40. The irradiation method is one of the popular techniques to prepare hydrogels. The important point of wound dressing is sterilization; therefore the radiation doses used in this study were higher than the minimum radiation sterilization dose. The gamma irradiation doses used in this research were 30-50 kGy, which was higher than 25 kGy recommended for medical sterilization. However, it was noticed that gamma irradiation doses in some studies were lower than 25 kGy. H. L. Abd El-Mohdy (2013) used 15, 20, and 25 kGy *(145)*. Erizal and Wikanta (2011) used the irradiation doses of 20-40 kGy *(140)*.

The hydrogel prepared in this research was in a sheet form. Wokalek H. (1991) *(132)* recommended that the thickness of hydrogel sheet should be between 3-5 mm. From Table A.1 and A.2 in appendix, the thickness of obtained hydrogels is about 3.6-4.1 mm, which is in the range of Wokalek's suggestion. Thickness of hydrogels is consistent with thickness of partial-thickness wound. Partial-thickness wound has a depth of 1-4 mm.

(162). This result also demonstrated that the preparation technique could reproduce the hydrogel with similar thickness. Thickness of hydrogels is similar to the thickness of commercial wound dressing (from the study of Uzun, M., Anand, S. C, and Shah, T. *(133)*, Table 2.9), which are Melolin* (3.4 mm), Biatain (3.4 mm), and CarboFlex™ (3.9 mm). Thickness of hydrogels is also close to the thickness of Mepilex®Border (4.2 mm), Allevyn Gentle Border (4.2 mm), and Aquacel® Surgical (4.2 mm). After the hydrogel sheets were prepared successfully, they were characterized, including water holding capacity and swelling ratio, WVTR, tensile properties, *in vitro* biodegradation, and gel fraction.

To determine the water holding capacity and swelling ratio of hydrogels, PBS that stimulated body fluid was used in the testing. The research by Kim et al. *(134)* reported that a suitable water holding capacity of wound dressing polymer should be in the range of 90-96%. Their dressing could absorb water efficiently and did not accumulate exudates. Table 4.1 shows water holding capacities of hydrogels, which are around 96%. The results were in agreement with Kim's recommendation. The gelatin/PVA hydrogels produced in this research demonstrated high swelling ratio at around 100-250% as shown in Figure 4.1. After 24 h immersion in PBS, the weight of swollen hydrogels was approximately 16-33 times compare with the weight of dried gel. The study of Uzun, M., Anand, S. C, and Shah, T. *(133)* reported the weight of the wet commercial wound dressings was around 4-19 times compare with the dry mass (Table 2.10), after immersing under sodium chloride, calcium chloride dihydrate and de-ionised water for 30 min.

The hydrogels with increasing quantities of PVA or increasing irradiation dose had decreasing water swelling ratios. The decreased swelling ratio could be the result from the higher crosslink density of the hydrogels, which happened when the crosslinked solution was exposed to a higher irradiation dose *(163)*. The main characteristic of hydrogel is the ability to absorb a lot of water. The hydrogels in this study can absorb and retain water very well. Gelatin and PVA, which were the main components of the hydrogels, are hydrophilic substances. Methionine, tyrosine, and cystine, which found in

gelatin, are polar amino acids. These hydrophilic amino acids in gelatin result in an excellent contact with water *(164).* PVA is also hydrophilic. The side chain of PVA has a large number of hydroxyl groups, which cause PVA hydrophilic *(165)*.

Water vapor transmission rate (WVTR), which is referred to as moisture vapor transmission rate (MVTR), is one of the essential factors of wound dressing. WVTR of the hydrogels in this study decreased when the amount of PVA or irradiation dose increased.Commercial wound dressing products exhibit a wide range of WVTR, which is between 76-9360 g/m^2/day *(131)*. Although there are broad ranges of WVTR for commercial wound dressings, a suitable range of WVTR is quite limited. The research by Queen et al. revealed that WVTR of 2000-2500 g/m^2/day could preserve wound moisture properly *(138)*. WVTR of the hydrogels in this study, shown in Figure 4.2, were approximately between 3000-5400 g/m^2/day. Some commercial wound dressing show the approximate WVTR value as the hydrogels in this study, such as Omiderm (Omikron Scientific Ltd., Rehovot, Israel). The WVTR of Omiderm is 5,000 g/ m^2/day *(166)*. WVTR of hydrogels in this study was higher than Queen's suggestion. However, the high WVTR dressing still has its own advantage. It could avoid exudates accumulation *(167).* Jonkman, M. F. and colleagues (1988) *(168)* studied wound healing under three conditions, which are covering with polyetherurethane (PEU) wound dressing, occlusive polyurethane wound dressing (OpSite), and air exposure. They discovered that the application of PEU wound dressing, which is highly water vapor permeable, can stimulate the epithelization more than two other methods for wound healing. In 1990, Jonkman, M. F. and colleagues *(169)* found that the enhanced epithelization is related with an abundant condensation of fibrin(ogen) and fibronectin.

Moreover, the research by Queen et al. *(170)* showed that an adhesive bandage covering on hydrogels could reduce the WVTR. High WVTR may be the result from the test method. Wu and colleagues (2007) *(171)* compared MVTR measurement test method. Three methods, which are ASTM F1249, ASTM E96(E), and ASTM E96(B), were

compared. Test method using different temperatures and condition cause dissimilar results. MVTR values from ASTM F1249 method (37.8°C) is approximately 10 times higher than the MVTR values for the same film tested by ASTM E96(B) method (23°C). High WVTR values in our study (3000-5400 g/m^2/day) may be the result of testing temperature at 37°C, which is considered high compared to the temperature used in another method, such as ASTM E96(B) method (23°C).

Mechanical testing of hydrogels is extremely difficult because of their soft surfaces and abundant fluid inside hydrogels *(172)*. ASTM D638, which is a standard test for tensile properties of plastics, was selected to test our hydrogel because PVA is a thermoplastic. However, the hydrogels in this study were very slippery and soft. When the hydrogel samples were pulled too fast or too slow, the sample broke or slipped from the grip. Another issue is a narrow section of the sample that can be torn easily. To solve these problems, we decided to adjust ASTM D638. The pull speed of 22 mm/min was selected. The 6 mm standard width of narrow section was extended to 10 mm. The overall width of sample was extended from 19 mm (the width of type IV) to 25 mm, which was specified in catalogue of plastic testing such as Zwick Roell *(173)*.

Mechanical properties is one of the important characteristic of wound dressing. Wound dressing with greater flexibility can comfortably bend on skin curve *(140)*. Flexibility depends on the type of wound dressing. Film dressing has less flexibility compared with hydrogel dressing. Peh, K. and colleague (2000) *(174)* reported that Omiderm® film dressing has an elongation at break of 56 %. Chitosan-AA and Chitosan-LA film dressing have elongation at break of 21 % and 67 %, respectively. Erizal, E. and Wikanta, T. (2011) *(140)* reported that polyethylene oxide-chitosan hydrogel wound dressings have elongation at break of 90-145% approximately. Tensile test was used to investigate the mechanical property of the hydrogel in this study. Results of percentage strain at maximum load were shown in Figure 4.4. The percentage strain at maximum load of the hydrogels was increased when the amount of PVA was increased. It could be

explained that the brittleness of gelatin was lessen by the toughness or viscoelastic properties of PVA *(175)*. At the same time, the increasing irradiation dose resulted in decreasing of percentage strain at maximum load. Results of stress at maximum load were also described in Figure 4.5. Stress at maximum load of the neat gelatin hydrogels was decreased when the irradiation dose was increased. A preliminary study showed that, the stiffness of the gelatin hydrogels irradiated at 40 kGy (71.15 ± 27.22 kN/m) was higher than the stiffness of the gelatin/PVA 80:20 hydrogel irradiated at 40 kGy (58.58 ± 37.25 kN/m) *(176)*. The mechanical testing results of hydrogel have a wide range of SD. These results could be the effect of the inexact received irradiation dose. The hydrogels in this study were aimed to be irradiated at 30, 40, and 50 kGy. The values of the received irradiation doses in the form of mean values ± SD were 29.98 ± 2.55, 41.50 ± 2.72, and 50.77 ± 0.70 kGy. In addition, several factors could influence the mechanical properties of hydrogels *(177)*. For example, water loss or evaporation during testing may cause an increasing moduli *(178)*.

The next testing is degradation. *In vitro* biodegradation of hydrogels was investigated in PBS containing lysozyme. Lysozyme is an enzyme that can be detected in wound and blister fluid *(153)*. In this part, time interval of degradation is 24-hour period (same as once-daily wound dressing change). There was no significant difference between remaining weight of all hydrogels. As seen in Figure 4.6, the hydrogels with higher irradiated dose or more PVA content demonstrated higher remaining weight. Remaining weight of 100:0 hydrogel which irradiated at 30 kGy was the least. Remaining weight of 60:40 hydrogel which irradiated at 50 kGy was the highest. Crosslinking process produces gel fraction and sol fraction. The gel fraction is “the network content of the polymer” and the sol fraction is “a fraction of unattached polymer” *(179)*. The gel fraction was used as an indirect estimation of the degree of crosslinking. At first, the hydrogels were dried. Then, they were immersed in an excess solvent to get rid of sol fraction. The gelatin/PVA hydrogels with more PVA content had more gel fraction, which can be related to the differences in the dissolution properties of gelatin and PVA *(180)*. The higher

irradiation dose causes an increase in the degree of crosslinking and leads to higher gel fraction.

In this part, the gelatin hydrogels and gelatin/PVA were characterized physical and mechanical properties. Water holding capacity, swelling ratio, and WVTR are the properties that associated with water. Water holding capacity and WVTR were decreased when amount of PVA was increased. Polymer in this study is PVA with high degrees of hydrolysis (99+% hydrolyzed). The high degrees of hydrolysis PVA is difficult to dissolve in water *(181)*. Water holding capacity, swelling ratio, and WVTR were decreased when irradiation dose was increased. The hydrogels that were irradiated with higher irradiation dose had an increasing degree of crosslinking. The degree of crosslinking had an effect on structure and swelling behavior of hydrogel *(182, 183)*. An increase in the degree of crosslinking also causes the hydrogel become less flexible *(184)*. It has been noticed that percentage strain at maximum load were decreased when irradiation dose was increased (Figure 4.4).

After considering all results, we selected the gelatin/PVA 60:40 hydrogels, irradiated at 30 kGy, for further study on AgNPs incorporation since they had suitable water holding capacity, high remaining weight after degradation test, and the highest percentage strain at maximum load. Although the 60:40 hydrogels, which were irradiated at 50 kGy, had the highest remaining weight after degradation test, but they had less percentage strain at maximum load.

Part II: Preparation and Characterization of Gelatin/PVA Hydrogel Containing AgNPs

In this part, $AgNO_3$ was used to create AgNPs for antibacterial activity. $AgNo_3$ was added in the gelatin/PVA 60:40 hydrogels irradiated at 30 kGy to produce the AgNP/gelatin/PVA hydrogels. Purposes of this part are to prove the existence of AgNPs and to investigate the effects of AgNPs in hydrogel. Then the properties of AgNP/gelatin/PVA hydrogels were tested again.

The values of swelling ratio of the AgNP/gelatin/PVA hydrogels were higher than the gelatin/PVA hydrogels (Figure 4.8). This incident occurred due to a certain part of radiation was used for Ag^+ reducing. Therefore, the AgNP/gelatin/PVA hydrogels were crosslinked by the remaining radiation but the gelatin/PVA hydrogels were obtained entire irradiation dose. The hydrogels without AgNPs could have a greater crosslink density *(121).* The values of WVTR of AgNP/gelatin/PVA hydrogels were quite similar (Figure 4.9). There was no significant difference.

The next experiment is a tensile test. From Figure 4.10, it was found that the hydrogels with higher amount of $AgNO_3$ had less percentage strain at maximum load. The functional groups of gelatin, which are -OH, C=O, and -NH groups *(185)*, and functional group of PVA, which is -OH group, bound with Ag^+ and form AgNPs. This nanoparticle formation may interrupt the matrix of hydrogel and lead to a lower percentage strain *(186)*. The stress at maximum load also decreased with more amount of $AgNO_3$.

The following test is an *in vitro* biodegradation. Time intervals of degradation of AgNP/gelatin/PVA hydrogel were divided into four intervals, which were 6, 12, 18, and 24 h, as shown in Figure 4.12. Time interval of changing dressing on burn wounds was advised by World Health Organization (WHO). Daily or twice daily changing is recommended for daily treatment of burn *(187)*. Remaining weights of the AgNP/gelatin/PVA hydrogels were approximately 37-52% and 49-83% at 24 h interval and 12 h interval respectively. In clinical use, there is a secondary dressing cover the hydrogel, which is a primary dressing. Therefore, the remaining weight at 12 h could be sufficient. After that, gel fraction was investigated. Gel fraction of AgNP/gelatin/PVA hydrogels was decreased when the amount of $AgNO_3$ was increased. These results could be explained by the binding of Ag^+ with the functional groups of gelatin and PVA, which was described in the previous section. The morphology of AgNP/gelatin/PVA hydrogels, examined by SEM, showed that the hydrogels had porous network structures, with pore diameter between 1-5 μm. The porous characteristic of wound dressing is permeable for water

vapor and wound exudates. The permeability of wound exudate can prevent bullae formation *(188)*.

Next process is chemical composition analysis. There are many techniques to analyze chemical composition such as nuclear magnetic resonance (NMR), Mass spectrometry (MS), and FTIR. Each technique has different limitations. An NMR sample must be dissolved in a deuterated solvent and solution sample has to be prepared properly *(189, 190).* Our crosslinked hydrogels were not soluble, therefore solution-state NMR was not a suitable technique. Another kind of NMR was a solid-state NMR. A weakness of solid-state NMR is broad spectra, which is broader than solution-state NMR spectra. The solid-state NMR outcome is not as well as solution NMR *(190)*. MS technique also has its own limitation. Molecular weight of MS sample is limited to the tens of kilodalton range *(191)*. Therefore, MS may not be suitable for our hydrogels. We examined the functional group of our hydrogels using FTIR technique. FTIR is used to investigate molecular structures in many biomaterial researches *(192-194)*. From Figure 4.15, the neat gelatin hydrogel had the spectrum with a peak at 3289 cm^{-1} attributed to –NH stretching, C=O stretching at 1630 cm^{-1}, and N-H bending at 1528 cm^{-1}. The FTIR spectrum of the gelatin/PVA hydrogel was similar to the spectrum of neat gelatin hydrogel. However, the peaks at 3289 cm^{-1}, in the spectra of neat gelatin and gelatin/PVA hydrogel, were broad indicating hydrogen bonds between the hydroxyl groups of PVA, gelatin and amide groups of gelatin. FTIR spectrum of the AgNP/gelatin/PVA hydrogel exhibited a broad peak compared to other spectrum. This might be due to the effect of reduced AgNPs on the functional groups of the polymers *(145)*.

We used UV-vis analysis to characterize the formation of AgNP. A peak of the characteristic SPR band of AgNPs is approximately 410-430 nm *(104, 157-160)*. Intensity of the characteristic peak of hydrogels with greater percentage of $AgNO_3$ loaded was higher. It can be explained that the AgNPs were formed with higher yields *(157).* There is bare absorbance at 410-430 nm for the hydrogels without $AgNO_3$ because of the absence

of AgNPs. EDX analysis also used to prove the existence of silver in our hydrogels. The EDX spectrum of all AgNP/gelatin/PVA hydrogels had characteristic L-series peaks of silver. This result confirmed the persistence of silver element.

The result of TEM indicated that the AgNPs in this study were very small, about 2-8 nm, which is good for antibacterial activity. H. L. Abd El-Mohdy (2013) *(145)* also synthesized AgNPs but in a larger size about 37 nm. The others used other substances for antibacterial purpose. Erizal and Wikanta (2011) *(140)* used chitosan. Singh and Pal (2011) *(147)* used sterculia gum. In this study, the functional groups of hydrogel polymer bind the AgNPs, therefore the nanoparticles do not agglomerate into a large size. This is one of the advantages of the *in situ* synthesis of AgNPs. Most of the preparation methods of the hydrogel with nanoparticles usually start with prefabrication of nanometal, and follow by impletion of nanoparticles into hydrogel ingredient *(195)*. Later, the agglomeration of AgNPs may occur, and explode the abundant of silver to the body which can cause toxicity *(196, 197)*.

This study investigated the release characteristic of silver by mimic the wound dressing. The hydrogels were placed on the CA sheet and on the body of the Franz cell. With this method, the hydrogels can release silver from only one side of the material, just like the wound dressing released the drug from only one side that attached to the wound area. Silver was released rapidly at the beginning and slowed down after 6 h (Figure 4.20). This situation was explained that the Ag^+ released in the earliest stage of the experiment originated from the silver particles at the surface of the hydrogels. The Ag^+ came out quickly and did not require the diffusion process migrate from the inside of the hydrogels. After that, the majority of the released Ag^+ transported from the inside of the hydrogels to the surface. This process needed diffusion *(198)*. Media that be used in the silver-release experiment is PBS, which is biological media. However, percent of released-silver is low. This incident could be caused by using PBS as media. Cations from PBS can effect AgNP agglomeration and silver dissolution. Ag^+ from AgNPs bind chloride ions from media and

construct AgCl complexes, which have low solubility. Obtainable Ag^+ decreased due to precipitation of these complexes (199)

Part III: Determination of the Effects of Gelatin/PVA Hydrogels Containing AgNPs to Fibroblast Cells and Bacteria

Silver is a common antiseptic agent in topical treatment of wound. Ability of Ag^+ to destruct bacteria can be toxic to cells. Therefore, cytotoxicity test was used to determine the toxicity to human dermal fibroblasts. MTT assay can measure the cell proliferation and viability. From Figure 4.21, all of cell viabilities were greater than 80%. Durations of cytotoxicity testing are 24 h (1 d) and 72 h (3 d), which are the same as covering period of commercial dressing. Durations of use of Acticoat™ are 1-3 days *(75)*. Cell viability of control group and gelatin/PVA hydrogels without AgNPs had no significant difference. Cell viability of hydrogel with $AgNO_3$, except hydrogel with $AgNO_3$ 0.25 wt% for 3 days, were significantly different compared to control group. This finding indicated that gelatin and PVA did not have serious toxicity to fibroblasts, while AgNPs had some toxic. Cell viability of hydrogel with $AgNO_3$ were 84-92% approximately. The wavelength in our study was 570 nm. The wavelength can be used in the range of 550-600 nm *(200)*.

Cytotoxicity of commercial silver antimicrobial dressings has been investigated by Ziegler and colleagues *(201)*. Three silver antimicrobial dressings (Acticoat, Actisorb silver 220, and Atrauman Ag) were tested with human keratinocyte cell line. Atrauman Ag and Actisorb silver 220 showed low cytotoxicity. Viability of keratinocytes with Atrauman Ag and Actisorb silver 220 were 90% and 80%, respectively, whereas Acticoat exhibited high cytotoxicity with 2% of cell viability. The eluate from cytotoxic test was determined the concentration of Ag^+ to find out the relationship between the result of cytotoxic test and the concentration of Ag^+. Acticoat, the most toxic, released the highest Ag^+ concentration of 71.4 ppm. Atrauman Ag and Actisorb silver 220 released Ag^+ concentration of 2.3 and 0.38 ppm respectively. Our hydrogels exhibited low toxicity with at least 80% of cell viability. From the result of silver-release assay (Figure 4.20), our

hydrogels with $AgNO_3$ released low concentration of Ag^+, which was less than 0.9 μg/mL (ppm) in 24 h.

Other cell tests in our study were antimicrobial activity assays and zone of inhibition test. Bacteria in this study were Gram-negative bacteria (represented by *E. coli*), Gram-positive bacteria (represented by *S. aureus*), and antibiotic resistant bacteria (represented by MRSA). Wound infection could postpone healing *(202)*. *E. coli* and *S. aureus* were reported as two of the most commonly pathogen, which cause hospital infections *(203)*. *S. aureus* also was the most common bacteria found in venous ulcer *(204)*. MRSA was the cause of sepsis in burn wound *(205).* Figure 4.22 showed anti-bacterial efficacy of hydrogels. The hydrogels with AgNPs had high anti-bacterial efficacy. However, it has been noticed that the hydrogels without AgNPs (0.00 wt%) also had moderately anti-bacterial efficacy. Antibacterial efficacy of the hydrogels without AgNPs against *E. coli* was approximately 40%, and against MRSA was approximately 60% while against *S. aureus* was only a few percent. These moderately anti-bacterial efficacies to *E. coli* and MRSA were suspicious. Safety data sheet of gelatin did not report the toxicity *(206)*. Toxicological effects of PVA was reported only oral LD50 of rat *(207)*. Gamma irradiation did not leave any toxic residues *(208)*. Reducing of viable bacterial colonies after exposure to hydrogels without AgNPs could be caused from limitations and error of our laboratory experiment.

Bacteria are fast-growing organisms. Generation time or doubling time of *E. coli* in optimal condition is about 20 min *(209)*. Generation time of *S. aureus* and MRSA is 30 min *(210, 211)*. In general, the incubation time at 35°C to prepare bacterial suspension equivalent to 0.5 McFarland standard is 2-6 h *(212)*. We incubated bacterial suspension for 24 h due to the laboratory limitation. Our bacterial suspension could move on the death phase or decline phase, which store toxic and autolytic enzymes *(213)*. These toxic and enzymes may have negatively impact on remaining bacteria. Anti-bacterial efficacies of hydrogels with various amount of AgNPs (0.25, 0.50, 0.75, and 1.00 wt%) were very

similar. This incident occurred because the period of incubation with hydrogels was too long (3 h). Actually, the incubation period should be divided, such as 30, 60, 90, 120 min. Anti-bacterial efficacies of hydrogels in short incubation time could be different depending on $AgNO_3$ amount.

Many AgNP/gelatin/PVA hydrogels were soft after the test because reduction of AgNPs reduced the crosslinking density of the hydrogels. The diameter of hydrogels in antibacterial activity test was increased when the amount of $AgNO_3$ was increased. The hydrogels with greater amount of $AgNO_3$ had decreased gel fraction, which imply the less degree of crosslinking. The decreased degree of crosslinking cause the increased diameter. The result appears to contradict swelling ratio result, which was decreased when the amount of $AgNO_3$ was increased. Media in swelling test is PBS. AgNP aggregated and precipitated in PBS *(214)*. This incident may influence swelling ratio result. However, there was no bacterial growth in the area of soft hydrogels. Thus the diameter of the soft hydrogels could claim as the clear zone. The NB agar under the gelatin/PVA hydrogels without $AgNO_3$ had opaque appearance indicated the presence of bacteria growth, so it did not count as a clear zone. The length of the clear zone hardly appeared while the percentage of anti-bacterial efficacy was very high. The conflict was explained by the reason that the inhibition of bacterial growth on agar related with the diffusion of the released Ag^+ from the hydrogels. But the hydrogels in antimicrobial activity assays was shaken, therefore the part of Ag^+ was released out by shaking force. The results of the effects of AgNP/gelatin/PVA hydrogels to bacteria supported our hypothesis that AgNPs could prevent the growth of bacteria on the hydrogel.

5.2 Conclusions

The developed gelatin/PVA hydrogels containing AgNPs was accomplished through gamma irradiation method. Gamma irradiation could crosslink polymer, produce AgNPs from $AgNO_3$, and sterile material within single step. The properties of hydrogel, which are water holding capacity, swelling ratio, WVTR, mechanical property, *in vitro*

biodegradation and gel fraction, were tested. The physical properties testing revealed that the addition of PVA can enhance elasticity and resistance to degradation of the hydrogels. The higher irradiation dose caused an increase in the degree of crosslinking of the hydrogels. However, the hydrogels with more content of $AgNO_3$ had the decreasing degree of crosslinking.

The AgNPs were prepared in this study. Ag^+ from silver nitrate aggregated to form AgNPs. The presence of AgNPs in the hydrogel structure was confirmed by TEM micrographs, monitoring of the surface plasmon peak using UV-vis spectrophotometer, and confirming the existence of silver using EDX. The indirect cytotoxicity of hydrogels with AgNPs showed that all of hydrogels with AgNPs had low cytotoxocity to fibroblasts.

The ability to use gelatin/PVA hydrogels containing AgNPs as an antibacterial wound dressing was investigated using *E. coli*, *S. aureus*, and MRSA. The results showed that the hydrogels with AgNPs can eliminate bacteria effectively. The highest $AgNO_3$-loaded content (1.00 wt%) hydrogel had the best antibacterial property. But the hydrogel with the lowest $AgNO_3$-loaded content (0.25 wt%) had the better mechanical property. The gelatin/PVA hydrogel with low content of $AgNO_3$-loaded (0.25 wt%) could be developed to use as the effective sterile antibacterial wound dressing in the form of hydrogel sheet.

The gelatin/PVA hydrogels containing AgNPs in this study were expected to be used as an antibacterial wound dressing for dry or slightly moist wounds. Wound healing mechanisms of gelatin/PVA hydrogels containing AgNPs are to provide moist wound environment and to prevent wound infection. Highly water vapor permeability and moisture from hydrogel is supposed to promote epithelialization. Hydrogel could absorb some wound exudate. AgNPs and Ag^+ are expected to perform antibacterial activity. Hydrogels in this study are suggested to apply to minor or partial thickness burn wounds

in the proliferative phase. It is recommended to change the hydrogel dressing every 12 h.

5.3 Recommendations

The further investigation should focus on the effect of hydrogels to wound healing. The pH value is an important factor for the reactions in the wound healing process *(215)*. Aggregation of silver particles is related to pH *(216, 217)*. Therefore, the effect on pH of AgNP/gelatin/PVA hydrogels should be further studied. The next steps of investigation should be an evaluation of healing potential of hydrogels in animal test.

REFERENCES

1. Posnett J, Gottrup F, Lundgren H, Saal G. The resource impact of wounds on health-care providers in Europe. J Wound Care 2009;18(4):154-61.

2. American Burn Association. Burn incidence and treatment in the United States: 2012 fact sheet 2013 [3 December 2013]. Available from: http://www.ameriburn.org/resources_factsheet.php.

3. Centers for Disease Control and Prevention. National diabetes fact sheet: national estimates and general information on diabetes and prediabetes in the United States. Atlanta, GA: U.S. Department of Health and Human Services, Centers for Disease Control and Prevention, 2011.

4. Singh N, Armstrong DG, Lipsky BA. Preventing foot ulcers in patients with diabetes. JAMA. 2005;293:217-28.

5. Rogers LC, Lavery LA, Armstrong DG. The right to bear legs-an amendment to healthcare: how preventing amputations can save billions for the US Health-care System. J Am Podiatr Med Assoc. 2008;98:166-8.

6. Gordois A, Scuffham P, Shearer A, Oglesby A, Tobian JA. The health care costs of diabetic peripheral neuropathy in the US. Diabetes Care. 2003;26:1790-5.

7. Bank of Thailand. Imports classified by economic classification. In: EC_XT_004_S2, editor. 2013.

8. Watanasit Y, Jitsurong S, Wansu F, Chichareon V. The application of cellulose (Thainanocell®) wound dressing on acute wound with partial-thickness loss. Songkla Med J. 2009;27(3):235-47.

9. Chang KW, Alsagoff S, Ong KT, Sim PH. Pressure ulcers--randomised controlled trial comparing hydrocolloid and saline gauze dressings. The Medical journal of Malaysia. 1998;53(4):428-31.

10. Boateng JS, Matthews KH, Stevens HNE, Eccleston GM. Wound healing dressings and drug delivery systems: a review. J Pharm Sci. 2008;97(8):2894-923.

11. Weller C, Sussman G. Wound dressings update. J Pharm Pract Res. 2006;36(4):318-24.

12. Eccleston GM. Wound dressings. In: Aulton ME, editor. Pharmaceutics: The science of dosage form design. 3rd edition ed. UK: Churchill Livingstone; 2007. p. 264–71.

13. Morgan DA. Wound management products in the drug tariff. Pharm J. 1999;263:820-5.

14. Phillips GO, Williams PA. Handbook of hydrocolloids. P. Murphy, editor. Cambridge, England: Woodhead Publishing limited; 2000

15. Hoare TR, Kohane DS. Hydrogels in drug delivery: progress and challenges. Polymer. 2008;49:1993-2007.

16. IAEA. Good radiation practice (GRP). IAEA (ed) Guidelines for industrial radiation sterilization of disposable medical products (cobalt-60 gamma irradiation). Vienna, Austria: IAEA; 1990. p. 12-24.

17. Hara M. Various cross-linking methods for collagens: merit and demerit of methods by radiation. J Oral Tissue Eng. 2006;3(3):118-24.

18. Djagny V, Wang Z, Xu S. Gelatin: a valuable protein for food and pharmaceutical industries: review. Crit Rev Food Sci Nutr. 2001;41(6):481-92.

19. Tabata Y, Ikada Y. Protein release from gelatin matrices. Adv Drug Deliv Rev. 1998;31:287-301.

20. Wan J. Microfluidic-based synthesis of hydrogel particles for cell microencapsulation and cell-based drug delivery. Polymers. 2012;4:1084-108.

21. Cascone MG, Sim B, Dowries S. Blends of synthetic and natural polymers as drug delivery systems for growth hormone. Biomaterials. 1995;16:569-74.

22. Burczak K, Gamian E, Kochman A. Long-term in vivo performance and biocompatibility of poly(vinyl alcohol) hydrogel macrocapsules for hybrid-type artificial pancreas. Biomaterials. 1996;17(24):2351-6.

23. Rosiak J, Ulańśki P. Synthesis of hydrogels by irradiation of polymers in aqueous solution. Radiat Phys Chem. 1999;55(2):139–51.

24. Danno A. Gel formation of aqueous solution of polyvinyl alcohol irradiated by gamma rays from cobalt-60. J Phys Soc Jpn. 1958;13(7):722-7.

25. Huang M-H, Yang M-C. Evaluation of glucan/poly(vinyl alcohol) blend wound dressing using rat models. Int J Pharm. 2008;346(1-2):38–46.

26. Berger TJ, Spadaro JA, Chapin SE, Becker RO. Electrically generated silver ions: quantitative effects on bacterial and mammalian cells. Anti Microb Agents. 1996:357-8.

27. Atiyeh BS, Costagliola M, Hayek SN, Dibo SA. Effect of silver on burn wound infection control and healing: Review of the literature. Burns. 2007;33(2):139-48.

28. Morones JR, Elechiguerra JL, Camacho A, Holt K, Kouri JB, Ramírez JT, et al. The bactericidal effect of silver nanoparticles. Nanotechnology. 2005;16(10):2346-53.

29. Rujitanaroj P, Pimpha N, Supaphol P. Preparation, characterization, and antibacterial properties of electrospun polyacrylonitrile fibrous membranes containing silver nanoparticles. J Appl Polym Sci. 2010;116(4):1967-76.

30. Krklješ A, Nedeljkovi**ć** JM, Ka**č**arevi**ć**-Popovi**ć** ZM. Fabrication of Ag-PVA hydrogel nanocomposite by **γ**-irradiation. Polym Bull. 2007;58:271-9.

31. Dorland WAN. Dorland's Illustrated Medical Dictionary. 32nd ed. ed. Philadelphia: Elsevier - Health Sciences Division; 2012.

32. สุมิตรา พงษ์ศิริ. บาดแผลและการหายของบาดแผล [13 มิถุนายน 2558]. Available from: http://www.dent.cmu.ac.th/mis/dis/UserFiles/File/surg/SheetDOS381/Sheet%20Wound%20Healing_45.pdf.

33. Percival JN. Classification of wounds and their management. Surgery 2002;20:114-7.

34. Harding KG, Morris HL, Patel GK. Science, medicine and the future: Healing chronic wounds. Br Med J. 2002;324:160-3.

35. Snyder RJ. Treatment of nonhealing ulcers with allografts. Clin Dermatol 2005;23 (4):388-95.

36. Taylor JE, Laity PR, Hicks J, Wong SS, Norris K, Khunkamchoo P, et al. Extent of iron pick-up in deforoxamine-coupled polyurethane materials for therapy of chronic wounds. Biomaterials 2005;26(30):6024-33.

37. Different types of wounds: Wound care centers. Available from: http://www.woundcarecenters.org/wound-basics/different-types-of-wounds.html.

38. Lazarus G, Cooper D, Knighton D, Margolis D, Pecoraro R, Rodeheaver G, et al. Definitions and guidelines for assessment of wounds and evaluation of healing. Wound Rep Reg. 1994;2:165-70.

39. Schultz GS. Molecular regulation of wound healing. In: Bryant RA, editor. Acute and chronic wounds: Nursing management. 2nd edition ed. St. Louis, MO: Mosby; 1999. p. 413-29.

40. Diegelmann R, Evans M. Wound healing: an overview of acute, fibrotic and delayed healing. Front Biosci. 2004;9:283-9.

41. Gurtner G, Werner S, Barrandon Y, Longaker M. Wound repair and regeneration. Nature. 2008;453:314-21.

42. Haas AF. Wound healing. Dermatol Nurs. 1995;7(28-34).

43. Werner S, Grose R. Regulation of wound healing by growth factors and cytokines. Physiol Rev. 2003;83:835-70.

44. Werner S, Krieg T, Smola H. Keratinocyte-fibroblast interactions in wound healing. The Journal of investigative dermatology. 2007;127:998-1008.

45. Szabowski A M-SN, Andrecht S, Kolbus A, Schorpp-Kistner M, Fusenig NE, Angel P. c-Jun and JunB antagonistically control cytokine-regulated mesenchymal-epidermal interaction in skin. Cell. 2000;103(5):745-55.

46. Levenson S, Geever E, Crowley L, Oates JI, Berard C, Rosen H. Healing of rat skin wounds. Ann Surg. 1965;161(2):293-308.

47. Guo S, DiPietro LA. Factors Affecting Wound Healing. Journal of Dental Research. 2010;89(3):219-29.

48. Rodriguez PG, Felix FN, Woodley DT, Shim EK. The role of oxygen in wound healing: a review of the literature. Dermatologic surgery : official publication for American Society for Dermatologic Surgery [et al]. 2008;34(9):1159-69.

49. Tandara AA, Mustoe TA. Oxygen in wound healing--more than a nutrient. World journal of surgery. 2004;28(3):294-300.

50. Hohn DC, MacKay RD, Halliday B, Hunt TK. Effect of oxygen tension on microbicidal function of leukocytes in wounds and in vitro. Surgical forum. 1976;27(62):18-20.

51. Schreml S, Szeimies RM, Prantl L, Karrer S, Landthaler M, Babilas P. Oxygen in acute and chronic wound healing. The British journal of dermatology. 2010;163(2):257-68.

52. Principles of best practice: Wound infection in clinical practice. An international consensus London: World Union of Wound Healing Societies (WUWHS) MEP Ltd; 2008 [14 June 2015]. Available from: www.mepltd.co.uk.

53. Edwards R, Harding KG. Bacteria and wound healing. Current opinion in infectious diseases. 2004;17(2):91-6.

54. Winter GD. Formation of the scab and the rate of epithelization of superficial wounds in the skin of the young domestic pig. Nature. 1962;193(4812):293-4.

55. Katz MH, Alvarez AF, Kirsner RS, Eaglstein WH, Falanga V. Human wound fluid from acute wounds stimulates fibroblast and endothelial cell growth. J Am Acad Dermatol. 1991;25(6 Pt 1):1054-8.

56. Nemeth AI, Eaglstein WH. Wound dressings and local treatment in leg ulcers: diagnosis and treatment. In: Westerhof W, editor. Leg ulcers: diagnosis and treatment. Amsterdam: Elsevier Science Publishers; 1993. p. 325–33.

57. Shepherd AA. Nutrition for optimum wound healing. Nursing standard (Royal College of Nursing (Great Britain) : 1987). 2003;18(6):55-8.

58. Gogia PP. Physiology of wound healing. In: Gogia PP, editor. Clinical wound management. Thorofare, NJ: Slack Incorporated; 1995. p. 8-12.

59. Arnold M, Barbul A. Nutrition and wound healing. Plastic and reconstructive surgery. 2006;117(7 Suppl):42s-58s.

60. Campos AC, Groth AK, Branco AB. Assessment and nutritional aspects of wound healing. Current opinion in clinical nutrition and metabolic care. 2008;11(3):281-8.

61. Burgess C. Topical vitamins. J Drugs Dermatol. 2008;7(7 Suppl):s2-s6.

62. Swift ME, Burns AL, Gray KL, DiPietro LA. Age-related alterations in the inflammatory response to dermal injury. The Journal of investigative dermatology. 2001;117(5):1027-35.

63. Gosain A, DiPietro LA. Aging and wound healing. World journal of surgery. 2004;28(3):321-6.

64. Purna Sai K. MB. Collagen based dressings - a review. Burns. 2000;26:54-62.

65. Paul W, Sharma C. Chitosan and alginate wound dressings: a short review. Trends Biomater Artif Organs. 2004;18(1):18-23.

66. Thomas S, Hay P. Fluid handling properties of hydrogel dressings. Ostomy Wound Manage 1995;41(3):54-6, 8-9.

67. Morgan N. What you need to know about hydrogel dressings. Wound Care Advisor. 2013;2(6):21-3.

68. Eisenbud D, Hunter H, Kessler L, Zulkowski K. Hydrogel wound dressings: where do we stand in 2003? Ostomy Wound Manage. 2003;49(10):52-7.

69. Hydrogels: Amorphous: Kestrel Health Information, Inc.; 2008-2014 [cited 2014 1 September 2014]. Available from: http://www.woundsource.com/product-category/dressings/hydrogels-amorphous.

70. Hydrogels: Impregnated: Kestrel Health Information, Inc.; 2008-2014 [cited 2014 1 September 2014]. Available from: http://www.woundsource.com/product-category/dressings/hydrogels-impregnated.

71. Lay-Flurrie K. The properties of hydrogel dressings and their impact on wound healing. Prof Nurse. 2004;19(5):269-73.

72. Hydrogels: Sheets: Kestrel Health Information, Inc.; 2008-2014 [cited 2014 2 September 2014]. Available from: http://www.woundsource.com/product-category/dressings/hydrogels-sheets.

73. Harris A, Komray RR. Cost-effective management of pharyngocutaneous fistulas following laryngectomy. Ostomy Wound Manage. 1993;39(8):36-7, 40-2, 4.

74. Dinh T, Pham H, Veves A. Emerging treatments in diabetic wound care. Wounds. 2002;14:2-10.

75. Guidelines for use of Nanocrystalline Silver Dressing - Acticoat™. In: Health Do, editor. Western Australia: Department of Health, Western Australia; 2011.

76. Roberts C, Ivins N, Widgerow A. ACTICOAT™ AND ALLEVYN™ Ag Made Easy. Wounds International. 2011;2(2):s7-s12.

77. Queen D, Walker M, Parsons D, Rondas A. AQUACEL Ag dressings made easy. Wounds International. 2011;2(2):1-6.

78. Carsin H, Wassermann D, Pannier M, Dumas R, Bohbot S. A silver sulphadiazine-impregnated lipidocolloid wound dressing to treat second-degree burns. J Wound Care. 2004;13(4):145-8.

79. Gray D. Product focus: Reduced cellular toxicity and clinical performance of Atrauman® Ag. Wounds International. 2010;1(5):44-6.

80. Clark R, Bradbury S. SILVERCEL® Non-adherent made easy. Wounds International. 2010;1(5):1-6.

81. Adlington L. NHS Lincolnshire Formulary of wound management products. Lincolnshire N; 2012.

82. บริษัท เอส อาร์ โอเมดดิคอล จำกัด. พลาสเตอร์เทปปิดแบบต่างๆ และแผ่นฟิลม์ปิดแผลกันน้ำ และชุดแผล ฯลฯ 2014 [updated 28 มิถุนายน 2014; cited 2014 29 มิถุนายน 2014]. Available from: http://sromedical.com/service/40/.

83. Gelatin Handbook [Internet]. Gelatin Manufacturers Institute of America. 2012.

84. Riaz M, Chaudry M. Halal food production. Florida: CRC Press; 2005.

85. America Gmio. GMIA standard methods for the testing of edible gelatin. Official Procedure of the Gelatin Manufacturers Institute of America, Inc.; 2013.

86. Liassaf. J Polym Lett. 1972;16(225).

87. Prissanaroon-Ouajai W. Lab1 Poly(vinyl alcohol). Powerpoint of lecture note "411318 Polymer Chemistry Lab". Bangkok, King Mongkut's University of Technology North Bangkok.

88. Katz DA. Polyvinyl alcohol slime [14 June 2015]. Available from: http://www.chymist.com/PVA%20Slime.pdf.

89. Guidance for radiation accident management: Radiation emergency assistance center/Training site (REAC/TS). Available from: http://orise.orau.gov/reacts/guide/define.htm.

90. Gamma irradiators for radiation processing. International atomic energy agency (IAEA).

91. Laughlin WL, Boyd AW, Chadwich KH, Donald JC, Miler A. Dosimetry for radiation processing. Taylor & Francis Ed, editor. New York, USA1989.

92. Kaplan I. Nuclear Physics. Boston, USA: Addison-Wesley Pub. Co.; 1955.

93. Rosenthal I. Electromagnetic radiations in Food Science. Berlin: Springer Verlag; 1992.

94. Fellows P. Irradiation. Food Processing Technology. 2nd ed. ed. Cambridge: Woodhead Publishing Limited; 2000. p. 196 - 209.

95. สายสนม ประดิษฐดวง. การให้ความร้อนด้วยพลังงานไมโครเวฟและการฉายรังสีอาหาร. วิทยาศาสตร์และเทคโนโลยีการอาหาร. พิมพ์ครั้งที่ 2 ed. กทม.: สำนักพิมพ์ มหาวิทยาลัยเกษตรศาสตร์; 2540. p. 173 - 95.

96. Kojima T, Bessho M, Furuta M, Okuda S, Hara M. Characterization of biopolymer hydrogels produced by γ-ray irradiation. Radiat Phys Chem. 2004;71(1-2):235–8.

97. Ulanski P, Bothe E, Rosiak JM, von Sonntag C. OH-radical-induced crosslinking and strand breakage of poly(vinyl alcohol) in aqueous solution in the absence and presence of oxygen. A pulse radiolysis and product study. Macromol Chem Phys. 1994;195(4):1443–61.

98. Zhu Y, Qian Y, Li X, Zhang M. γ-Radiation synthesis and characterization of polyacrylamide–silver nanocomposites. Chem Commun. 1997(12):1081-2.

99. Temgire M, Joshi S. Optical and structural studies of silver nanoparticles. Radiat Phys Chem. 2004;71(5):1039–44.

100. Chen P, Song L, Liu Y, Fang Y-E. Synthesis of silver nanoparticles by γ-ray irradiation in acetic water solution containing chitosan. Radiat Phys Chem. 2007;76(7):1165-8.

101. Xu X, Yin Y, Ge X, Wu H, Zhang Z. γ-Radiation synthesis of poly(acrylic acid)–metal nanocomposites. Mater Lett. 1998;37(6):354–8.

102. Shin HS, Yang HJ, Kim SB, MS L. Mechanism of growth of colloidal silver nanoparticles stabilized by polyvinyl pyrrolidone in gamma-irradiated silver nitrate solution. J Colloid Interface Sci. 2004;274(1):89-94.

103. Kumar M, Varshney L, Francis S. Radiolytic formation of Ag clusters in aqueous polyvinyl alcohol solution and hydrogel matrix. Radiat Phys Chem. 2005;73(1):21-7.

104. Zhou Y, Zhao Y, Wang L, Xu L, Zhai M, Wei S. Radiation synthesis and characterization of nanosilver/gelatin/carboxymethyl chitosan hydrogel. Radiat Phys Chem. 2012;81(5):553–60.

105. Thomas V, Bajpai M, Bajpai SK. In situ formation of silver nanoparticles within chitosan-attached cotton fabric for antibacterial property. J Ind Text. 2011;40(3):229-45.

106. Aquino KAdS. Sterilization by gamma irradiation. In: Feriz Adrovic, editor. Gamma Radiation: InTech; 2012.

107. Whitby JL, Gelda AK. Use of incremental doses of cobalt 60 radiation as a means to determining radiation sterilization dose. Journal of Parenteral Drug Association. 1979;33:144-55.

108. Barbosa-Canovas GV, Pothakamury UR, Palou E, Swanson BG. Nonthermal preservation of foods. New York: Marcel Dekker, Inc.; 1998.

109. Nanotechnology 101 What is nanotechnology? : National Nanotechnology Initiative; [14 June 2015]. Available from: http://www.nano.gov/nanotech-101/what/definition.

110. Allhoff F, Lin P, Moore D. What is nanotechnology and why does it matter?: from science to ethics: John Wiley and Sons; 2010

111. Scale of Things Chart: Office of Basic Energy Sciences (BES) for the U.S. Department of Energy; 2006.

112. Sharma VK, Yngard, R. A., Lin, Y. Silver nanoparticles: green synthesis and their antimicrobial activities. Adv Colloid Interface Sci. 2009;145(1-2):83-96.

113. Jiang H, Moon K, Zhang Z, Pothukuchi S, Wong CP. Variable frequency microwave synthesis of silver nanoparticles. J Nanopart Res. 2006;8(1):117-24.

114. Tran QH, Nguyen VQ, Le A-T. Silver nanoparticles: synthesis, properties, toxicology, applications and perspectives. Adv Nat Sci: Nanosci Nanotechnol. 2013;4.

115. Kapoor S, Lawless D, Kennepohl P, Meisel D, Serpone N. Reduction and aggregation of silver ions in aqueous gelatin solutions. Langmuir. 1994;10(9):3018–22.

116. Shenashen MA, El-Safty SA, Elshehy EA. Synthesis, morphological control, and properties of silver nanoparticles in potential applications. Particle & Particle Systems Characterization. 2014;31:293-316.

117. Kruis FE, Fissan H, Rellinghaus B. Sintering and evaporation characteristics of gas-phase synthesis of size-selected PbS nanoparticles. Mat Sci Eng. 2000;B 69-70:329-34.

118. Magnusson MH, Deppert K, Malm J-O, Bovin J-O, Samuelson L. Gold nanoparticles: production, reshaping, and thermal charging. J Nanopart Res. 1999;1(2):243-51.

119. Remita S, Fontaine P, Lacaze E, Borensztein Y, Sellame H, Farha R, et al. X-ray radiolysis induced formation of silver nano-particles: A SAXS and UV–visible absorption spectroscopy study. Nuclear Instruments and Methods in Physics Research B. 2007;263:436-40.

120. Abu Bakar NHH, Ismail J, AbuBakar M. Synthesis and characterization of silver nanoparticles in natural rubber. Mater Chem Phys. 2007;104:276-83.

121. Sikareepaisan P. Gelatin and alginate hydrogels as bio-interactive dressings. Bangkok: Chulalongkorn University.; 2011.

122. Sakamoto M, Fujistuka M, Majima T. Light as a construction tool of metal nanoparticles: Synthesis and mechanism. Journal of Photochemistry and Photobiology C: Photochemistry Reviews. 2009;10:33-56.

123. Sintubin L, Verstraete W, Boon N. Biologically produced nanosilver: current state and future perspectives. Biotechnol Bioeng. 2012;109(10):2422-36.

124. Kalimuthu K, Babu RS, Venkataraman D, Bilal M, Gurunathan S. Biosynthesis of silver nanocrystals by *Bacillus licheniformis*. Colloids and Surfaces B: Biointerfaces. 2008;65:150-3.

125. Campbell DJ, Xia Y. Plasmons: Why should we care? J Chem Educ. 2007;84(1):91-6.

126. Krutyakov YA, Kudrinskiy AA, Olenin AY, Lisichkin GV. Synthesis and properties of silver nanoparticles: advances and prospects. Russian Chemical Reviews. 2008;77(3):233 - 57.

127. Huang T, Xu X-HN. Synthesis and characterization of tunable rainbow colored colloidal silver nanoparticles using single-nanoparticle plasmonic microscopy and spectroscopy. J Mater Chem. 2010;20(44):9867-76.

128. Nowack B, Krug HF, Height M. 120 years of nanosilver history: implications for policy makers. Environ Sci Technol. 2011;45:1177-83.

129. Li Q, Mahendra S, Lyon DY, Brunet L, Liga MV, Li D, et al. Antimicrobial nanomaterials for water disinfection and microbial control: Potential applications and implications. Water research. 2008;42:4591-602.

130. Sondi I, Salopek-Sondi B. Silver nanoparticles as antimicrobial agent: a case study on *E. coli* as a model for gram-negative bacteria. J Coll Inter Sci. 2004;275(1):177-82.

131. Wu P, Fisher AC, Foo PP, Queen D, Gaylor JDS. In vitro assessment of water vapour transmission of synthetic wound dressings. Biomaterials. 1995;16(3):171-5.

132. Wokalek H, inventorHydrogel sheet wound dressings. United States patent 5,076,265. 1991 Dec. 31, 1991.

133. Uzun M, Anand SC, Shah T. In Vitro Characterisation and Evaluation of Different Types of Wound Dressing Materials. Journal of Biomedical Engineering and Technology. 2013;1(1):1-7.

134. Kim IY YM, Seo JH, Park SS, Na HS, Lee HC, Kim SK, Cho CS. Evaluation of semi-interpenetrating polymer networks composed of chitosan and poloxamer for wound dressing application. Int J Pharm. 2007;341(1-2):35-43.

135. Balakrishnan B, Mohanty M, Umashankar PR, Jayakrishnan A. Evaluation of an in situ forming hydrogel wound dressing based on oxidized alginate and gelatin. Biomaterials. 2005;26(32):6335-42.

136. Silverman RA, Lender J, Elmets CA. Effects of occlusive and semi-occlusive dressings on the return of barrier function to transepidermal water loss in standardized human wounds. J Am Acad Dermatol. 1989;20:755-60.

137. Pirone L, Monte K, Shannon R, Bolton L. Wound healing under occlusion and non-occlusion in partial-thickness and full-thickness wounds in swine. Wounds. 1990;2:74-81.

138. Queen D, Gaylor JDS, Evans JH, Courtney JM, Reid WH. The preclinical evaluation of the water vapor transmission rate through burn wound dressings. Biomaterials. 1987;8:367-71.

139. Lang SM, Webster DF. Wound dressing, manufacture and use. Google Patents; 1984.

140. Erizal E, Wikanta T. Synthesis of polyethylene oxide (PEO)–chitosan hydrogel prepared by gamma radiation technique. Indonesian Journal of Chemistry. 2011;11(1):16-20.

141. Sung JH, Hwang MR, Kim JO, Lee JH, Kim YI, Kim JH, et al. Gel characterisation and in vivo evaluation of minocycline-loaded wound dressing with enhanced wound healing using polyvinyl alcohol and chitosan. International Journal of Pharmaceutics. 2010;392(1-2):232-40.

142. Kamoun EA, Kenawy ERS, Tamer TM, El-Meligy MA, Eldin MSM. Poly (vinyl alcohol)-alginate physically crosslinked hydrogel membranes for wound dressing

applications: Characterization and bio-evaluation. Arabian Journal of Chemistry. 2015;8(1):38–47.

143. Shi L, Yang N, Zhang H, Chen L, Tao L, Wei Y, et al. A novel poly(gamma-glutamic acid)/silk-sericin hydrogel for wound dressing: Synthesis, characterization and biological evaluation. Materials Science and Engineering C. 2015;48:533-40.

144. Yu H, Xu X, Chen X, Lu T, Zhang P, Jing X. Preparation and antibacterial effects of PVA-PVP hydrogels containing silver nanoparticles. J Appl Polym Sci. 2007;103(1):125-33.

145. El-Mohdy HLA. Radiation synthesis of nanosilver/poly vinyl alcohol/cellulose acetate/gelatin hydrogels for wound dressing. Journal of Polymer Research. 2013;20(177).

146. Singh R, Singh D. Radiation synthesis of PVP/alginate hydrogel containing nanosilver as wound dressing. Journal of Materials Science: Materials in Medicine. 2012;23(11):2649-58.

147. Singh B, Pal L. Radiation crosslinking polymerization of sterculia polysaccharide–PVA–PVP for making hydrogel wound dressings. Int J Biol Macromol. 2011;48:501-10.

148. ASTM. ASTM Standard E96-00. Standard test methods for water vapour transmission of materials. Annual book of ASTM standards, vol 406. Philadelphia2000.

149. Mao JS, Liu HF, Yin YJ, Yao KD. The properties of chitosan-gelatin membranes and scaffolds modified with hyaluronic acid by different methods. Biomaterials. 2003;24(9):1621-9.

150. ASTM D638-03 Standard Test Method for Tensile Properties of Plastics ASTM International. USA: ASTM International; 2003.

151. Sabudin S, Derman MA, Zainol I, Noorsal K. In vitro cytotoxicity and cell seeding studies of a chitosan-silver composite for potential wound management applications. Journal of Engineering Science. 2012;8:29-37.

152. Theapsak S, Watthanaphanit A, Rujiravanit R. Preparation of chitosan-coated polyethylene packaging films by DBD plasma treatment. Appl Mater Interfaces. 2012;4(5):2474-82.

153. Frohm M, Gunne H, Bergman AC, Agerberth B, Bergman T, Boman A, et al. Biochemical and antibacterial analysis of human wound and blister fluid. Eur J Biochem. 1996;237(1):86-92.

154. Mulvaney P. Surface plasmon spectroscopy of nanosized metal particles. Langmuir. 1996;12(3):788-800.

155. Rashid M, Sabir S. Biosynthesis of self-dispersed silver colloidal particles using the aqueous extract of *P. peruviana* for sensing *dl*-Alanine. ISRN Nanotechnology. 2014;2014.

156. Derrick MR, Stulik D, Landry JM. Infrared Spectroscopy in Conservation Science: Getty Conservation Institute; 1999.

157. Liu F-K, Hsu Y-C, Tsai M-H, Chu T-C. Using **γ**-irradiation to synthesize Ag nanoparticles. Materials Letters. 2007;61:2402–5.

158. Liu Y, Chen S, Zhong L, Wu G. Preparation of high-stable silver nanoparticle dispersion by using sodium alginate as a stabilizer under gamma radiation Radiation Physics and Chemistry. 2009;78:251-5.

159. Rujitanaroj P, Pimpha N, Supaphol P. Wound-dressing materials with antibacterial activity from electrospun gelatin fiber mats containing silver nanoparticles. Polymer. 2008;49:4723-32.

160. Rattanaruengsrikul V, Pimpha, N., and Supaphol P. Development of gelatin hydrogel pads as antibacterial wound dressings. Macromolecular Bioscience. 2009;9:1004-15.

161. Kaye GWC, Laby TH. Tables of physical and chemical constants: Longman; 1995.

162. Sussman C, Bates-Jensen BM. Wound care: a collaborative practice manual: Wolters Kluwer Health / Lippincott Williams & Wilkins; 2007.

163. Savas H, Guven O. Gelation, swelling and water vapor permeability behavior of radiation synthesized poly(ethylene oxide) hydrogels. Radiat Phys Chem. 2002;64:35-40.

164. Neuman R. The amino acid composition of gelatins, collagens and elastins from different sources. Arch Biochem. 1949;24(2):289-98.

165. Haweel CK, Ammar SH. Preparation of polyvinyl alcohol from local raw material. Iraqi Journal of Chemical and Petroleum Engineering 2008;9(1):15-21.

166. Behar D, Juszynski M, Ben Hur N, Golan J, Eldad A, Tuchman Y, et al. Omiderm, a new synthetic wound covering: Physical properties and drug permeability studies. Journal of Biomedical Materials Research. 1986;20(6):731-8.

167. Rennekampff HO, Hansbrough JF, Kiessig V, Abiezzi S, Woods Jr. V. Wound closure with human keratinocytes cultured on a polyurethane dressing overlaid on a cultured human dermal replacement. Surgery. 1996;120(1):16-22.

168. Jonkman MF, Bruin P, Hoeksma EA, Nieuwenhuis P, Klasen HJ, Pennings AJ, et al. A clot-inducing wound covering with high vapor permeability: enhancing effects on epidermal wound healing in partial-thickness wounds in guinea pigs. Surgery. 1988;104(3):537-45.

169. Jonkman MF, Hoeksma EA, Nieuwenhuis P. Accelerated Epithelization Under a Highly Vapor-Permeable Wound Dressing Is Associated with Increased Precipitation of Fibrin(ogen) and Fibronectin. J Investig Dermatol. 1990;94(4):477-84.

170. Queen D EJ, Gaylor JD, Courtney JM, Reid WH. The physical effects of an adhesive dressing top layer on burn wound dressings. Burns. 1986;12(5):351-6.

171. Wu PC, Jones G, Shelley C, Woelfli B. Novel microporous films and their composites. Journal of Engineered Fibers and Fabrics. 2007;2(1):49-59.

172. Kwon HJ, Rogalsky AD. Mechanical characterization of hydrogel. Plastics Research online. 2010.

173. Testing of plastics and rubber. In: Roell Z, editor.

174. Peh K, Khan T, Ch'ng H. Mechanical, bioadhesive strength and biological evaluations of chitosan films for wound dressing. Journal of pharmacy & pharmaceutical

sciences : a publication of the Canadian Society for Pharmaceutical Sciences, Societe canadienne des sciences pharmaceutiques. 2000;3(3):303-11.

175. Chun H-J, Kim J-J, Lee S-H, Kim U-Y, Kim K-Y. Dialysis performance of the modified poly(vinyl alcohol) membranes. Polymer Journal. 1990;22(6):477-81.

176. Leawhiran N, Pavasant P, Soontornvipart K, Supaphol P. Radiation synthesis of nanosilver/gelatin/PVA hydrogel for biomedical application. Poster session presented at The third international symposium Frontiers in Polymer Science, Sitges, Spain. 2013, May.

177. Ahearne M, Yang Y, El Haj AJ, Then KY, Liu K-K. Characterizing the viscoelastic properties of thin hydrogel-based constructs for tissue engineering applications. Journal of The Royal Society Interface. 2005;2(5):455-63.

178. Anseth KS, Bowman CN, Brannon-Peppas L. Mechanical properties of hydrogels and their experimental determination. Biomaterials. 1996;17:1647-57.

179. Nandi S, Winter HH. Swelling behavior of partially cross-linked polymers: a ternary system. Macromolecules. 2005;38(10):4447-55.

180. Nam SY, Nho YC, Hong SH, Chae GT, Jang HS, Suh TS, et al. Evaluations of poly(vinyl alcohol)/alginate hydrogels cross-linked by γ -ray irradiation technique. Macromolecular Research. 2004;12(2):219-24.

181. Hassan C, Peppas N. Structure and Applications of Poly(vinyl alcohol) Hydrogels Produced by Conventional Crosslinking or by Freezing/Thawing Methods. Biopolymers · PVA Hydrogels, Anionic Polymerisation Nanocomposites. Advances in Polymer Science. 153: Springer Berlin Heidelberg; 2000. p. 37-65.

182. Flory PJ, Rehner J. Statistical Mechanics of Cross-Linked Polymer Networks II. Swelling. The Journal of Chemical Physics. 1943;11(11):521-6.

183. Brannon-Peppas L, Peppas NA. Equilibrium swelling behavior of pH-sensitive hydrogels. Chemical Engineering Science. 1991;46(3):715-22.

184. Peppas NA, Bures P, Leobandung W, Ichikawa H. Hydrogels in pharmaceutical formulations. European journal of pharmaceutics and biopharmaceutics : official journal of Arbeitsgemeinschaft fur Pharmazeutische Verfahrenstechnik eV. 2000;50(1):27-46.

185. Rosiak JM, Ulanski P, Kadłubowski S. Conventional and Radiation Synthesis of Polymeric Nano- and Microgels and Their Possible Applications. IAEA; Vienna2005. p. 99-120.

186. Nguyen T-H, Kim Y.-H., Song H-Y, Lee B-T. Nano Ag loaded PVA nano-fibrous mats for skin applications. J Biomed Mater Res B Appl Biomater. 2011;96B(2):225-33.

187. Surgical care at the district hospital [Manual]: World Health Organization; 2003.

188. Hinrichs WLJ, Lommen EJCMP, Wildevuur CRH, Feijen J. Fabrication and characterization of an asymmetric polyurethane membrane for use as a wound dressing. J Appl Biomater. 1992;3:287-303.

189. NMR Sample Preparation from NMR Facility Notes J.B. Stothers NMR Facility, Department of Chemistry, Western University [5 November 2014]. Available from: http://publish.uwo.ca/~chemnmr/usingthefacility/NMR_Sample_Preparation_2.0.pdf.

190. NMR Service - Solid Samples J.B. Stothers NMR Facility, Department of Chemistry, Western University [5 November 2014]. Available from: http://publish.uwo.ca/~chemnmr/service/solids_service_2.html.

191. Koizumi H, Whitten WB, Reilly PT. Trapping of intact, singly-charged, bovine serum albumin ions injected from the atmosphere with a 10-cm diameter, frequency-adjusted linear quadrupole ion trap. J Am Soc Mass Spectrom. 2008;19(12):1942-7.

192. Reis EF, Campos FS, Lage AP, Leite RC, Heneine LG, Vasconcelos WL, et al. Synthesis and characterization of poly (vinyl alcohol) hydrogels and hybrids for rMPB70 protein adsorption. Materials Research. 2006;9(2):185-91.

193. Manjula MK, Lokanatha Rai KM, Raj JM, Manjula CS, Siddaramaiah, Ranganathaiah C. Microwave assisted improvement in physico-mechanical properties of poly(vinyl alcohol)/poly(ethylene imine)/gelatin blends. Journal of Polymer Research. 2010;17(1):89-98.

194. El Bahy GS, El-sayed E-SM, Mahmoud AA, Gweily NM. Preparation and characterization of poly vinyl alcohol /gelatin blends. Journal of Applied Sciences Research. 2012;8(7):3544-51.

195. El-Sherif H, El-Masry, M, Kansoh, A. Hydrogels as Template Nanoreactors for Silver Nanoparticles Formation and Their Antimicrobial activities. Macromol Res. 2011;19:1157-65.

196. Klasen HJ. A historical review of the use of silver in the treatment of burns II. Renewed interest for silver. Burns. 2000;26:131-8.

197. Tsipouras N, Rix CJ, Brady PH. Passage of silver ions through membrane-mimetic materials, and its relevance to treatment of burn wounds with silver sulfadiazine cream. Clin Chem. 1997;43(2):290-301.

198. Damm C, Munstedt H. Kinetic aspects of the silver ion release from antimicrobial polyamide/silver nanocomposites. Appl Phys A. 2008;91(3):479–86.

199. Reidy B, Haase A, Luch A, Dawson K, Lynch I. Mechanisms of Silver Nanoparticle Release, Transformation and Toxicity: A Critical Review of Current Knowledge and Recommendations for Future Studies and Applications. Materials. 2013;6(6):2295.

200. MTT Cell Proliferation Assay American Type Culture Collection, USA [3 February 2015]. Available from: http://www.atcc.org/~/media/DA5285A1F52C414E864C966FD78C9A79.ashx.

201. Ziegler K, Gorl R, Effing J, Ellermann J, Mappes M, Otten S, et al. Reduced cellular toxicity of a new silver-containing antimicrobial dressing and clinical performance in non-healing wounds. Skin Pharmacol Physiol. 2006;19(3):140-6.

202. Vowden P, Vowden K, Carville K. Antimicrobial dressings made easy. Wounds International. 2011;2(1):1-6.

203. Jarvis WR, Martone WJ. Predominant pathogens in hospital infections. J Antimicrob Chemother. 1992;29:19-24.

204. Halbert AR, Stacey MC, Rohr JB, Jopp-McKay A. The effect of bacterial colonization on venous ulcer healing. Australas J Dermatol. 1992;33(2):75-80.

205. Cook N. Methicillin-resistant Staphylococcus aureus versus the burn patient. Burns. 1998;24(2):91-8.

206. Safety data sheet Gelatin, from porcine skin. Sigma-Aldrich Pte Ltd, 2012.

207. Safety data sheet Poly(vinyl alcohol). Sigma-Aldrich Pte Ltd, 2012.

208. Facts about food irradiation. Vienna, Austria: International Atomic Energy Agency, 1999.

209. Todar K. Todar's Online Textbook of Bacteriology 2008-2012 [cited 2014 19 October 2014]. Available from: http://textbookofbacteriology.net/growth_3.html.

210. Keren I, Kaldalu N, Spoering A, Wang Y, Lewis K. Persister cells and tolerance to antimicrobials. FEMS Microbiol Lett. 2004;230(1):13-8.

211. Karauzum H, Ferry T, de Bentzmann S, Lina G, Bes M, Vandenesch F, et al. Comparison of adhesion and virulence of two predominant hospital-acquired methicillin-resistant Staphylococcus aureus clones and clonal methicillin-susceptible S. aureus isolates. Infect Immun. 2008;76(11):5133-8.

212. โรงพยาบาลธรรมศาสตร์เฉลิมพระเกียรติ. เอกสารคุณภาพห้องปฏิบัติการเทคนิคการแพทย์ โรงพยาบาลธรรมศาสตร์เฉลิมพระเกียรติ การตรวจวิเคราะห์ทางห้องแบคทีเรีย. 2551. p. 44.

213. Parija SC. Textbook of Microbiology & Immunology: Elsevier Health Sciences; 2014.

214. Park K, Lee Y. The stability of citrate-capped silver nanoparticles in isotonic glucose solution for intravenous injection. Journal of toxicology and environmental health Part A. 2013;76(22):1236-45.

215. Schneider LA, Korber A, Grabbe S, Dissemond J. Influence of pH on wound-healing: a new perspective for wound-therapy? Arch Dermatol Res. 2007;298(9):413-20.

216. Chen SF, Zhang H. Aggregation kinetics of nanosilver in different water conditions. Advances in Natural Sciences: Nanoscience and Nanotechnology. 2012;3(3):035006.

217. Paladini F, Meikle ST, Cooper IR, Lacey J, Perugini V, Santin M. Silver-doped self-assembling di-phenylalanine hydrogels as wound dressing biomaterials. Journal of Materials Science: Materials in Medicine. 2013;24:2461-72.

APPENDIX

DATA TABLES

Table A.1 Thickness of hydrogels (in mm)

Hydrogels Gelatin:PVA	Irradiation dose (kGy)		
	30	40	50
100:0	3.688 ± 0.383	3.623 ± 0.339	3.853 ± 0.146
80:20	3.947 ± 0.078	3.860 ± 0.086	3.904 ± 0.215
60:40	3.735 ± 0.167	3.879 ± 0.108	4.063 ± 0.066

Table A.2 Thickness (mm) of of AgNP/gelatin/PVA hydrogels compared with 60:40 gelatin/PVA hydrogel without AgNPs (30 kGy)

$AgNo_3$ wt%				
0.00	0.25	0.50	0.75	1.00
3.735 ± 0.167	3.890 ± 0.169	3.944 ± 0.304	3.911 ± 0.113	3.877 ± 0.110

Table A.3 Swelling ratio and WVTR of hydrogels

Hydrogels Gelatin:PVA (kGy)	Swelling ratio (%)	WVTR ($g/m^2/day$)
100:0 (30)	196.80 ± 27.15	5400.00 ± 522.46
80:20 (30)	180.82 ± 45.78	4758.33 ± 113.42
60:40 (30)	171.00 ± 31.41	4170.83 ± 220.20
100:0 (40)	139.82 ± 3.17	4816.67 ± 268.77
80:20 (40)	138.92 ± 10.52	4679.17 ± 365.79
60:40 (40)	128.94 ± 12.93	3425.00 ± 159.59
100:0 (50)	123.77 ± 3.61	4516.67 ± 104.83
80:20 (50)	119.05 ± 14.48	4262.50 ± 489.10
60:40 (50)	117.51 ± 3.65	3008.33 ± 239.25
60:40 (30) $AgNO_3$ 0.25 wt%	226.74 ± 0.96	4645.83 ± 349.18
60:40 (30) $AgNO_3$ 0.50 wt%	231.25 ± 3.18	4462.50 ± 261.01
60:40 (30) $AgNO_3$ 0.75 wt%	210.53 ± 9.95	4287.50 ± 100.00
60:40 (30) $AgNO_3$ 1.00 wt%	166.46 ± 6.39	4250.00 ± 189.16

Table A.4 Percentage strain at maximum load, and Gel fraction of hydrogels

Hydrogels Gelatin:PVA (kGy)	Percentage strain at maximum load (%)	Stress at maximum load (N/mm^2)	Gel fraction (%)
100:0 (30)	97.00 ± 20.14	0.0439 ± 0.0037	78.03 ± 1.39
80:20 (30)	141.32 ± 28.29	0.0403 ± 0.0078	71.24 ± 4.74
60:40 (30)	159.98 ± 12.88	0.0402 ± 0.0059	79.39 ± 0.36
100:0 (40)	58.64 ± 11.21	0.0319 ± 0.0023	76.02 ± 2.21
80:20 (40)	128.25 ± 25.00	0.0329 ± 0.0083	73.87 ± 4.07
60:40 (40)	140.11 ± 22.66	0.0305 ± 0.0033	84.47 ± 0.88
100:0 (50)	50.47 ± 11.09	0.0281 ± 0.0016	77.48 ± 0.94
80:20 (50)	113.22 ± 16.17	0.0362 ± 0.0044	80.97 ± 0.19
60:40 (50)	123.69 ± 28.30	0.0330 ± 0.0051	89.27 ± 3.48
60:40 (30) $AgNO_3$ 0.25 wt%	179.56 ± 15.79	0.0256 ± 0.0075	77.52 ± 1.92
60:40 (30) $AgNO_3$ 0.50 wt%	165.52 ± 27.82	0.0185 ± 0.0022	71.17 ± 1.22
60:40 (30) $AgNO_3$ 0.75 wt%	113.53 ± 10.19	0.0136 ± 0.0033	65.08 ± 2.51
60:40 (30) $AgNO_3$ 1.00 wt%	99.93 ± 10.29	0.0123 ± 0.0061	64.66 ± 3.85

Table A.5 Remaining weight (%) after 24 h *in vitro* biodegradation of hydrogels without AgNPs

Irradiation dose (kGy)	Hydrogels		
	100:0	80:20	60:40
30	38.2 ± 20.3	52.1 ± 12.1	62.5 ± 7.4
40	49.6 ± 17.6	58.6 ± 9.1	54.7 ± 18.5
50	63.9 ± 14.8	60.4 ± 13.5	75.1 ± 2.5

Table A.6 Remaining weight (%) after *in vitro* biodegradation of hydrogels with and without AgNPs

Time intervals (h)	$AgNO_3$ wt%				
	0.00	0.25	0.50	0.75	1.00
6	77.1 ± 2.1	91.3 ± 1.6	65.0 ± 0.5	66.2 ± 5.5	54.0 ± 4.5
12	66.4 ± 5.8	83.2 ± 2.3	59.8 ± 0.9	52.0 ± 1.4	49.1 ± 3.2
18	65.3 ± 4.3	76.8 ± 0.8	44.1 ± 6.8	45.6 ± 4.5	42.5 ± 6.2
24	62.5 ± 7.4	51.9 ± 3.4	42.0 ± 5.9	38.2 ± 2.7	36.9 ± 5.3

Table A.7 Release profiles of silver (μg/mL) from AgNP/gelatin/PVA hydrogels

Time intervals (h)	$AgNO_3$ wt%			
	0.25	0.50	0.75	1.00
0	0.000 ± 0.000	0.000 ± 0.000	0.000 ± 0.000	0.000 ± 0.000
1	0.112 ± 0.065	0.136 ± 0.061	0.169 ± 0.022	0.171 ± 0.026
3	0.195 ± 0.017	0.309 ± 0.070	0.302 ± 0.075	0.351 ± 0.073
6	0.350 ± 0.039	0.442 ± 0.033	0.538 ± 0.022	0.522 ± 0.042
12	0.471 ± 0.048	0.549 ± 0.037	0.621 ± 0.016	0.678 ± 0.096
24	0.548 ± 0.018	0.610 ± 0.027	0.685 ± 0.058	0.771 ± 0.034

Table A.8 Viability of NHDF that was cultured for 1 d (24 h) and 3 d (72 h)

Samples	Time intervals (d)	
	1	3
Control	100.00 ± 0.00	100.00 ± 0.00
$AgNO_3$ 0.00 wt%	99.08 ± 2.50	92.60 ± 8.10
$AgNO_3$ 0.25 wt%	91.74 ± 3.99	90.97 ± 6.69
$AgNO_3$ 0.50 wt%	90.06 ± 3.12	88.64 ± 2.88
$AgNO_3$ 0.75 wt%	89.52 ± 3.64	86.27 ± 5.53
$AgNO_3$ 1.00 wt%	85.09 ± 4.43	83.80 ± 4.42

Table A.9 Percentage of anti-bacterial efficacy of *E. coli*, *S. aureus*, and MRSA

Bacteria	$AgNO_3$ wt%				
	0.00	0.25	0.50	0.75	1.00
E. coli	43.9 ± 30.7	91.5 ± 11.5	98.6 ± 0.4	98.4 ± 1.6	97.4 ± 0.5
S. aureus	1.6 ± 4.1	99.4 ± 1.1	99.2 ± 0.4	100.0 ± 0.0	100.0 ± 0.0
MRSA	62.3 ± 8.6	99.9 ± 0.1	100.0 ± 0.0	100.0 ± 0.0	100.0 ± 0.0

VITA

Miss Nuchanan Leawhiran was born in Bangkok on 13th November 1979. She graduated from Faculty of Science, Chulalongkorn University with a Bachelor degree of science in Biology in academic year 2001. In 2004, she received her Master degree of Science in Medical Science, Faculty of medicine, Chulalongkorn University.

Her publication and presentations during Bachelor degree and Master degree are listed as follows;

Publication: - Vejchapipat, P., Leawhiran, N., Poomsawat, S., Theamboonlers, A., Chittmittrapap, S., and Poovorawan, Y. (2006). Amelioration of Intestinal Reperfusion Injury by Moderate Hypothermia is Associated with Serum sICAM-1 Levels. J Surg Res. 130, 152–157.

Presentations: - The elevation of serum sICAM-1 following intestinal ischemia-reperfusion is ameliorated by moderate hypothermia. the 19th Congress of the Association of Pediatric Surgeons, Hong Kong, Republic of China. 28th November – 1st December 2004. (Poster Presentation)

- Leawhiran, N., and Chutmongkonkul, M., Investigation of Protozoa and Helminth parasites in Macaca fascicularis. The 9th Academic conference, Faculty of Science, Chulalongkorn University (Poster Presentation)

After graduation, she worked from 2005-2006 in Faculty of Public Health, Mahidol University. In the last quarter of 2006, she moved to worked in Faculty of Medicine Siriraj Hospital, Mahidol University. She has enrolled at Chulalongkorn University in the Degree of Doctor of Philosophy Program in Biomedical Engineering, Faculty of Engineering in 2009.

Some parts of this work were presented and published as follows;

Publication: - Leawhiran, N., Pavasant, P., Soontornvipart, K., and Supaphol, P. (2014). Gamma irradiation synthesis and characterization of AgNP/gelatin/PVA hydrogels for antibacterial wound dressings. J Appl Polym Sci. DOI:10.1002/APP.41138.

Presentations: - Leawhiran, N., Pavasant, P., Soontornvipart, K., and Supaphol, P., Radiation synthesis of nanosilver/gelatin/PVA hydrogel for biomedical application. Frontiers in Polymer Science, Sitges, Spain. 21st -23rd May 2013. (Poster Presentation)